Effect of surfactants on the therapeutic efficacy of atovaquone nanosuspensions against acute and reactivated murine toxoplasmosis

Dissertation

To obtain the academic degree
Doctor rerum naturalium (Dr. rer. nat.)
Submitted to the Department of Biology, Chemistry
and Pharmacy of Freie Universität, Berlin - Germany

By

Hend Shubar
(From Tripoli, Libya)

Institute of Microbiology and Hygiene
Charité—University Medicine, Berlin
Campus Benjamin Franklin, Berlin, Germany

July 2009

Prof. Dr. Oliver Liesenfeld

Prof. Dr. Hans-Hubert Borchert

Disputation date: ___23. September 2009_____

DEDICATION

I dedicate this dissertation to my loving husband Bashir Sherif and my beautiful son Ahmed Bashaar Sherif for being so patient, and so supporting to me while I have spent periods of time away from them working on this project, and for their patience, encouragement and unconditional love.

I would also like to dedicate this dissertation to my beautiful mother for her love and kindness.

Finally, I dedicate this dissertation to my late father (god bless his soul), the man who guided me by his invaluable suggestions throughout my life, the man who encouraged me by all his means to complete my education, but Allah chose him to be in another world at this time.

ACKNOWLEDGEMENTS

While I am in Berlin for my PhD I have learnt and understand many things. I am thankful for all the people who helped me. Without their guidance, assistance and organizations, this study would not have been possible.

First of all I thank Prof. Oliver Liesenfeld for taking me as his student and for being my supervisor and introducing me to the field of parasitology. I thank him for the opportunity to work on a very interesting project, for his support and for correcting my thesis. Thanks for standing beside me in all cases.

I would also like to thank Prof. Hubert Borchert for being my supervisor at the faculty of pharmacy. I thank him for reviewing my thesis.

I thank Dr. Ildiko Dunay for helping me in the first steps of my project. She did a lot of basic work from which I began my research.

I am also thankful to Petra Huck for teaching me the technique of cell culture and flow cytometry and for helping me performing in-vitro experiments.

I thank Berit Söhl-Kielczynski for being my technical assistant for the past four years and for helping me deal with animals and for performing the HPLC analysis. She was beside me in every experiment.

I thank also Uwe Lohmann for teaching me the technique of PCR and for helping me performing PCR analysis.

I would also like to thank Dr. Markus Heimesaat for providing critical assistance when all seemed dark and guidance when the project seemed endless. I thank him for helping me deal with animals, and treating my mice when I was not available. I thank him also for sorting problems I faced during my work.

Special thanks to Sabrina Lachenmaier for being my closest colleague, for supporting and for the extreme help she offered me during my study. Thanks for the wonderful time we spent together, thanks for the advices and for sorting out things whenever I ran in to trouble during my stay in Berlin (thank you Sabrina for everything).

I thank Daniela Struck for helping me deal with animals, and for her help with the mouse experiments.

I thank our collaborators for being helpful to me:
Thank you to Ms. Sigrid Ziesch and Dr. Rudolf Fitzner from the Institute of Clinical Chemistry and Pathobiochemistry, Charité University Medicine for performing the HPLC analysis.

Thank you to Dr. Faris Nadiem Bushrab, Dr. Rachmat Mauludin, and Prof. Rainer Müller from the Department of Pharmaceutical Technology, Biotechnology and Quality Management, Free University of Berlin, for synthesizing atovaquone nanosuspensions.

I would like to acknowledge the Libyan General Peoples Committee Secretary For Higher Education for financially supporting my PhD and giving me the opportunity to get to know Germany in other aspects than only science.

I am very grateful to all my lab mates, Solvy Wolke, Uschi Rüschendorf, Michaela Wattrodt, Lara Bajohr, Anna Gomes, Melba Munoz, Susanne Matschi, Pinar Önal, Agata Dukaczewska, Seong-Ji Han, Frederik Heinrich, all of them made the lab a nice place to work.

Finally, I would like to thank Profs. Helmut Hahn and Ulf Göbel for giving me the chance to do my PhD in the Institute of Microbiology and Hygiene.

TABLE OF CONTENT

1 List of figures 11

2 List of tables 14

3 List of abbreviations 15

4 Introduction 17

4.1 Toxoplasmosis 17

4.1.1 Infection with *T. gondii* 17

4.1.2 Epidemiology 20

4.1.3 Toxoplasmic encephalitis 21

4.1.4 Therapy 22

4.1.4.1 Pyrimethamine 23

4.1.4.2 Sulfadiazine 23

4.1.4.3 Clindamycin 24

4.1.4.4 Atovaquone 24

4.2 Biological barriers to drug delivery 26

4.2.1 The gastrointestinal barrier 26

4.2.1.1 Structure and function of the gastrointestinal barrier 26

4.2.1.2 Transport at the gastrointestinal barrier 28

4.2.2 The blood-brain barrier 30

4.2.2.1 Structure and function of the BBB 30

4.2.2.2 Transport at the BBB 32

4.3 Drug targeting 33

4.3.1 Nanoparticles 34

4.3.1.1 Nanoparticles for oral drug delivery 35

4.3.1.2 Nanoparticles for brain drug delivery 36
4.3.2 Surfactants (stabilizers) 37
4.3.2.1 Tween® 80 (polysorbate 80) 37
4.3.2.2 Poloxamers 39
4.3.2.2.1 Poloxamer 188 40
4.3.2.3 Sodium dodecyl sulphate (SDS) 41
5 Aims of research 43
6 Material and methods 44
6.1 Chemicals and plastic ware 44
6.2 Apparatus 47
6.3 Cell lines 49
6.4 *T. gondii* strains 49
6.5 Animals 49
6.6 Software 50
6.7 Methods 51
6.7.1 In-vitro experiments 51
6.7.1.1 Preparation of ANSs 51
6.7.1.2 Characterization of ANSs 52
6.7.1.2.1 Particle size measurement 52
6.7.1.2.2 Zeta potential measurement 52
6.7.1.2.3 Microscopic imaging 52
6.7.1.3 MTT colorimetric cell viability assay 53

6.7.1.4 Mono-culture model of intestinal barrier 53
6.7.1.5 Mono-culture model of blood-brain-barrier 54
6.7.1.6 Co-culture model of blood-brain-barrier 54
6.7.1.7 High-performance liquid chromatography (HPLC) 56
6.7.1.8 Flow cytometry analysis of atovaquone efficacy using *T. gondii* expressing GFP 57
6.7.2 In-vivo experiments 58
6.7.2.1 Pharmacokinetics of atovaquone compounds in mice 58
6.7.2.2 Infection with *T. gondii* 58
6.7.2.3 Murine model of acute toxoplasmosis 58
6.7.2.4 Murine model of reactivated toxoplasmosis 59
6.7.2.4.1 Oral treatment with atovaquone compounds 60
6.7.2.5 Histology 61
6.7.2.5.1 Hematoxylin and eosin staining 61
6.7.2.5.2 Peroxidase antiperoxidase staining 61
6.7.2.6 Polymerase chain reaction (PCR) 62
6.7.2.6.1 DNA extraction 62
6.7.2.6.2 Quantitative LightCycler PCR 62
6.7.2.7 Statistical analysis 63
7 Results 64
7.1 Characterization of atovaquone preparations 64
7.2 Cytotoxicity of atovaquone compounds 66
7.3 Transport of atovaquone across the intestinal barrier in a mono-culture model 68
7.4 Transport of atovaquone across the BBB in a mono-culture model 70

7.5 Transport of atovaquone across the BBB in a co-culture model 71

7.6 Antiparasitic effect of atovaquone in-vitro 73

7.7 Pharmacokinetics of ANSs in mice 75

7.8 Therapeutic efficacy of atovaquone in a murine model of acute toxoplasmosis... 76

7.8.1 Therapeutic efficacy of atovaquone preparations at 50 mg/kg body weight 76

7.8.1.1 Atovaquone concentrations in serum and organs 76

7.8.1.2 Antiparasitic effect of atovaquone 78

7.8.2 Therapeutic efficacy of atovaquone preparations at 100 mg/kg body weight 84

7.8.2.1 Atovaquone concentrations in serum and organs 84

7.8.2.2 Antiparasitic effect of atovaquone 86

7.9 Therapeutic efficacy of atovaquone in a murine model of reactivated toxoplasmosis 92

7.9.1 Therapeutic efficacy of atovaquone preparations at 50 mg/kg body weight 92

7.9.1.1 Atovaquone concentrations in serum and organs 92

7.9.1.2 Antiparasitic effect of atovaquone 94

7.9.2 Therapeutic efficacy of atovaquone preparations at 100 mg/kg body weight 100

7.9.2.1 Atovaquone concentrations in serum and organs 100

7.9.2.2 Antiparasitic effect of atovaquone 102

8 Discussion 111

9 Summary 123

10 References 125

11 Addition 134

1 List of figures

Fig. 1: Life cycle of *T. gondii* and clinical manifestations of toxoplasmosis 19

Fig. 2: Murine oocysts in cat feces (A), tachyzoites in cell culture (B), and a tissue cyst containing bradyzoites (C) in the brain of a *T. gondii* infected mouse 20

Fig. 3: Histologic changes in brains of mice with reactivated TE.....22

Fig. 4: Chemical structure of atovaquone 25

Fig. 5: Schematic sections of a Peyer's patch and overlying FAE (A); M cell transport of particulate delivery vehicles is depicted in (B).....28

Fig. 6. Multiple pathways for intestinal absorption of compounds 29

Fig. 7: Schematic representation of the BBB.....31

Fig. 8: Schematic diagram of cells and transport mechanism operative at the BBB.....33

Fig. 9: Chemical structure of polysorbates 80.....38

Fig. 10: Schematic graph of a pluronic block copolymer molecule (A) and a micelle with a solubilized drug (B) 40

Fig. 11: Chemical structure of sodium dodecyl sulphate (SDS) 42

Fig. 12: Schematic design of atovaquone nanosuspensions for oral use.....51

Fig. 13: Schematic view of the intestinal mono-culture barrier model 54

Fig. 14: Schematic view of the BBB in-vitro co-culture model using freshly isolated rat PRBECs and rat astrocytes.....56

Fig. 15: Murine model of acute toxoplasmosis in C57BL/6 mice.....59

Fig. 16: Murine model of reactivated toxoplasmosis in IRF-8$^{-/-}$ mice 60

Fig. 17: Light microscopy of ANSs and micronized suspension (Wellvone®) 66

Fig. 18: Viability of cell lines after 20h incubation with Wellvone® and ANSs stabilized by P188 or SDS as determined by MTT.....67

Fig. 19: Percentages of atovaquone transported through a mono-culture model of the intestinal barrier.....69

Fig. 20: Percent passage of ANSs and Wellvone® through a mono-culture model of the BBB.....70

Fig. 21: Percentages of atovaquone transported through a co-culture model of the BBB 72

Fig. 22: Antiparasitic effects of ANSs and Wellvone® against *T. gondii* as determined by flow cytometry 74

Fig. 23: Atovaquone concentrations in serum of C57BL/6J mice after a single oral treatment with atovaquone compounds (ANS/P188, ANS/SDS and Wellvone®) measured by HPLC 75

Fig. 24: Atovaquone concentrations in serum (A), lungs (B), and livers (C) of infected C57BL/6J mice after oral treatment with atovaquone compounds at 50 mg/kg body weight measured by HPLC 77

Fig. 25: Numbers of inflammatory foci (H&E) in brains (A) and livers (B) of C57BL/6J mice orally infected with *T. gondii* and treated orally with atovaquone compounds at 50 mg/kg body weight 79

Fig. 26: Numbers of parasitophorous vacuoles and free parasite antigen as determined by immunoperoxidase staining in lungs (A), livers (B), and brains (C) of C57BL/6J mice orally infected with ME49 *T. gondii* and treated orally with atovaquone compounds at 50 mg/kg body weight 81

Fig. 27: *T. gondii* DNA load as determined by LightCycler-PCR in lungs (A) and brains (B) of C57BL/6J mice orally infected with 10 cysts ME49 *T. gondii* and treated orally with atovaquone compounds at 50 mg/kg body weight 83

Fig. 28: Atovaquone concentrations in serum (A), lungs (B), livers (C), and brains (D) of infected C57BL/6J mice after oral treatment with atovaquone compounds at 100 mg/kg body weight measured by HPLC 85

Fig. 29: Inflammatory foci (H&E) in brains (A) and livers (B) of C57BL/6J mice orally infected with *T. gondii* and treated orally with atovaquone compounds at 100 mg/kg body weight 87

Fig. 30: Numbers of parasitophorous vacuoles and free parasite antigen as determined by immunoperoxidase staining in lungs (A), livers (B), and brains (C) of C57BL/6J mice orally infected with ME49 *T. gondii* and treated orally with atovaquone compounds at 100 mg/kg body weight 89

Fig. 31: *T. gondii* DNA load as determined by LightCycler-PCR in lungs (A) and brains (B) of C57BL/6J mice orally infected with 10 cysts ME49 *T. gondii* and treated orally with atovaquone compounds at 100 mg/kg body weight 91

Fig. 32: Atovaquone concentrations in serum (A), lungs (B), livers (C), and brains (D) of infected IRF-8$^{-/-}$ mice after oral treatment with atovaquone compounds at 50 mg/kg body weight measured by HPLC 93

Fig. 33: Inflammatory foci (H&E) in brains (A) and livers (B) of IRF-8$^{-/-}$ mice orally infected with ME49 *T. gondii* and treated orally with atovaquone compounds at 50 mg/kg body weight 95

Fig. 34: Numbers of parasitophorous vacuoles and free parasite antigen as determined by immunoperoxidase staining in lungs (A), livers (B), and brains (C) of IRF-8$^{-/-}$ mice orally infected with ME49 *T. gondii* and treated orally with atovaquone compounds at 50 mg/kg body weight..... 97

Fig. 35: Histologic changes in brains of IRF-8$^{-/-}$ mice with TE orally infected with ME49 *T. gondii* and treated orally with atovaquone compounds at 50 mg/kg..... 98

Fig. 36: *T. gondii* DNA load as determined by LightCycler-PCR in brains of IRF-8$^{-/-}$ mice orally infected with 10 cysts ME49 *T. gondii* and treated orally with atovaquone compounds at 50 mg/kg body weight..... 99

Fig. 37: Atovaquone concentrations in serum (A), lungs (B), livers (C), and brains (D) of infected IRF-8$^{-/-}$ mice after oral treatment with atovaquone compounds at 100 mg/kg body weight measured by HPLC 101

Fig. 38: Inflammatory foci (H&E) in brains (A) and livers (B) of IRF-8$^{-/-}$ mice orally infected with ME49 *T. gondii* and treated orally with atovaquone compounds at 100 mg/kg body weight 103

Fig. 39: Numbers of parasitophorous vacuoles and free parasite antigen as determined by immunoperoxidase staining in lungs (A), livers (B), and brains (C) of IRF-8$^{-/-}$ mice orally infected with ME49 *T. gondii* and treated orally with atovaquone compounds at 100 mg/kg body weight..... 105

Fig. 40: *T. gondii* DNA load as determined by LightCycler-PCR in brains of IRF-8$^{-/-}$ mice orally infected with 10 cysts ME49 *T. gondii* and treated orally with atovaquone compounds at 100 mg/kg body weight..... 106

Fig. 41: Atovaquone concentrations in serum (A) and brains (B) of infected IRF-8$^{-/-}$ mice after oral treatment with atovaquone compounds at 50 mg/kg body weight (ANSs and Wellvone®) and 100 mg/kg body weight (Wellvone®) measured by HPLC..... 108

Fig. 42: *T. gondii* DNA load as determined by LightCycler-PCR in brains of IRF-8$^{-/-}$ mice orally infected with 10 cysts ME49 *T. gondii* and treated orally with atovaquone compounds at 50 mg/kg body weight (ANSs and Wellvone©) and 100 mg/kg body weight (Wellvone®)..... 110

2 List of tables

Table 1: Products and plastic ware 44

Table 2: Apparatus 47

Table 3: Cell lines 49

Table 4: *T. gondii* strains 49

Table 5: Mice and rats 49

Table 6: Software 50

Table 7: LD and PCS diameters of ANSs compared to the micronized suspension (Wellvone®) 64

Table 8: Zeta potentials (ZP) of ANSs and the micronized suspension (Wellvone®) 65

3 List of abbreviations

ANSs	Atovaquone nanosuspensions
AZT	Azithromycin
BBB	Blood-brain barrier
BSA	Bovine serum albumin
bEnd3	Mouse brain microvascular endothelial cell line
bFGF	Basic Fibroblast Growth Factor
DMEM	Dulbecco's modified Eagle medium
DAB	Diaminobenzidine
FCS	Fetal calf serum
GFP	Green fluorescent protein
HPLC	High performance liquid chromatography
H&E	Hematoxylin and Eosin
HSA	Human serum albumin
HAART	Highly active antiretroviral therapy
J774A.1	Mouse macrophage-like cell line
LD	Laser diffractometry
LDL	Low-density lipoprotein
MODE-K	Mouse duodenal epithelial cell line
M cells	Microfold cells
NEAAs	Non-essential amino acids
P188	Poloxamer 188
PCR	Polymerase chain reaction
P/S	Penicillin/streptomycin

PDS	Plasma-derived bovine serum
PRBECs	Primary rat brain endothelial cells
Pgp	P-glycoprotein
PAP	Peroxidase anti-peroxidase
PBS	Phosphate-buffered saline
PI	Polydispersity index
PCS	Photon correlation spectroscopy
PBCA	Poly butyl cyanoacrylate
RBMECs	Rat brain microvascular endothelial cells
SDS	Sodium dodecyl sulphate
T. gondii	*Toxoplasma gondii*
TEER	Transendothelial electrical resistance
Tween® 80	Polysorbate 80
TJs	Tight junctions
TE	Toxoplasmic encephalitis
ZP	Zeta potential
Z-ave	Mean particle size

4 Introduction

4.1 Toxoplasmosis

4.1.1 Infection with *T. gondii*

Toxoplasma gondii is an obligate intracellular protozoan pathogen that was first described in 1908 by Nicolle and Manceaux. The species designation originated from the name of the North African rodent (*Ctenodactylus gondi*) from which this parasite was isolated. The genus name is derived from the Greek work “toxon”, meaning bow and referring to the crescent shape of the organism. Toxoplasma belongs to the phylum Apicomplexa, which consists of intracellular parasites that have a characteristically polarized cell structure and a complex cytoskeletal and organellar arrangement at their apical end (Dubey et al 1998). Sexual replication of the parasite occurs only in the intestine of the cat, resulting in production of oocysts (Fig. 1) whereas asexual parasites invade and proliferate in virtually any nucleated cell (Hu et al 2002a). During acute infection, several million oocysts are shed in the feces of cats for 7–21 days. After sporulation oocysts containing sporozoites (Fig. 2A) are infective when ingested by mammals (including man) and give rise to the tachyzoite stage (Montoya & Liesenfeld 2004). Tachyzoites (Fig. 2B) are crescentic or oval and are the rapidly multiplying stages of the parasite. They enter all nucleated cells by active penetration and form a cytoplasmic vacuole. After repeated replication, host cells are disrupted and tachyzoites are disseminated via the blood stream and infect many tissues, including the CNS, eye, skeletal and heart muscle, and placenta. Replication leads to cell death and rapid invasion of neighboring cells. Tachyzoites cause a strong inflammatory response and tissue destruction resulting in clinical manifestations of toxoplasmosis. Tachyzoites are transformed into bradyzoites due to the host immune response (Montoya & Liesenfeld 2004). Tissue cysts (Fig. 2C) contain hundreds and thousands of bradyzoites and form within host cells in the

brain as well as in skeletal and heart muscles where they persist for the life of the host. Bradyzoites can be released from cysts, transform back into tachyzoites, and cause reactivation of infection in immunocompromised patients (Montoya & Liesenfeld 2004). Cysts are infective stages for intermediate and definitive hosts. The majority of strains so far identified in Europe, North America and other parts of the world fall into one or another of just three distinct genotypes (known as types I, II and III) (Boothroyd & Grigg 2002). *Toxoplasma* isolates from human toxoplasmosis are mainly from type II. Type I and atypical genotypes are found mostly in severe cases of human toxoplasmosis and/or in extreme geographic locations (Darde 2004).

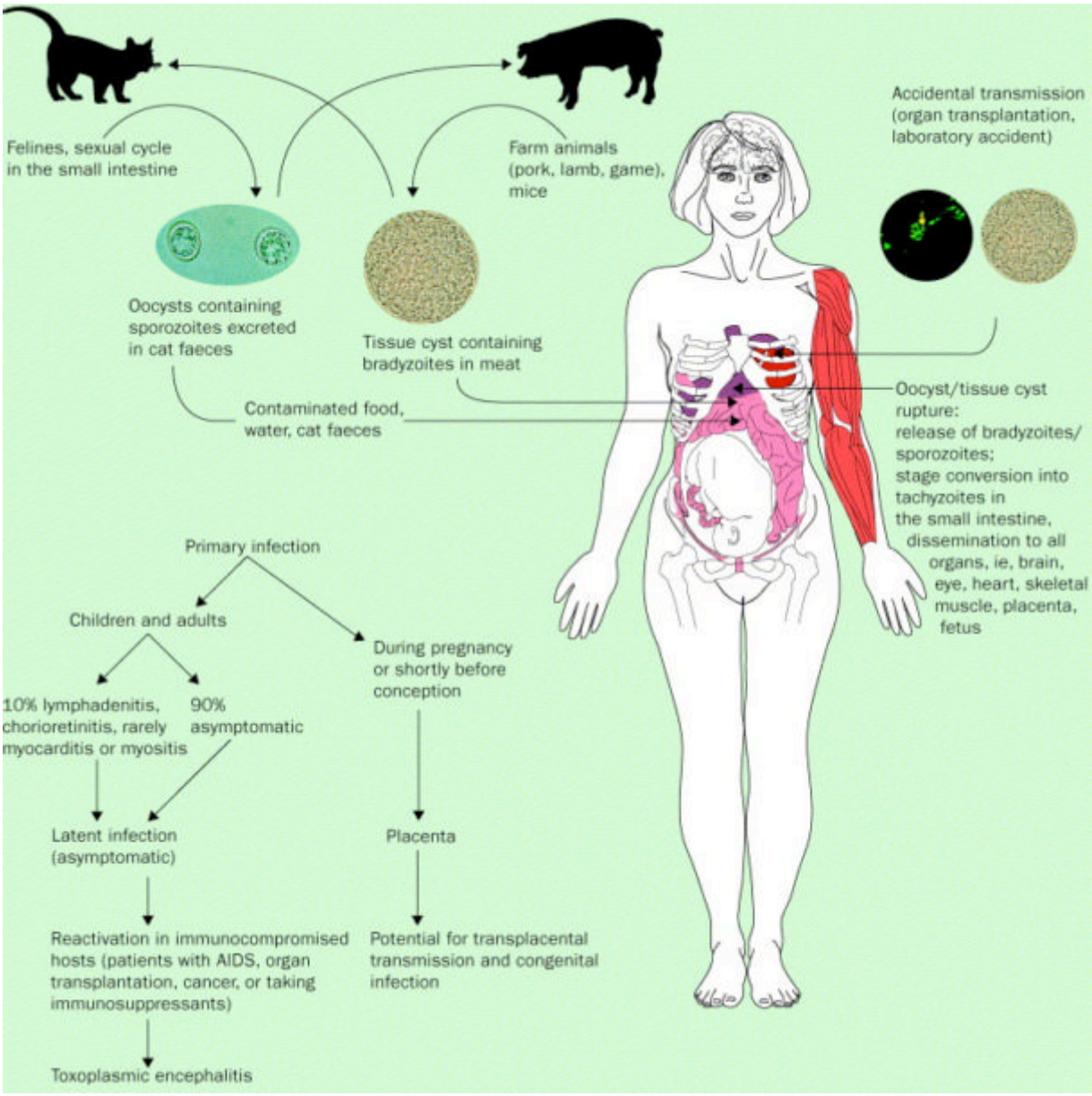

Fig. 1: Life cycle of *T. gondii* and clinical manifestations of toxoplasmosis (Montoya & Liesenfeld 2004)

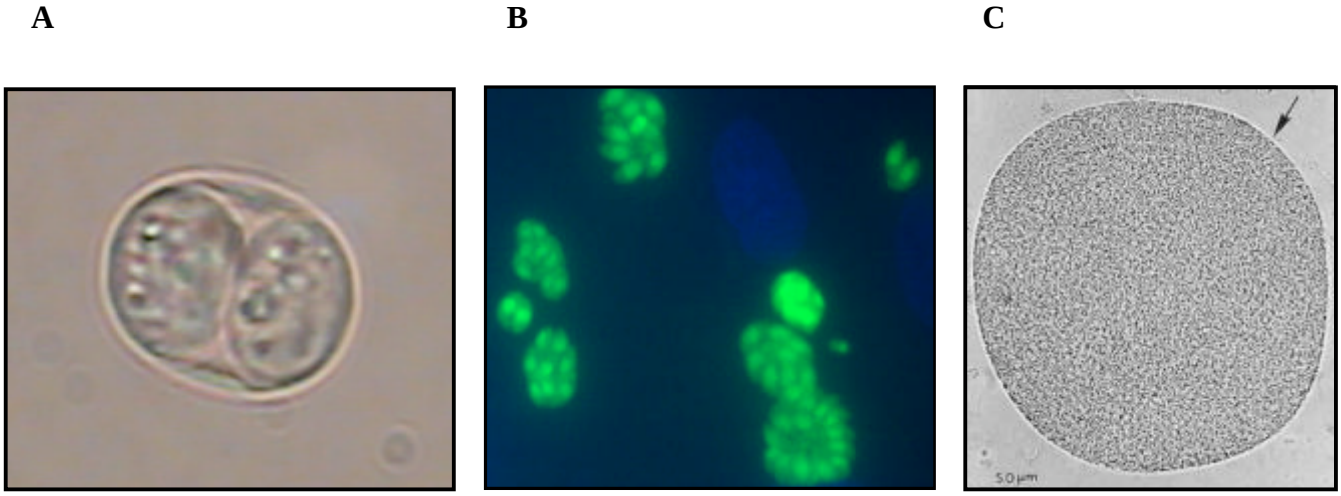

Fig. 2: Murine oocysts in cat feces (1000x magnification) (A), tachyzoites in cell culture (630x magnification) (B), and a tissue cyst containing bradyzoites (C) in the brain of a *T. gondii* infected mouse

4.1.2 Epidemiology

T. gondii is found worldwide in many species and in every population group of humans investigated. However, the definitive host is the cat. Approximately half a billion humans have antibodies to *T. gondii*. The incidence of infection in humans and animals varies in different parts of a country (Weiss & Dubey 2009). The cause for these variations is not yet known: environmental conditions, cultural habits, and animal species are among factors that may determine the degree of natural spread of *T. gondii*. Only a small proportion (<0.1 %) of people acquire infection congenitally. Immunocompetent mothers of congenitally infected children do not give birth to infected children in subsequent pregnancies. Ingestion of infected tissues and oocysts, and congenital infection are the main modes of transmission of *T. gondii* (Dubey 2008, Dubey & Jones 2008). Overall, <1% of humans and livestock acquire *T. gondii*

infection transplacentally. The proportion of the human population that becomes infected by ingesting *T. gondii*-infected meat, food or water contaminated with oocysts is unknown and currently there are no tests to distinguish infections acquired via tissue cysts in meat or via oocysts in contaminated environment (Dubey & Jones 2008). The low prevalence in young children and surge of infections in teen age suggests that transmission by meat is important in the USA (Dubey & Jones 2008).

4.1.3 Toxoplasmic encephalitis

Immunocompromised hosts with defective T-cell functions (up to 40% of patients with AIDS or organ transplant recipients) are at risk of reactivation of the infection by rupture of cysts (the latent form of infection). Toxoplasmic encephalitis (TE) is the most common clinical manifestation of reactivated disease in AIDS patients who do not receive highly active antiretroviral therapy (HAART) or antiparasitic prophylaxis. Reactivation of disease causes death of the patient if left untreated (Dunay et al 2004). Damage to the CNS by *T. gondii* is characterized by the presence of foci of necrosis in the brain parenchyma and meningeal inflammation in humans (Montoya & Liesenfeld 2004) and in mice (Fig. 3).

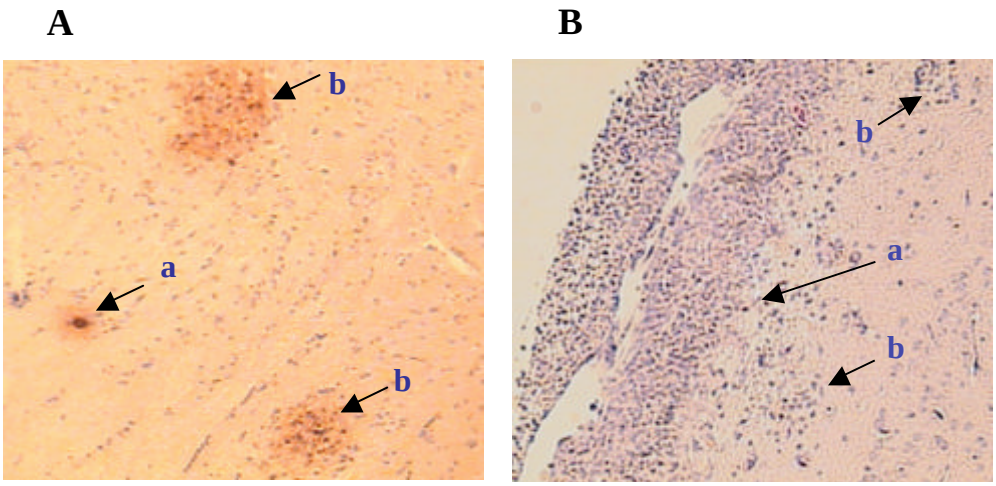

Fig. 3: Histologic changes in brains of mice with reactivated TE. (A) *T. gondii* cysts (a) or free parasites (b). (B) Meningeal inflammation due to immune cells (a) and inflammatory foci in brain parenchyma (b)

4.1.4 Therapy

Therapy of TE in immunocompromised patients consists of a phase of acute treatment followed by lifelong maintenance treatment to prevent reactivation. In AIDS patients on HAART with stable CD4 cell counts of >200 cells/µl for more than 6 months (indicating a recovery of the immune system), maintenance therapy can be withdrawn (Bertschy et al 2006). Acute primary standard therapy of choice for the treatment of TE is the combination of pyrimethamine plus sulfadiazine or clindamycin (Chirgwin et al 2002). Acute treatment with pyrimethamine plus sulfadiazine should be followed by lifelong maintenance therapy (secondary prophylaxis) with the same drugs in lower dosages (Montoya & Liesenfeld 2004) in patients not on HAART. Alternative treatment options including AZT, clarithromycin, dapsone, and trimethoprim/sulfamethoxazole are of lower efficacy and less well studied (Fung & Kirschenbaum 1996).

4.1.4.1 Pyrimethamine

Pyrimethamine belongs to the diaminopyrimidines group of drugs. The antiparasitic effect is due to its affinity to the parasite's dihydrofolate reductase enzyme (DHFR) and, to a lesser extent, for the corresponding human DHFR (Schmidt et al 2005). For the maintenance therapy of TE, pyrimethamine (25 to 50 mg orally daily) in combination with sulfadiazine (500 to 1000 mg orally four times daily) is the drug regimen of choice; this recommendation is based on efficacy and clinical benefit seen in randomized clinical trials (A1 strength of recommendation by the Centers for Disease Control and Prevention, the National Institutes of Health, and the Infectious Diseases Society of America) (Kaplan et al 2009). However, pyrimethamine therapy may cause severe side effects including hematologic toxicity (Kaplan et al 2009). To reduce hematologic toxicity, folinic acid (Leucovorin®) is administered in combination with pyrimethamine (Frenkel 1957, Kaplan et al 2009, Myatt et al 1953).

4.1.4.2 Sulfadiazine

Sulfadiazine belongs to the sulfonamide group of drugs. Their antiparasitic activity is related to the inhibition of the parasites enzyme dihydropteroate synthase (DHPS), and this, in turn, prevents the appropriate use of para-aminobenzoic acid for the synthesis of folic acid (Schmidt et al 2005). In combination with pyrimethamine it is the drug of choice for the acute and maintenance therapy of TE (1,000 to 2,000 mg administered orally four times a day for 6 to 8 weeks for the acute therapy, followed by 500 to 1000 mg administered orally four times a day for the maintenance therapy) (Jordan et al 2004, Kaplan et al 2009, Masur et al 2002). Sulfadiazine causes severe allergic side effects, mainly rash, in 5-15% of patients; discontinuation of this regimen results in up to 40% of patients (Kaplan et al 2009, Porter & Sande 1992).

4.1.4.3 Clindamycin

Clindamycin (7-chloro-lincomycin) is a semisynthetic derivative of lincomycin. It inhibits protein synthesis in prokaryotic ribosomes and is thought to act on *T. gondii* prokaryote-type organelle called plastid (Fitzhugh 1998, Pfefferkorn et al 1992, Weiss & Kim 2007). It has remarkable but delayed in-vitro anti-*T. gondii* activity, achieved at low drug concentrations (Pfefferkorn et al 1992). It is used as an alternative acute and maintenance therapy to TE (300 to 450 mg orally every 6 to 8 h) (Kaplan et al 2009, Masur et al 2002) in combination with pyrimethamine (BI strength of recommendation). This combination is associated with severe side effects, mainly rash, and diarrhea caused by overgrowth of toxinogenic strains of *Clostridium difficile* (antibiotic-induced diarrhea). Alternatively, the combination with atovaquone (750 mg orally every 6 to 12 h) with or without pyrimethamine may be used; the evidence for the efficacy of these alternative treatments is based on clinical experience, descriptive studies, or reports of consulting committees (CIII strength of recommendation) and are therefore insufficient to support recommendation (Kaplan et al 2009, Masur et al 2002).

4.1.4.4 Atovaquone

Atovaquone (566C80), a hydroxy-1,4-naphthoquinone (Fig. 4), is a structural analog of protozoan ubiquinone, a mitochondrial protein involved in electron transport (Baggish & Hill 2002). The commercial preparation of atovaquone is a yellow crystalline solid in a citrus-flavored liquid suspension (750 mg atovaquone/5 ml of suspension [Wellvone®]; GlaxoSmithKline). Atovaquone was first released in 1992 as a tablet but this formulation was replaced by a suspension because of poor and unreliable bioavailability (Rolan et al 1994). Atovaquone is highly lipophilic with a low aqueous solubility. It is 99.9% bound to plasma

protein. Bioavailability is greater when administered with food than in the fasting state. Average absolute bioavailability of a 750 mg single dose of atovaquone suspension administered with food is 47% (compared to 23% for Wellvone® tablets). Undesirable effects of atovaquone may be -in rare cases- nausea and skin rash, it may also increase liver enzymes level. Atovaquone is used in combination with proguanil (Malarone TM; GlaxoSmithKline) as a safe and reliable treatment of malaria (Kuhn et al 2005). Atovaquone at ng/ml concentration has a high level of activity against *T. gondii* tachyzoites in-vitro (Araujo et al 1991, Romand et al 1993). Atovaquone is a well-tolerated drug that appears to be an effective alternative for patients with toxoplasmosis who are intolerant of standard therapies (Chirgwin et al 2002, Katlama et al 1996, Kovacs 1992, Torres et al 1997).

However, neither atovaquone nor any of the drugs investigated so far achieves complete killing of bradyzoites and clearance of all cysts. This effect would be desirable to prevent reactivation of infection in immunocompromised patients. Therefore, new drugs or improved delivery systems for existing drugs are urgently needed.

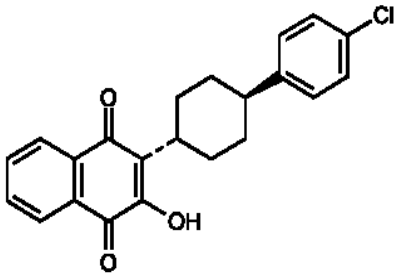

Fig. 4: Chemical structure of atovaquone

4.2 Biological barriers to drug delivery

Drug molecules encounter several membrane barriers in living systems. They include the gastrointestinal and the blood brain barriers (Kerns & Li 2008). Thus, these barriers have to be taken into account when designing drugs with improved absorption characteristics (Wang et al 2005).

4.2.1 The gastrointestinal barrier

4.2.1.1 Structure and function of the gastrointestinal barrier

Different types of cells and structures compose the intestinal epithelium. Epithelium of villi is mainly constituted of enterocytes and goblet cells (des Rieux et al 2006). Enterocytes control the passage of macromolecules and pathogens, and, at the same time, allow the digestive absorption of dietary nutrients. Goblet cells secrete the mucus gel layer, a viscous fluid composed primarily of highly glycosylated proteins (mucins) suspended in a solution of electrolytes. Dispersed through the intestinal mucosa, intraepithelial and lamina propria lymphoid cells as well as lymphoid cells in organized lymphoid structures called Peyer's patches and cryptopatches represent the mucosa-associated lymphoid system. The organized mucosa-associated lymphoid system (O-MALT) is of utmost important, mainly due to the presence of cells with a microfold (M) surface (des Rieux et al 2006). These M cells are located scattered within the epithelium overlaying the Peyer's patches called follicle-associated epithelium (FAE) (Fig. 5).

M cells deliver foreign material from the lumen to the underlying organized MALT to induce immune responses (des Rieux et al 2006). M cells are specialized for antigen sampling, but they are also exploited as a route of host invasion by many pathogens (Gebert et al 1996, Kraehenbuhl & Neutra 2000). Furthermore, M cells represent a potential portal for oral

delivery of peptides and proteins and for mucosal vaccination, since they possess a high transcytotic capacity and are able to transport a broad range of materials, including nanoparticles (Clark et al 2000, Frey & Neutra 1997). Uptake of particles, microorganisms and macromolecules by M cells occurs through adsorptive endocytosis by way of clathrin-coated pits and vesicles, fluid phase endocytosis, and phagocytosis (Buda et al 2005). In addition, M cells, compared with normal epithelial cells have reduced levels of membrane hydrolase activity, which can influence the uptake of protein-containing or protein-decorated nanoparticles (des Rieux et al 2006). The relatively sparse nature of the glycocalyx facilitates the adherence of both microorganisms and inert particles to their surfaces (Florence 2005). Although less numerous than enterocytes, M cells present enhanced transcytosis abilities which rendered them interesting targets for oral drug delivery application.

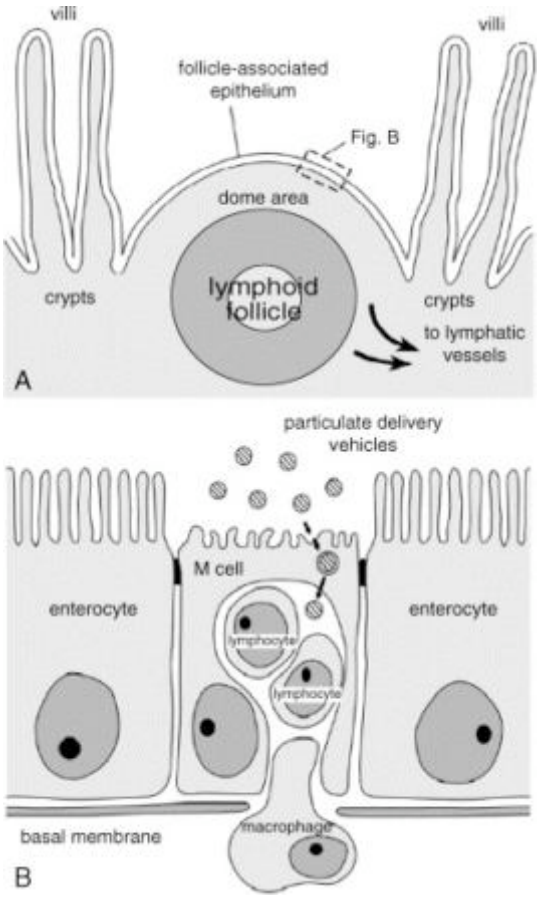

Fig. 5: Schematic sections of a Peyer's patch and overlying FAE (A); M cell transport of particulate delivery vehicles is depicted in (B) (des Rieux et al 2006)

4.2.1.2 Transport at the gastrointestinal barrier

Oral drug delivery is the route of choice for drug administration because of its non-invasive nature. It avoids pain and discomfort associated with injections as well as eliminating contaminations. Drug absorption across the intestinal membrane is a complex multi-pathway process as shown in Fig. 6 (Balimane et al 2006). Passive absorption occurs most commonly through the cell membrane of enterocytes (transcellular route) or via the tight junctions

between the enterocytes (paracellular route). Carrier-mediated absorption occurs via an active (or secondary active) process or by facilitated diffusion. Various efflux transporters, such as Pgp, breast cancer resistance protein (BCRP), and multidrug resistance protein 2 (MRP-2) are functional possibly limiting absorption. Intestinal enzymes could be involved in metabolizing drugs to alternate moieties for absorption. Finally, receptor-mediated endocytosis may also play a role.

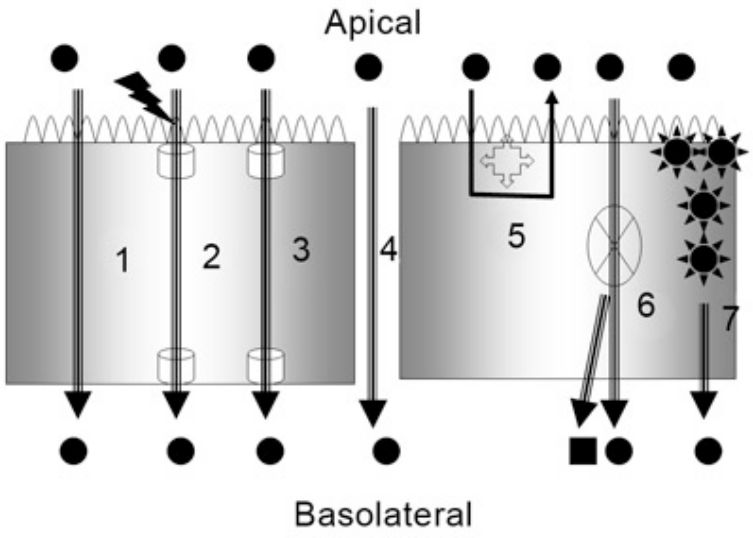

Fig. 6. Multiple pathways for intestinal absorption of compounds: (1) passive, transcellular; (2) active or secondary active; (3) facilitated diffusion; (4) passive, paracellular; (5) absorption limited by Pgp and/or other efflux transporters; (6) intestinal first-pass metabolism followed by absorption of parent and metabolite; and (7) receptor-mediated transport (Balimane et al 2006)

4.2.2 The blood-brain barrier

4.2.2.1 Structure and function of the BBB

Existence of the BBB was already observed in the late 1800s, when immunologist Paul Ehrlich found that intravenously administered dyes failed to stain certain regions of the brain, whereas other body tissues were stained (Ribatti et al 2006). Ehrlich thought the dyes did not have a staining affinity for the brain, but his student, Edwin Goldman, showed that the dyes could stain brain tissues but could not cross a barrier into the brain. The BBB is a diffusion barrier, which impedes influx of most compounds from blood to brain. Three cellular elements of the brain microvasculature compose the BBB: endothelial cells, astrocytes, and pericytes (Fig. 7). Tight junctions (Tj), present between cerebral endothelial cells, form a diffusion barrier, which selectively excludes most blood-borne substances from entering the brain. Astrocytic end-feet tightly sheathe the vessel wall and appear to be critical for the induction and maintenance of the TJ-barrier (Ballabh et al 2004). The TJ consists of three integral membrane proteins, namely, claudin, occludin, junction adhesion molecules, and cytoplasmic accessory proteins including zonulae occludentes, cingulin, and others (Ballabh et al 2004). The electrical resistance across the endothelium is extremely high, i.e 1,500 - 2,000 $\Omega \times cm^2$, and the passage of molecules through the paracellular pathway is greatly restricted. In addition, brain capillaries are covered by a continuous basal membrane enclosing pericytes. The outer surface of the basal membrane is contacted by astrocytic or glial foot processes. The function of these cells has not yet been completely elucidated, but secretion of soluble growth factor(s) by astrocytes may play a role in the establishment and maintenance of the brain endothelial cell phenotype (Fricker & Miller 2004). The BBB is reinforced by a high concentration of Pgp, an active-drug-efflux-transporter protein in the luminal membranes of the cerebral capillary endothelium. This efflux transporter actively

removes a broad range of drug molecules from the endothelial cell cytoplasm before they cross into the brain parenchyma (Misra et al 2003).

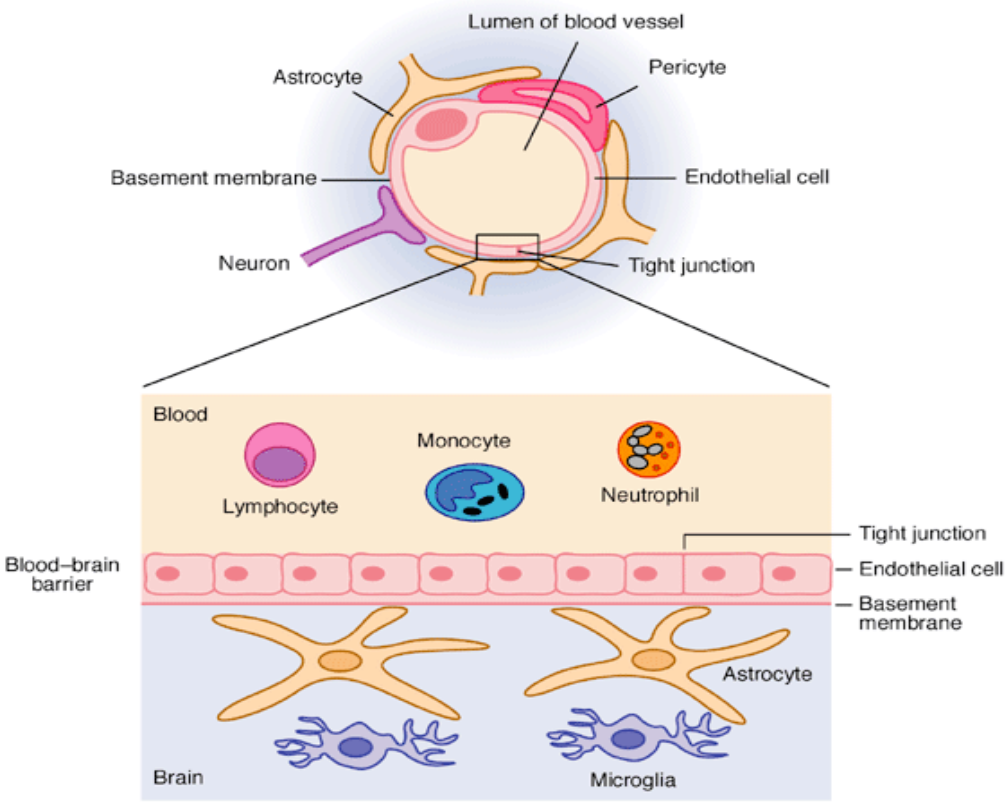

Fig. 7: Schematic representation of the BBB consisting of tight junctions between endothelial cells of the blood vessels in the brain thereby protecting it from harmful substances (Francis et al 2003)

4.2.2.2 Transport at the BBB

Normally, the tight junctions severely restrict penetration of water-soluble compounds, including polar drugs. However, the large surface area of the lipid membranes of the endothelium offers an effective diffusive route for lipid-soluble agents. The endothelium contains transport proteins (carriers) for glucose, amino acids, purine bases, nucleosides, choline and other substances. Some transporters are energy-dependent (e.g., Pgp) and act as efflux transporters. Certain proteins, such as insulin and transferrin, are taken up by specific receptor-mediated endocytosis and transcytosis and native plasma proteins such as albumin are poorly transported, but cationization can increase their uptake by adsorptive-mediated endocytosis and transcytosis. Fig. 8 shows pathways for drug delivery across the brain endothelium; most CNS drugs enter via the transcellular lipophilic pathway route (Abbott et al 2006).

The various strategies to increase drug delivery into the brain include (i) chemical delivery systems, such as lipid-mediated transport, (ii) biological delivery systems, in which pharmaceuticals are re-engineered to cross the BBB via specific endogenous transporters localized within the brain capillary endothelium, (iii) disruption of the BBB, e.g. by modification of the Tj which causes a controlled and transient increase in the permeability of brain capillaries. The use of molecular Trojan horses such as peptidomimetic monoclonal antibodies can lead to transport of large molecules across the BBB and particulate drug carrier systems (Patel et al 2009) exist. In addition, various drug delivery systems (e.g. liposomes, microspheres, nanoparticles, nanogels and bionanocapsules) have been used to enhance drug delivery to the brain (Patel et al 2009).

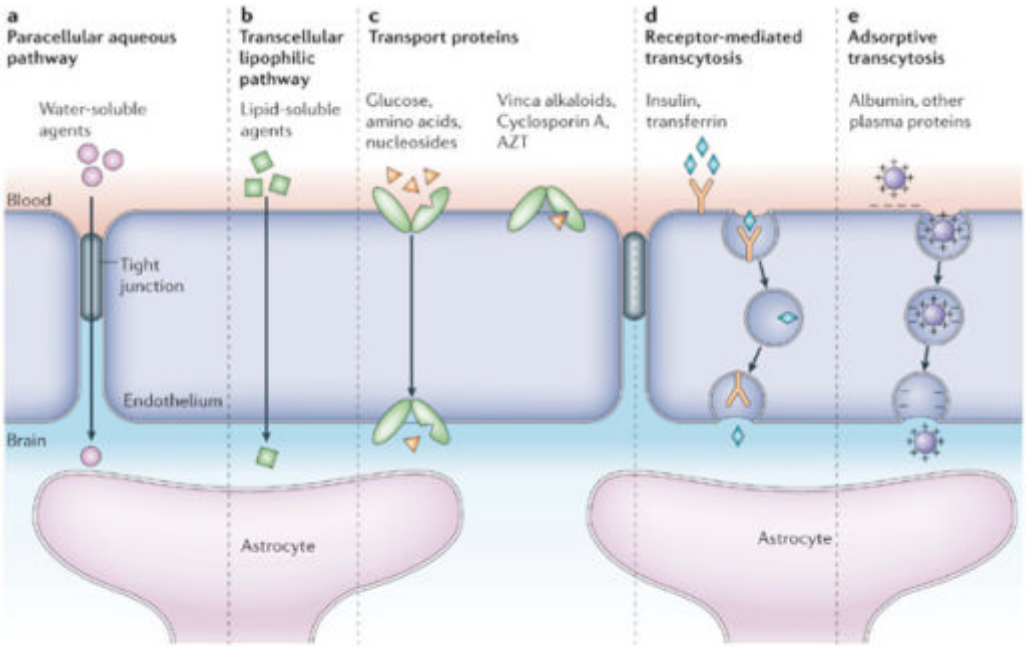

Fig. 8: Schematic diagram of cells and transport mechanism operative at the BBB (Abbott et al 2006)

4.3 Drug targeting

Drug delivery is an interdisciplinary and independent field of research gaining the attention of pharmaceutical industry and medical doctors (Orive et al 2003). A targeted and safe drug delivery could improve the performance of some classical therapeutics already on the market and, moreover, will have implications for the development and success of new therapeutic strategies, such as peptide and protein delivery. Many innovative technologies for effective drug delivery have been developed, including implants, nanotechnology, cell and peptide encapsulation, microfabrication, chemical modification and others (Orive et al 2003). Many pharmacological properties of conventional ("free") drugs can be improved through the use of

drug delivery systems, which include particulate carriers, composed primarily of lipids and/or polymers, and their associated therapeutics, for e.g., liposomes, micelles, polymeric nanoparticles, and dendrimers, which mask the unfavorable biopharmaceutical properties of the molecule and replaces them with the properties of the materials used for construction of the nano-delivery system (Devalapally et al 2007). Another approach involves the covalent conjugation of molecules with carrier and targeting moieties (e.g. polymer-drug conjugates, antibody-drug conjugates, etc.) that override the drug's poor biopharmaceutical properties and improve the pharmacokinetics and bio-distribution (Devalapally et al 2007). This approach was used for site-specific or targeted delivery to alter the pharmacokinetics of the drug by increasing the plasma elimination half-life, prevents degradation or metabolism of the drug in the systemic circulation, and may alter the organ and subcellular distribution of the drug. Advances in nanomedicines are also applied for site-specific drug and gene delivery strategies, especially for the treatment of cancer and other life threatening diseases (Duncan 2003, LaVan et al 2002).

4.3.1 Nanoparticles

The use of materials in nanoscale provides freedom to modify fundamental properties such as solubility, diffusivity, blood circulation half-life, drug release characteristics, and immunogenicity (Zhang et al 2008). In the last two decades, a number of nanoparticle-based therapeutic and diagnostic agents have been developed for the treatment of cancer, diabetes, pain, asthma, and allergy (Brannon-Peppas & Blanchette 2004, Kawasaki & Player 2005). These nanoscale agents may provide more effective and/or more convenient routes of administration, lower therapeutic toxicity, extend the product life cycle, and ultimately reduce health-care costs. As therapeutic delivery systems, nanoparticles allow targeted delivery and

controlled release (Zhang et al 2008). Nanoparticle-based drugs can be advantageous since they may improve the solubility of poorly water-soluble drugs, prolong the drug's systemic circulation, release drugs at a sustained rate, and thus lower the frequency of administration, deliver drugs in a target manner to minimize systemic side effects, and deliver two or more drugs simultaneously for combination therapy to generate a synergistic effect and suppress drug resistance (Emerich & Thanos 2007, Groneberg et al 2006).

4.3.1.1 Nanoparticles for oral drug delivery

Delivery of pharmaceuticals via the oral route remains problematic. Instability in the gastrointestinal environment and poor permeability across the intestinal epithelial cell barrier contribute to poor oral bioavailability for many compounds (Lambkin & Pinilla 2002). Current targeting strategies to overcome these issues are focused on three-part systems in which the drug is loaded into a protective particulate carrier coated with target-specific ligand which mediate site-specific delivery of the drug-carrier complex. Protection from gastrointestinal degradative processes combined with site-specific delivery to absorptive regions of the intestinal tract is purported to yield high local concentrations of the drug of choice in close proximity with the epithelial cell layer and hence, transport across the intestinal barrier through a variety of mechanisms (Lambkin & Pinilla 2002).

Nanoparticles are of special interest for intestinal delivery from the pharmaceutical point of view. First, they are more stable in the gastrointestinal tract than other colloidal carriers such as liposomes. They can protect encapsulated drugs from gastrointestinal environment. Second, the use of various polymeric materials enables the modulation of physicochemical characteristics (e.g. hydrophobicity, electrical charge), drug release properties (e.g. delayed, prolonged, triggered), and biological behavior (e.g. targeting, bioadhesion, improved cellular

uptake) of nanoparticles (Galindo-Rodriguez et al 2005). Finally, the particle surface can be modified by adsorption or chemical grafting of molecules such as poly ethylene glycol (PEG), poloxamers, and bioactive molecules (lectins, invasins, etc). Moreover, their submicron size and their large specific surface area favor their absorption compared to larger carriers.

4.3.1.2 Nanoparticles for brain drug delivery

Polymeric nanoparticles have attracted increasing interest as carriers for transporting therapeutic agents across the BBB since they are superior to liposomes and micelles in terms of prolonged bioavailability, high loading efficiency, low burst effect, and tunable surface chemistry (Gil et al 2009). Brain targeted polymeric nanoparticles have been found to increase the therapeutic efficacy and reduce the toxicity for a large number of drugs. By coating nanoparticles with surfactants, higher concentrations of drugs can be delivered to the brain (Chopra et al 2008, Kreuter 2001). The mechanism of nanoparticles-mediated transport of drugs across the BBB at present is not fully elucidated. The most likely mechanism is endocytosis by the endothelial cells lining the brain blood capillaries (Kreuter 2001). Other processes such as Tj modulation, inhibition of Pgp, passive diffusion (by large concentration gradient), brain endothelial uptake by phagocytosis also may occur (Kreuter 2001, Soppimath et al 2001). Moreover, these mechanisms may run in parallel or may be cooperative thus enabling drug delivery into the brain (Kreuter 2001). Drugs that have been successfully delivered into the brain using nanoparticles include the hexapeptide dalargin (Kreuter et al 1995), the dipeptide kytorphin (Schroeder et al 1998), loperamide (Alyautdin et al 1997), tubocurarine (Alyautdin et al 1998), rivastigmine (Wilson et al 2008a), and tacrine (Wilson et al 2008b). Recently, nanoparticles made of PBCA or poly(lactic-co-glycolic acid) (PLGA) coated with polysorbate 80 or P188 transported doxorubicin across the BBB for the treatment

of cerebral cancer (Kreuter & Gelperina 2008). Furthermore loperamide-loaded HSA nanoparticles with covalently bound transferrin or transferring-receptor monoclonal antibodies (OX26 or R17217) induced significant anti-nociceptive effects in the tail-flick test in mice after intravenous injection, demonstrating that transferrin or antibodies against the transferring receptor covalently coupled to HSA nanoparticles are able to transport loperamide and possibly other drugs across the BBB (Ulbrich et al 2009).

4.3.2 Surfactants (stabilizers)

As the total surface area of the particles in a nanosuspension is typically orders of magnitude larger compared to a conventional suspension, large quantities of additives may be necessary to ensure adequate stabilization. Therefore, whatever method used for the production of nanosuspensions, a careful evaluation of the type and concentration of the stabilizer used is key to the successful production of nanosuspensions (Van Eerdenbrugh et al 2009).

4.3.2.1 Tween® 80 (polysorbate 80)

Polysorbate 80 is an amphipathic, nonionic surfactant composed of fatty acid esters of polyoxyethylene sorbitan (polyoxyethylene sorbitan monooleate) (Fig. 9) (Ha et al 2002). It is commonly used for applications in the chemical, cosmetic, food, environmental, and pharmaceutical industries (Wuelfing et al 2006). It is the most common polysorbate currently used in formulation of protein biopharmaceuticals (Nema et al 1997). Many authors have shown that therapeutic agents can be transported across the BBB by binding them to PBCA nanoparticles coated with Tween® 80 (e.g. rivastigmine used for the treatment of Alzheimer's disease) (Wilson et al 2008a) and other drugs (dalargin, kytorphin, loperamide, and tubocurarine as mentioned above). The mechanism of entry may involve adsorption of

apolipoprotein E from plasma onto their surface (Kreuter 2001). The particles may thereby mimic LDL particles and interact with the LDL receptor leading to their uptake by endothelial cells. Recently it has been shown that nerve growth factor adsorbed on PBCA nanoparticles coated with Tween® 80 was effective in the treatment of Morbus Parkinson in a murine model (Kurakhmaeva et al 2008).

Polysorbate 80 was shown previously to be an efficient stabilizer for nanosuspensions; polysorbate 80 is well tolerated, safe, and well accepted for i.v. injection (Jacobs & Mueller 2002, Keck 2006).

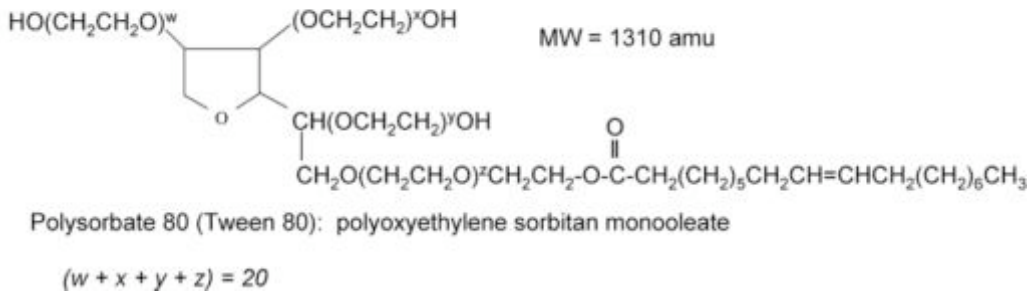

Fig. 9: Chemical structure of polysorbates 80. w, x, y, z refers to the total number of oxyethylene subunits on surfactant molecule (Kerwin 2008)

4.3.2.2 Poloxamers

Poloxamers or pluronics comprize triblock copolymers (Wu & Lee 2009). They consist of a single chain of hydrophobic polyoxypropylene sandwiched between two hydrophilic chains of polyoxyethylene (PEO-PPO-PEO) (Lundsted 1976, Schmolka 1991, Wu & Lee 2009) (Fig. 10). They act as stabilizing surfactants and show almost no toxicity. These surface modifiers can be used to reduce uptake by the mononuclear phagocytic system. Studies on bovine brain endothelial cells have demonstrated that poloxamer 235 (Pluronic P85) single chains ('unimers') inhibited the Pgp efflux pump thus enhancing drug accumulation in these cells (Miller et al 1997). Several poloxamers are available for use in humans such as Lutrol® F 127 (Poloxamer 407). It is used as a thickening agent and gel former, as a co-emulsifier, and as a viscosity enhancer in creams and liquid emulsions. Lutrol® F 127 also stabilizes topically and orally administered suspensions and is used in toothpaste and mouthwashes. In recent years, poloxamers have been shown to increase the transport of a broad spectrum of drugs through the BBB by a variety of mechanisms including inhibition of Pgp and multidrug-resistance associated protein efflux systems on BBB (e.g. Poloxamer 235), adsorption of different apolipoproteins in plasma on the surface of poloxamer-coated nanoparticles (e.g. Poloxamer 184 and Poloxamer 188), and binding to specific ligands and monoclonal antibodies (e.g. Poloxamer 235) (Zhang & Fang 2008).

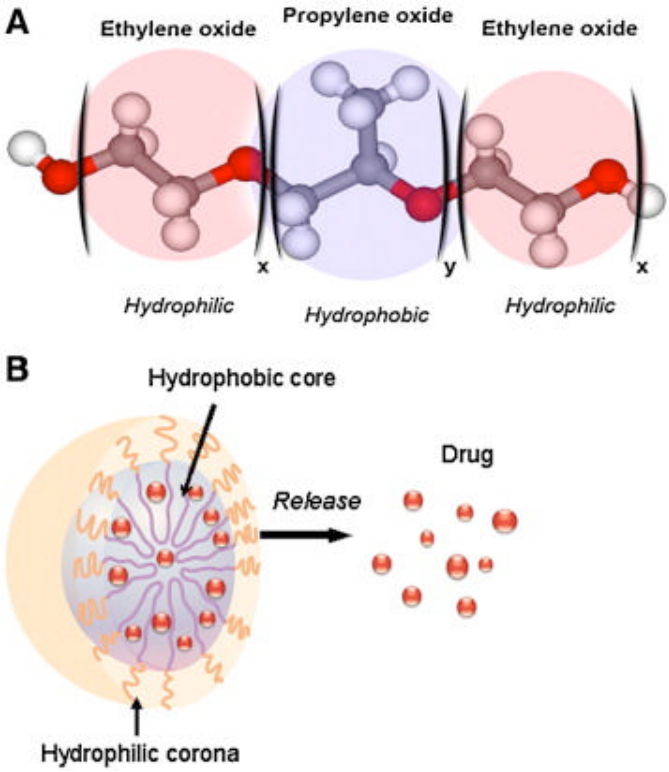

Fig. 10: Schematic graph of a pluronic block copolymer molecule (A) and a micelle with a solubilized drug (B) (Batrakova & Kabanov 2008)

4.3.2.2.1 Poloxamer 188

P188 (Lutrol® F 68, Pluronic® F-68, Flocor™, MW 8400 g/mol) is used in humans as a dispersing and wetting agent for oral, topical, and parenteral preparations (Wu et al 2005). This copolymer has been widely tested in numerous experimental and clinical situations (Adams-Graves et al 1997, Ballas et al 2004, Maynard et al 1998, Moghimi & Murray 1996, Orringer et al 2001, Palmer et al 1998, Toth et al 1997). For example, intravenous injection or infusion of P188 has been shown to be of significant benefit in the management of sickle cell

disease as well as in stroke and myocardial infarction, in which poloxamer accelerates thrombolysis, reduces re-occlusion and ameliorates re-perfusion injury (Moghimi et al 2004). P188 is well known as an efficient stabilizer and proved sufficient for efficient steric stabilization of nanocrystals (Keck 2006, Mueller 1991). It is licensed for intravenous administration (RheothRx®, GlaxoSmithKline).

4.3.2.3 Sodium dodecyl sulphate (SDS)

SDS ($NaC_{12}H_{25}SO_4Na$, MW 288.38 g/mol) (Fig. 11) is one of the most widely used detergents and has many applications in industry and science. The molecule has a tail of 12 carbon atoms, attached to a sulfate group, giving the molecule the amphiphilic properties required of a detergent. It lowers surface tension of aqueous solutions and is used as fat emulsifier, wetting agent, detergent in cosmetics, pharmaceuticals, and toothpastes; it is also used in protein biochemistry (Bischoff et al 1998, Weber & Osborn 1969, Wu et al 2005, Yamamoto et al 2008). It is an excellent electrostatic stabilizer with high affinity to particle surfaces leading to high zeta potentials (Soukupová et al 2008). It is licensed as a stabilizer for oral dosage (Keck 2006), e.g. Janumet® tablets (Merck), and Rythmol® capsules (GlaxoSmithKline).

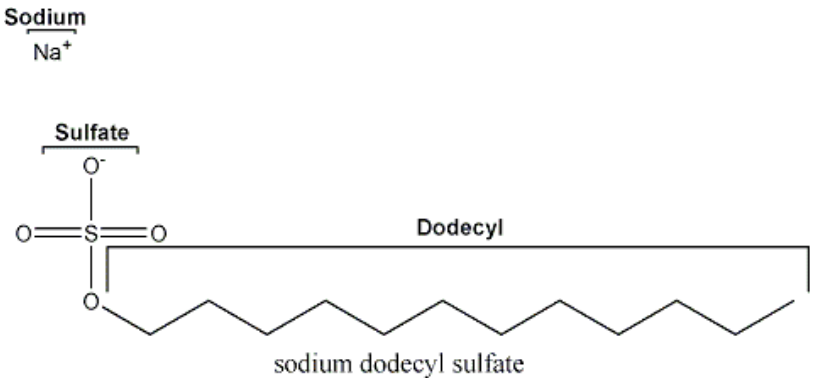

Fig. 11: Chemical structure of sodium dodecyl sulphate (SDS)

5 Aims of research

Since TE is a major cause of central nervous system morbidity and mortality in immunocompromised patients and standard therapy is associated with adverse effects, alternative treatment options are needed. Atovaquone is safe and highly effective against *T. gondii* in-vitro and may therefore be a suitable drug for the therapy of TE. However, the bioavailability of the present oral suspension (Wellvone®) is poor and little is known about the uptake into the brain. Therapeutic efficacy in patients with TE has not been shown convincingly. Since preparation of drug nanosuspensions coated with surfactants has been reported to enhance drug solubility and transport through intestinal and brain barriers, ANSs coated with surfactants may increase the capacity of atovaquone to cross barriers and thereby improve the therapeutic efficacy.

In the present study, the passage of host tissue barriers was therefore compared between ANSs coated with different surfactants and Wellvone® currently used in the treatment of patients with TE. In-vitro models of the BBB and intestinal barrier as well as murine models of acute and reactivated toxoplasmosis were applied. I specifically asked the following questions:

1. Do ANSs show increased passage through the intestinal barrier and BBB in comparison with the oral suspension Wellvone® in-vitro?
2. Does the coating of ANSs with surfactants including Tween® 80, P188 and SDS increase the oral bioavailability and brain uptake of atovaquone in-vivo?
3. Do ANSs coated with surfactants increase the therapeutic efficacy of atovaquone against murine acute and reactivated toxoplasmosis?

6 Material and methods

6.1 Chemicals and plastic ware

Table 1: Products and plastic ware

Products and plastic ware	Company	Location
12 well cell culture plates	Corning	Schiphol-Rijk, Netherlands
3 µm pore filters	Corning	Schiphol-Rijk, Netherlands
96 well plate	Nunc	Roskilde, Danmark
Acetonitrile	Merck	Darmstadt, Germany
Aerosol resistant tips	Molecular BioProducts	San Diego, California, USA
Atovaquone powder	GlaxoSmithKline	Munich, Germany
bFGF	Roche Applied Science	Mannheim, Germany
BSA	Sigma-Aldrich	Deisenhofen, Germany
Cannulae (26G, 22G)	BD Biosciences	Heidelberg, Germany
Cell scraper (23 cm)	Nunc	Wiesbaden, Germany
Collagen IV	Sigma-Aldrich	Deisenhofen, Germany
Collagenase	Sigma-Aldrich	Deisenhofen, Germany
Collagenase/Dispase	Sigma-Aldrich	Deisenhofen, Germany
Combitips	Eppendorf	Hamburg, Germany
DAB	Sigma-Aldrich	Steinheim, Germany
Disposable conical tubes	Nunc	Wiesbaden, Germany
DMEM	GIBCO	Grand Island, USA
DMSO	Sigma-Aldrich	Deisenhofen, Germany

Products and plastic ware	Company	Location
DNase l	Roche Applied Science	Mannheim, Germany
Eosin	Merck	Darmstadt, Germany
Eppendorf tubes (1.5 ml)	Eppendorf	Hamburg, Germany
Ethanol	Sigma-Aldrich	Deisenhofen, Germany
FACS tubes	BD Biosciences	Heidelberg, Germany
FCS	Biochrom	Berlin, Germany
Formaldehyde solution	Merck	Darmstadt, Germany
Gentamycin	Gibco/Invitrogen,	Grand Island, USA
Glycerol	Sigma-Aldrich	Deisenhofen, Germany
Halothan Eurim	Eurim Pharm	Piding, Germany
Hematoxylin	Merck	Darmstadt, Germany
Hexan	Merck	Darmstadt, Germany
Histology cassette	Simport	Beloeil, QC, Canada
Hydrogen peroxide (30%)	Merck	Darmstadt, Germany
Isoamyl alcohol	Merck	Darmstadt, Germany
Methanol	Sigma-Aldrich	Steinheim, Germany
Microscope slides (App.76 × 26 mm/3× 1 Inch)	R-Langenbrinck	Teningen, Germany
MTT	Sigma-Aldrich	Deisenhofen, Germany
NEAAs	Gibco/Invitrogen,	Grand Island, USA
PAP	Dako	Glostrup, Denmark
P/S	Biochrom	Berlin, Germany
Percoll™	Amersham Biosciences	Uppsala, Sweden

Products and plastic ware	Company	Location
Plasma-derived serum	First Link	West Midland, UK
Puromycin	Sigma-Aldrich	Deisenhofen, Germany
Reference pipets	Eppendorf	Hamburg, Germany
RPMI 1640 Medium	GIBCO	Grand Island, USA
SDS	Bio-rad	Munich, Germany
Serological pipets (1, 2,5, 10, 25 ml)	Falcon	Franklin Lakes, USA
Sulfadiazine	Sigma-Aldrich	Deisenhofen, Germany
Swine rabbit immunoglobulin	Dako	Glostrup, Denmark
Syringes (1, 5, 10 ml)	B.Braun	Melsungen, Germany
Thiomersal	Sigma-Aldrich	Deisenhofen, Germany
Tissue culture 50 ml flasks	Merck	Darmstadt, Germany
Trypanblue	Biochrom	Berlin, Germany
Trypsin-EDTA	Biochrom	Berlin, Germany
Tubes (15, 50 ml)	Sarstedt	Nümbrecht, Germany
Wellvone®	GlaxoSmithKline	Munich, Germany

6.2 Apparatus

Table 2: Apparatus

Apparatus	Company	Location
- 20^0C Freezer	Liebherr	Rostock, Germany
- 70^0C Freezer	Sanyo-Fisher Sales	Munich, Germany
Axiostar stereomicroscope	Zeiss	Oberkochen, Germany
Bio Photometer	Eppendorf	Hamburg, Germany
CO_2 incubator	Heraeus	Hanau, Germany
Coulter LS 230 analyser	Beckman-Coulter	Krefeld, Germany
Diavert stereomicroscope	Leitz	Stuttgart, Germany
Elvar stereomicroscope	Leitz	Stuttgart, Germany
FACSCalibur	BD Biosciences	Heidelberg, Germany
Haemocytometer	Assistent	Sonheim, Germany
HPLC Column (Spherisorb C1)	Waters	Eschborn, Germany
Integrator (model 3396III)	Hewlett Packard	Böblingen, Germany
Isocratic pump (model 510)	Waters	Eschborn, Germany
Laborfuge II	Heraeus	Hanau, Germany
Light microscope	Leitz	Wetzlar, Germany
LightCycler	Roche Applied Science	Mannheim, Germany
Lightcycler capillaries (20µl)	Roche Applied Science	Mannheim, Germany
Micron LAB 40 homogenizer	APV system	Unna, Germany
Microtom HM 355	Microm	Walldorf, Germany

Apparatus	Company	Location
Mortar	VWR	Darmstadt, Germany
PCS	Malvern Instruments	Malvern, UK
Precolumn (Xterra RP 18)	Waters	Eschborn, Germany
Sampler/Injector (Autosampler, Model 717)	Waters	Eschborn, Germany
Shaker	B.Braun	Melsungen, Germany
Shaker (KM-2 Akku)	Edmund Bühler	Tübingen, Germany
Tecan Spectra ELISA reader	Tecan	Crailsheim, Germany
Thermomixer	Eppendorf	Hamburg, Germany
Ultra turrax® T25 disperser	Janke and Kunkel	Staufen, Germany
Ultracentrifuge (L 5.65) (Ti 60 Rotor)	Heraeus	Hanau, Germany
Varifuge RF	Heraeus	Hanau, Germany
Water bath	GFL	Wunsdorf, Germany
Zitasizer 4	Malvern Instruments	Malvern, UK

6.3 Cell lines

Table 3: Cell lines

J774A.1	American Type Culture Collection, Manassas, VA, USA
MODE-K	Dr. Ulrich Steinhoff, Department of Immunology, Max Planck Institute for Infection Biology, Berlin, Germany
bEnd3	Dr. Kwang Sik Kim, Department of Molecular Microbiology and Immunology, Johns Hopkins University School of Medicine, Baltimore, Maryland, USA

6.4 *T. gondii* strains

Table 4: *T. gondii* strains

GFP-RH	Prof. Dominique Soldati, Department of Microbiology and Molecular Medicine, University of Geneva, Switzerland
ME49	Prof. J. Remington, Stanford University, USA

6.5 Animals

Table 5: Mice and rats

Wistar Rats	Forschungseinrichtung für Experimentelle Medizin (FEM), Charité, Berlin
NMRI Mice	Forschungseinrichtung für Experimentelle Medizin (FEM), Charité, Berlin
C57BL/6 Mice	Forschungseinrichtung für Experimentelle Medizin (FEM), Charité, Berlin
IRF-8$^{-/-}$ Mice	Forschungseinrichtung für Experimentelle Medizin (FEM), Charité, Berlin

6.6 Software

Table 6: Software

Acrobat Reader	Adobe System GmbH, Munich, Germany
Cellquest Pro	BD Biosciences, Heidelberg, Germany
Easy Measure (Version 1.0.30)	Inteq, London, UK
SQS 98 software	Perkin-Elmer, Überlingen, Germany
LightCycler Version 3.5	Roche Applied Science, Mannheim, Germany
Serion Evaluate	Virion, Rüschlikon, Switzerland
Mac OS 10 software	Apple

6.7 Methods

6.7.1 In-vitro experiments

6.7.1.1 Preparation of ANSs

ANSs for oral therapy were synthesized in the Department of Pharmaceutical Technology of the Free University, Berlin, by high pressure homogenization under aseptic conditions. The drug powder was dispersed in an aqueous surfactant solution using an Ultra Turrax® T 25. The coarse pre-dispersion obtained was homogenized in a Micron LAB 40 high pressure homogenizer applying pressure of 150 and 500 bar (2 cycles each), and 1500 bar (20 cycles). Particles were preserved by thiomersal at a concentration of 0.001% (wt/vol). Iso-osmolarity was achieved by adjusting with glycerole at a concentration of 2.25% (wt/vol).

ANSs contained 1% atovaquone and 1% of either Tween® 80, P188, or 0.2% SDS as stabilizers.

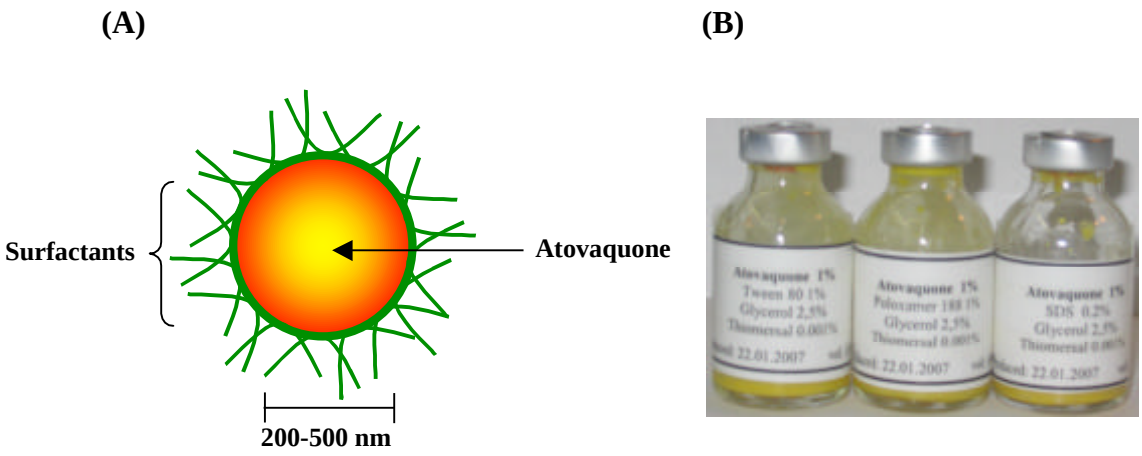

Fig. 12: Schematic design of atovaquone nanosuspensions for oral use

6.7.1.2 Characterization of ANSs

To characterise ANSs we determined the physicochemical properties including particle size, polydispersity index, and zeta potential.

6.7.1.2.1 Particle size measurement

The Z-ave and PI were determined by PCS and LD (Teeranachaideekul et al 2008). Prior to the measurement, samples were diluted with distilled water to a suitable scattering intensity and redispersed by handshaking before the measurement.

6.7.1.2.2 Zeta potential measurement

To investigate the physical stability of ANSs which is critical in the interaction of nanoparticles with cellular membranes (Mansouri et al 2006), we determined the ZP of ANSs using the Zetasizer Nano ZS. Measurements were performed in purified water. The pH was in the range of 5.5–6.0. The ZP values were calculated using the Helmholtz–Smoluchowsky equation.

6.7.1.2.3 Microscopic imaging

ANSs and Wellvone® suspension were analysed by light microscopy using a 1000-fold magnification to investigate the morphology of the nanocrystals and Wellvone® suspension. Each sample was analysed 3 times. Polarized light was used to determine the presence or absence of larger crystals or aggregates.

6.7.1.3 MTT colorimetric cell viability assay

The cytotoxicity of ANSs and Wellvone® suspension on J774A.1, MODE-K, and bEnd3 cells was assessed by the 3-(4,5-dimethylthiazol-2-yl)-2,5-diphenyltetrazolium bromide (MTT) assay (Mosmann 1983). Fifty microliters of MTT solution (2.5 mg of MTT/ml in PBS) were added to confluent monolayers of cells that had been incubated for 20h at 37°C in a 5% CO_2 incubator with ANS/P188, ANS/SDS, or Wellvone® in 1 and 3 µg/ml concentrations. The incubation was continued for 4h and absorbance was measured at 550 nm in an automated ELISA plate reader. Percent viability was determined by comparison to untreated cells that were considered 100% viable. All measurements of toxicity were performed in triplicate.

6.7.1.4 Mono-culture model of intestinal barrier

MODE-K cells were grown in cell culture flasks in DMEM supplemented with 10% (v/v) FCS, 1% (v/v) NEAA, and 1% (v/v) l-glutamine, at 37°C in a 5% CO_2 water saturated atmosphere. Cells were then grown onto 3 µm pore filters ($1x10^5$/insert) coated with 0.5 mg/ml collagen IV for 3 days (Fig. 13A). The integrity of the cell layer was evaluated by measurement of TEER with a Millicell-ERS apparatus containing two electrodes minutes before the transport experiments (Fig. 13B). One electrode was placed in the lid that extended into the medium in the insert (apical chamber) (0.5 ml/insert) while the other was placed in the base of the chamber which contained 1.5 ml of medium. The TEER (Ω x cm^2) of inserts containing the monolayers was measured and values were corrected for the background resistance measured across filters without cells. For transport studies, ANS/Tween® 80, ANS/P188, ANS/SDS, and Wellvone® were added to the apical chambers on day 4 at concentrations of 1 and 3 µg/ml (0.5 ml/insert). Basolateral contents were sampled at 1h (Fig. 13C) and analysed by HPLC for quantification of atovaquone.

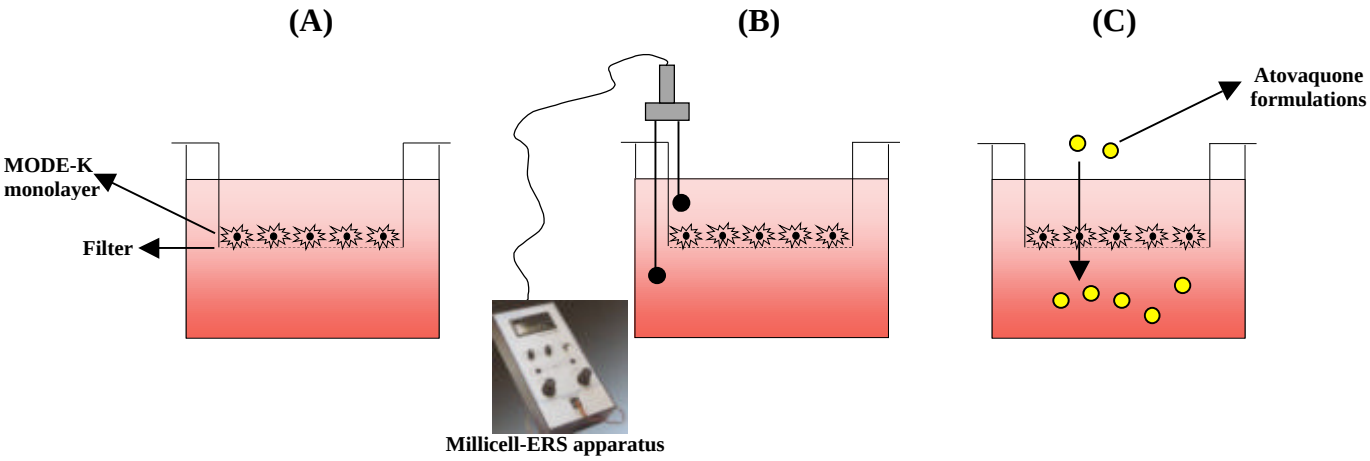

Fig. 13: Schematic view of the intestinal mono-culture barrier model. MODE-K monolayers were grown onto 3 µm pore filters (A). Integrity of cell layers was evaluated by TEER measurement (B). Atovaquone suspensions were then added to the apical chambers for tranport studies (C)

6.7.1.5 Mono-culture model of blood-brain-barrier

bEnd3 cells were grown to confluence on 3 µm pore filters ($1x10^5$/insert) coated with 0.5 mg/ml collagen IV for 3 days. For transport studies, ANS/Tween® 80, ANS/P188, ANS/SDS and Wellvone® were added to the apical chambers on day 4 at concentration of 1 and 3 µg/ml. Content of the basolateral chambers was sampled at 1h and evaluated by HPLC for quantification of atovaquone.

6.7.1.6 Co-culture model of blood-brain-barrier

PRBECs were isolated from brains of 2-weeks-old Wistar rats as previously described (Deli et al 1993, Veszelka et al 2007). Forebrains were collected and meninges were removed. The gray matter was minced to 1 mm^3 pieces and then digested with 1 mg/ml collagenase type-2

and 15 µg/ml DNaseI in DMEM for 1.5h at 37°C. The pellet containing the microvessels was further separated by centrifugation in DMEM containing 20% BSA to remove myelin sheats followed by digestion with 1 mg/ml collagenase-dispase and 6.6 µg/ml DNaseI for 1h at 37°C to remove pericytes from the basal membrane. The cell fraction containing the endothelial cell clusters was separated on a 33% percoll gradient, collected, and washed twice. Endothelial cells were plated onto 3 µm pore filters coated with 0.5 mg/ml collagen IV and 0.1 mg/ml fibronectin. Three µg/ml puromycin were added to endothelial cell medium [DMEM containing 20% plasma-derived bovine serum, 100 µg/ml P/S, 100 µg/ml heparin and 1 ng/ml bFGF] and incubated for three days to eliminate contaminating cells that express Pgp at low levels (Perriere et al 2005).

Astrocytes were isolated from 2-days-old Wistar rats (Gaillard et al 2001). Cortices were fragmented and incubated with 0.1% trypsin for 15 minutes at 37°C and then digested for 5 minutes with 100 µg/ml DNaseI. Astrocytes were then cultured in D-MEM containing 10% FCS, 1% P/S and 1x NEAA in 12 well plates at 37^0 C and 5% CO_2 for 4 weeks before used in co-cultures with PRBECs.

Three days after isolation of PRBECs filters were transferred to 12 well plates that were seeded with astrocytes and cultivated in endothelial cell medium supplemented with 200 ng/ml hydrocortisone (Deli et al 2005). On the following day the medium of the upper chamber was exchanged by endothelial cell medium containing 200 ng/ml hydrocortisone, 250 µM cAMP and 17.5 µM RO-20 for 24h to tighten endothelial junctions (Deli et al 2005, Perriere et al 2005). The integrity of the in-vitro BBB was analysed by measuring TEER (Ω x cm^2) as mentioned above.

Seven days after initiation of co-culture of PRBECs and astrocytes (Fig. 14), fresh medium was added to the lower compartment. ANS/Tween® 80, ANS/P188, ANS/SDS and Wellvone® were added to the apical chambers (after withdrawal of medium) at concentrations of 1 and 3

µg/ml (500 µl/insert). Following incubation for 1h at 37° C, the content of the basolateral chambers was collected and atovaquone concentrations were determined by HPLC.

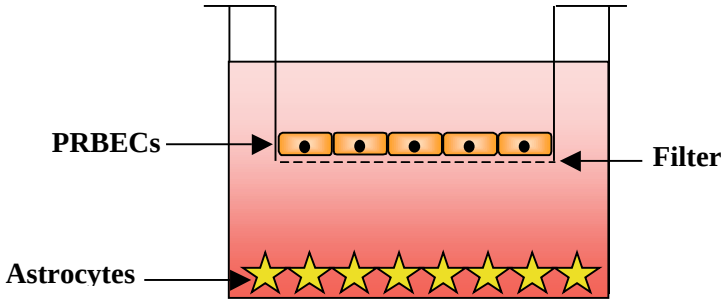

Fig. 14: Schematic view of the BBB in-vitro co-culture model using freshly isolated rat PRBECs and rat astrocytes

6.7.1.7 High-performance liquid chromatography (HPLC)

HPLC analysis was performed in the Department of Clinical Chemistry and Pathobiochemistry, Charité. Weighted samples of serum (200 µl), brain, liver, and lung (50 to 300 mg) were homogenized in 5 ml of extraction solution consisting of 2% (vol/vol) isoamyl alcohol and 98% (vol/vol) hexane in a glass-Teflon homogenizer. 0.1 ml homogenate was diluted in 5 ml of extraction solution. After the addition of 1 ml of phosphate buffer, samples were rotated for 20 minutes in a rotating mixer (Hannan et al 1996, Hansson et al 1996). Suspensions were centrifuged for 10 minutes at 2,800 g in a temperature-controlled centrifuge at 10°C. Four ml of supernatant was evaporated to dryness in a rotating vacuum centrifuge. The dry residue was dissolved in mobile phase (aqueous solution of 50% [vol/vol] acetonitrile and 5% [vol/vol] methanol, pH 2.65). The samples were chromatographed on a reversed-

phase column guarded with a C18 precolumn in isocratic mode. Absorbance of the eluate was monitored at 254 nm in a UV detector. The linear calibration function was calculated by means of least-squares regression analysis by using SQS 98 computer software. The detection limit of this method was 0.6 mg/l of serum. Limits of quantification for tissues were approx. 0.5 mg/kg tissue. Inter-assay precision for serum varied from 7.4 to 15.1%. Recovery from spiked serum was 98.1 to 108.1%. Replicate extractions yielded the following extraction rates for the first extraction: 100.0% (serum), 63.6% (brain), 78.1% (liver), and 78.1% (lung).

6.7.1.8 Flow cytometry analysis of atovaquone efficacy using *T. gondii* expressing GFP

T. gondii RH tachyzoites expressing GFP were maintained in continuous in-vitro culture in mouse macrophages (J744A.1).

GFP-tachyzoites of *T. gondii* were grown in RPMI 1640 medium supplemented with 10% heat inactivated FCS. Confluent monolayers of MODE-K cells (1 x 10^5/well in 24-well plates) were inoculated with GFP- tachyzoites at parasite-to-cell ratios of 3:1. After incubation at 37° C for 3h to allow parasite invasion, cultures were rinsed 3 times with PBS to remove extracellular parasites, and incubated with ANS/Tween® 80, ANS/P188, ANS/SDS and Wellvone® in concentrations of 3 µg/ml for 48h. Wells were washed with PBS to remove dead cells. Remaining attached cells were detached with cold PBS containing 5% FCS, 1% sodium azide, harvested, and fixed with 4% formaldehyde/PBS for flow cytometry analysis.

6.7.2 In-vivo experiments

6.7.2.1 Pharmacokinetics of atovaquone compounds in mice

Naive C57BL/6J female mice were treated orally with ANS/P188, ANS/SDS and Wellvone® at 50 mg/kg as a single dose (0.2 ml). Serum was collected 8, 24, and 48hr after treatment and evaluated by HPLC to determine atovaquone concentrations.

6.7.2.2 Infection with *T. gondii*

Cysts of the ME49 strain of *T. gondii* were obtained from brains of NMRI mice that had been infected i.p. with 10 cysts 3 to 4 months before. Mice were sacrificed by asphyxiation with CO_2, and their brains were removed and triturated in PBS. An aliquot of the brain suspension was used to determine the numbers of cysts by microscopy.

6.7.2.3 Murine model of acute toxoplasmosis

Female C57BL/6 mice were maintained under specific-pathogen-free conditions in the animal facility of the Charité (FEM) and were 6-12 weeks old when used. Mice were orally infected with 10 cysts (Fig. 15). On day 5 post infection treatment with ANSs and Wellvone® (50 and 100 mg/kg body weight) was started; all drugs were administered orally for 7 days. One day after the last dose of oral atovaquone therapy (12 days post infection), sera and organs were obtained for histological and pharmacological analysis.

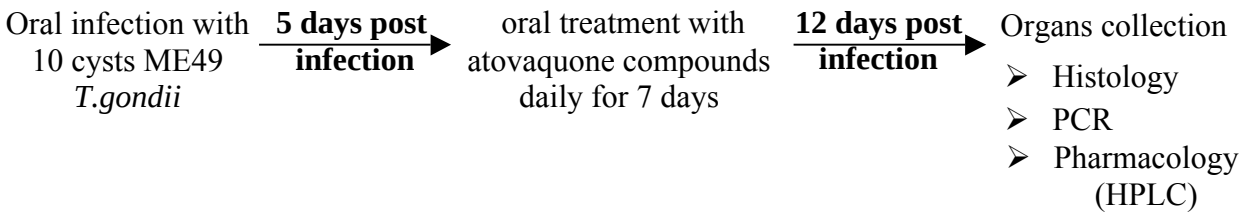

Fig. 15: Murine model of acute toxoplasmosis in C57BL/6 mice

6.7.2.4 Murine model of reactivated toxoplasmosis

Interferon regulatory factor (IRF)-$8^{-/-}$ mice are unable to upregulate IFN-γ production upon infection with 10 cysts of *T. gondii* and die within 15 days after infection (Dunay et al 2004, Scholer et al 2001). When mice are treated with sulfadiazine (400 mg/l) in drinking water for 4 weeks beginning 2 days after infection latent infection with cyst formation is established. Upon discontinuation of sulfadiazine reactivation of infection occurs and TE develops. Signs of the disease closely mimic signs of reactivated toxoplasmosis in immunocompromised patients including the presence of parasite-associated focal necrotic lesions in the brain parenchyma and meningeal inflammation (Fig. 16A and B).

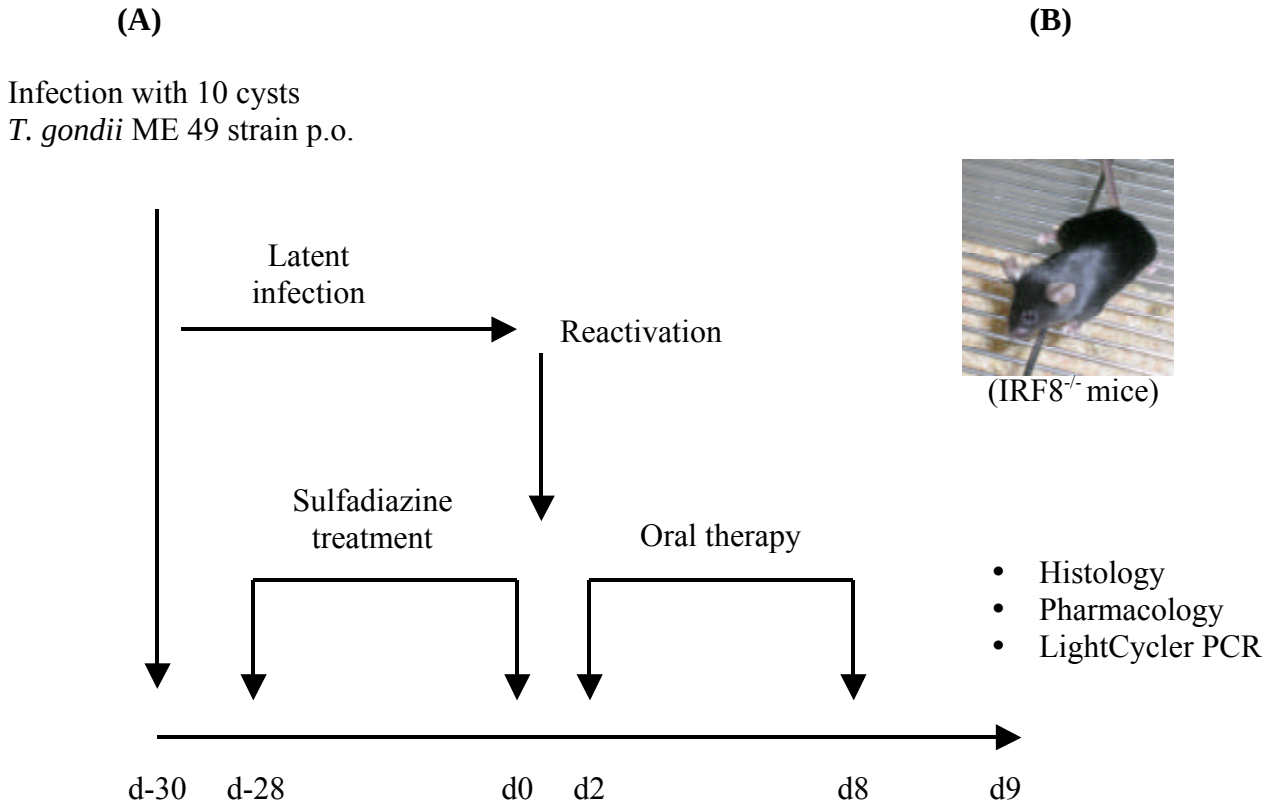

Fig. 16: Murine model of reactivated toxoplasmosis in IRF-8$^{-/-}$ mice. After reactivation of latent infection with *T. gondii,* oral therapy with atovaquone compounds was given for 7 days, d = day(s)

6.7.2.4.1 Oral treatment with atovaquone compounds

After discontinuation of sulfadiazine, mice were treated with ANSs and Wellvone® (50 and 100 mg/kg body weight) administered orally for 7 days (from day 2 to day 8 after discontinuation of sulfadiazine therapy). At day 9 after discontinuation of sulfadiazine (1 day after the last dose of oral atovaquone therapy), brains, livers, and lungs were removed and fixed in formalin for histology. Sera were obtained and stored at –70°C for HPLC analysis. There were 4 to 6 mice in each experimental group to study histological changes. HPLC analysis was performed on organs and serum samples of 3 to 4 mice per group.

6.7.2.5 Histology

Organs were excised, fixed in tissue blocks over night in a solution containing 5% formalin, and embedded in paraffin (Institute of Pathology, CBF, Charité) (Spector & Goldman 2006). Tissues were sectioned at 4-6 µm, and immunohistochemical staining was performed. Sagital sections of brains and cross sections of livers and lungs were stained with H&E according to standard procedures (Spector & Goldman 2006) and by the immunoperoxidase method with rabbit anti-*T. gondii* hyperimmunserum (Conley et al 1981).

6.7.2.5.1 Hematoxylin and eosin staining

Sections were deparaffinized in xylene, dehydrated through graded alcohols (from 100 to 70%), stained in hematoxylin solution and counterstained in eosin. Eosin was differentiated by a short dip in 70% ethanol solution and subsequently sections were dehydrated through graded alcohols (from 80 to 96%). Sections were then cleared in xylene, coverslipped, and left to dryness before light microscopy. The nuclei were stained blue, the cytoplasm was stained pink to red.

6.7.2.5.2 Peroxidase antiperoxidase staining

For staining by the immunoperoxidase method, deparaffinized sections were incubated with swine sera (1:10) and with the primary rabbit anti-*T. gondii* serum. After a rinse with modified PBS, sections were incubated with swine anti-rabbit immunoglobulin (1:100). Finally, sections were incubated with rabbit peroxidase anti-peroxidase (1:100) and with diaminobenzidine development solution after a rinsing step. The numbers of inflammatory foci and parasites were counted at x200 magnification in three optical fields. A total of three sections of each organ from four mice in each experimental group were evaluated for the

numbers of inflammatory foci and the numbers of *T. gondii* cysts, tachyzoites, and/or toxoplasma antigens.

6.7.2.6 Polymerase chain reaction (PCR)

6.7.2.6.1 DNA extraction

50-100 mg of mouse brain and lung were homogenized in a rotor-stator in 500 µl lysis buffer containing 100 mM Tris HCl pH 8.0, 200 mM NaCl, 5 mM EDTA pH 8.0, 0.2% SDS, and 200 µg/ml proteinase K. The homogenate was lysed for 30 minutes by shaking at 56°C in a thermomixer and centrifuged full speed for 15 minutes. DNA was precipitated by centrifugation after adding 500 µl of isopropanol to the supernatant. After washing with 70% ethanol, drying, and resuspending in 200 µl water, DNA concentrations were measured photometrically.

6.7.2.6.2 Quantitative LightCycler PCR

For the quantification of *T. gondii* we used primers amplificating a 162 bp fragment of the cryptic gene (Reischl et al 2003). The amplification mixture consisted of 2 µl of 10x reaction mix (LightCycler FastStart Master Hybridization Probes, Roche Applied Science, Mannheim, Germany), 2 mM $MgCl_2$, 1 µM of each oligonucleotide primer Tox9 (5'-AGG AGA GAT ATC AGG ACT GTA G-3') and 10as (5'-GCG TCG TCT CGT CTA GAT CG-3'), 0.2 µM of each oligonucleotide probe TOX-HP-1 (5'-GAG TCG GAG AGG GAG AAG ATG TT-FAM-3) and TOX-HP-2 (5'-RED-640-CCG GCT TGG CTG CTT TTC CTg-PH-3), and 500 ng of template DNA in a final volume of 20 µl. The amplification was performed using the following conditions: 1 cycle at 95°C for 10 min, 50 cycles at 95°C for 10 sec/52°C for 20 sec/72°C for 30 sec, and 1 cycle at 40°C for 30 sec with a single fluorescence detection point

at the end of the cycle. The temperature transition rate was 20°C/sec. Distilled water was used as negative control in each PCR. With each run a standard curve was performed using 500 to 5 pg *T. gondii* DNA. Fluorescence was analysed by LightCycler Data Analysis software. Crossing points (Cp) were established using the second derivative method.

6.7.2.7 Statistical analysis

Results are presented as mean ± SD. Statistical analysis was performed using the unpaired two-tailed Student's *t* test with $P<0.05$ indicating significant differences. All experiments were repeated twice unless otherwise stated.

7 Results

7.1 Characterization of atovaquone preparations

Atovaquone preparations (ANS/Tween® 80, ANS/P188, ANS/SDS and the commercial solution Wellvone®) were analysed by LD and PCS. Table 7 shows that 50% of ANS/Tween® 80, ANS/P188, and ANS/SDS had particle sizes of 0.757, 0.721, and 0.705 µm, respectively, whereas 50% of Wellvone® had a particle size of 2.766 µm. The mean size of ANS/Tween® 80, ANS/P188, and ANS/SDS was 415, 440, and 469 nm, respectively; in contrast, the particle size of micronized suspension Wellvone® (967 nm) was markedly bigger. ANS/Tween® 80, ANS/P188, and ANS/SDS had a narrow size distributions of 0.264, 0.249, and 0.391, respectively, whereas Wellvone® showed a very broad size distribution of 0.621.

Table 7: LD and PCS diameters of ANSs compared to the micronized suspension (Wellvone®); (mean no. ± SD, n = 3 for LD, n = 10 for PCS)

Formulations	LD (µm)			PCS	
	d50%	d90%	d99%	Z-ave (nm)	PI
ANS/Tween® 80	0.757 ± 0.027	1.832 ± 0.006	2.390 ± 0.013	415 ± 6	0.264 ± 0.127
ANS/P188	0.721 ± 0.005	1.835 ± 0.020	2.390 ± 0.040	440 ± 4	0.249 ± 0.073
ANS/SDS	0.705 ± 0.003	1.779 ± 0.010	2.367 ± 0.021	469 ± 13	0.391 ± 0.062
Wellvone®	2.766 ± 0.026	9.579 ± 0.031	12.987 ± 0.064	967 ± 152	0.621 ± 0.137

ANS/SDS had a highly negative surface charge of –76 mV. The zeta potentials of ANS/Tween® 80, ANS/P188, and Wellvone® were –20, –19, and +9 mV, respectively (Table 8).

Table 8: Zeta potentials (ZP) of ANSs and the micronized suspension (Wellvone®)

Formulations	Zeta potential (mV)
ANS/ Tween® 80	-20 ± 0.772
ANS/P188	-19 ± 0.748
ANS/SDS	-76 ± 0.612
Wellvone®	+9 ± 1.03

To further characterise ANSs we performed microscopy (Fig. 17). The differences in sizes were microscopically discernible. As indicated by their low PI ANSs displayed a homogenously distributed solution as single particles whereas Wellvone® displayed a more clustered distribution pattern.

These results indicate that ANSs are smaller in size and more uniform in shape than Wellvone® thus making them candidates to improve bioavailability of atovaquone.

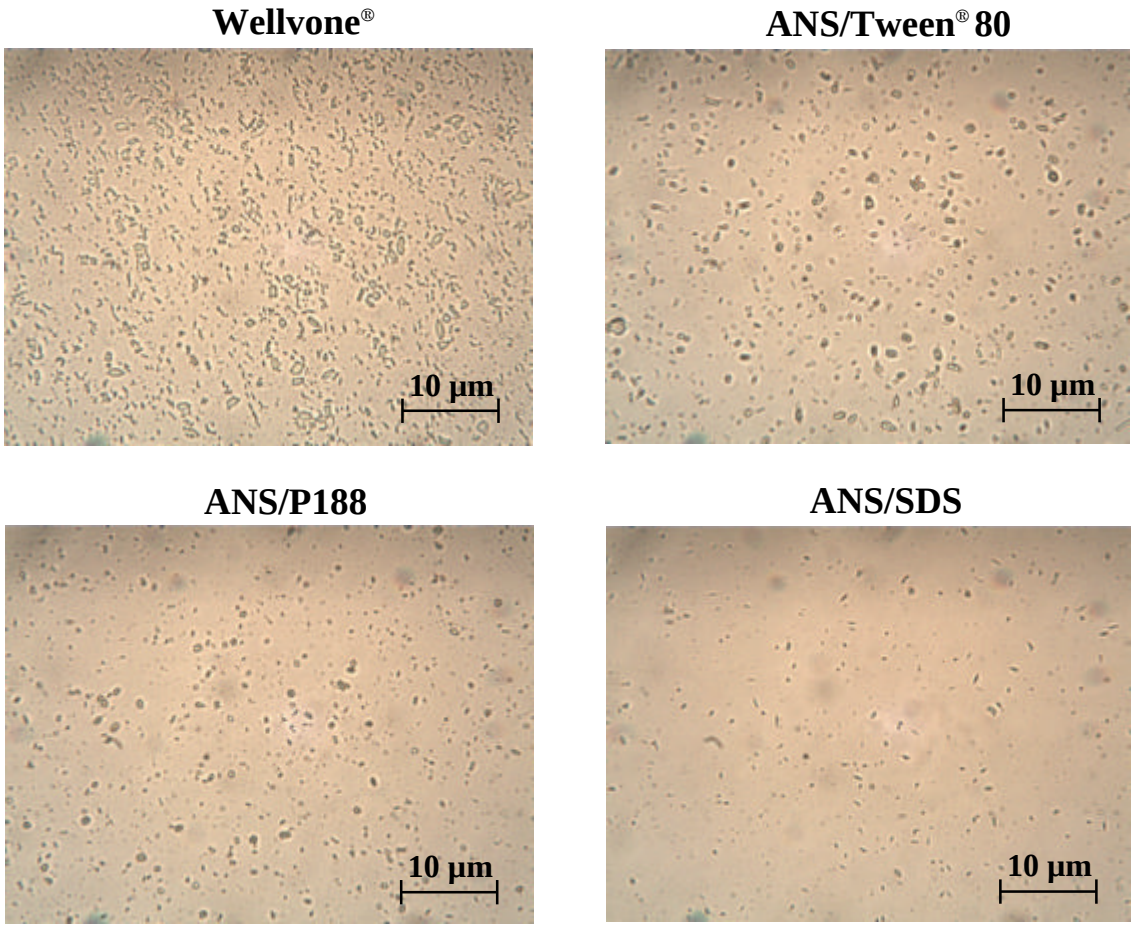

Fig. 17: Light microscopy of ANSs and micronized suspension (Wellvone®); 1000x-magnification

7.2 Cytotoxicity of atovaquone compounds

To exclude cytotoxicity of ANSs coated with P188 or SDS, I incubated J774A.1, MODE-K, and bEnd3 cells with physiological concentrations of ANSs and Wellvone®. The viability of these cell lines after 20h of incubation as determined by MTT assay is shown in Fig. 18. ANSs did not exert marked toxicity compared to untreated cell lines in-vitro. Viability ranged between 95 and 72% for J774A.1 cells treated after incubation of ANSs (Fig. 18). MODE-K cells treated with ANSs showed viabilities of between 100 and 80% and the viability of

bEnd3 cells ranged between 90% and 77%. The viability of Wellvone® and ANSs did not differ significantly.

Previously I tested cytotoxicity of ANSs coated with Tween® 80 (1 and 3 µg/ml) in J774A.1 cells (Shubar et al 2009). Viability of cells ranged between 93 and 71%.

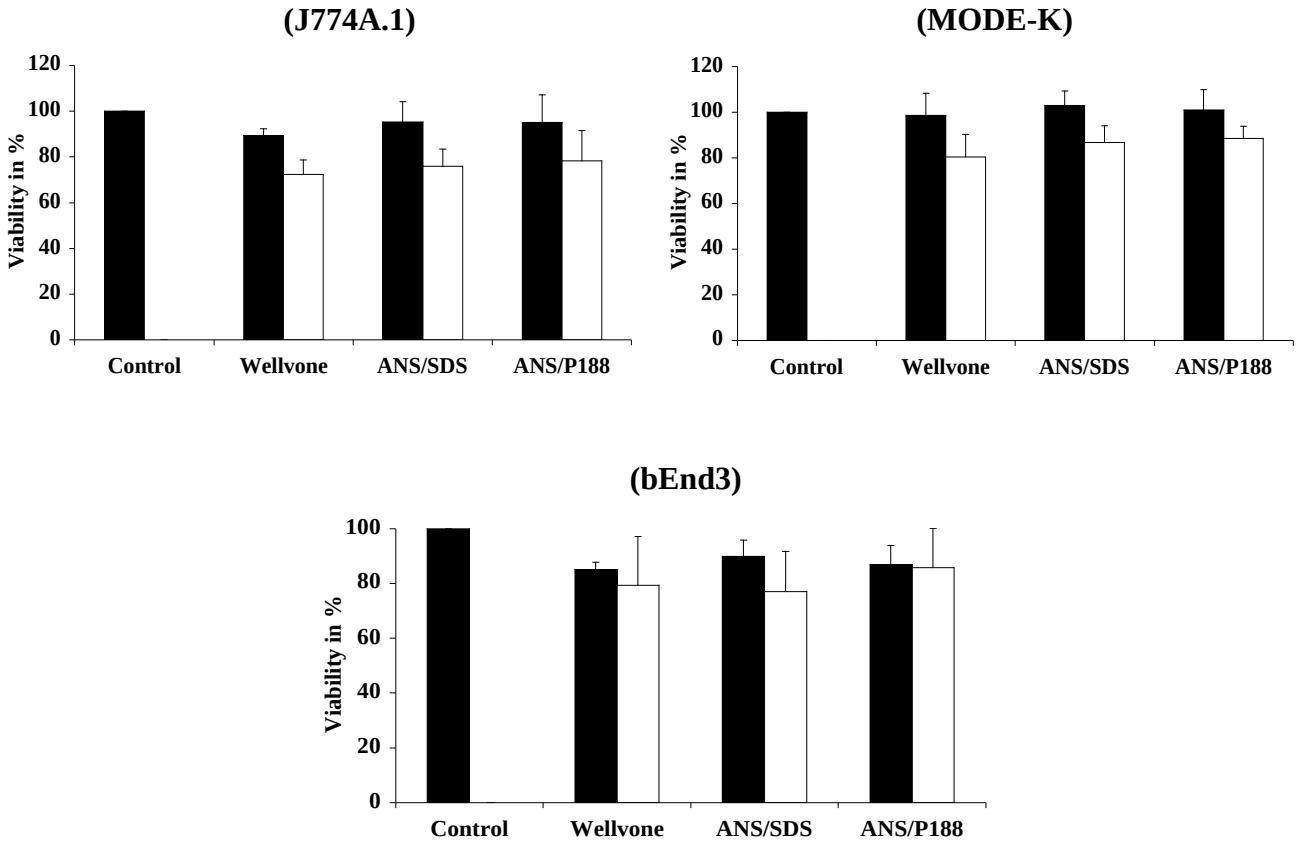

Fig. 18: Viability of cell lines after 20h incubation with Wellvone® and ANSs stabilized by P188 or SDS as determined by MTT. Control indicates untreated cells that were normalized to give a viability of 100%. Black and white bars indicate cells treated with 1 and 3 µg/ml of atovaquone compounds, respectively. Results shown are pooled data from 4 wells/atovaquone formulation ± SD

7.3 Transport of atovaquone across the intestinal barrier in a mono-culture model

Following the characterization and cytotoxicity testing of ANSs, I investigated the in-vitro transport of these nanosuspensions across a monolayer of enterocytes. Atovaquone concentrations in the content of the basolateral chamber of a transwell system were determined by HPLC 1h after addition to the apical chamber (Fig. 19). One µg/ml ANS/Tween® 80 and ANS/P188 crossed the transwell monolayer of MODE-K cells with significantly higher efficiency (11 and 12% recovery for ANS/Tween® 80 and ANS/P188, respectively) compared to Wellvone® (3.75%) (Fig. 19A), and 12.5 and 11% recovery were observed for ANS/Tween® 80 and ANS/P188, respectively, compared to Wellvone® (6%) at a concentration of 3 µg/ml (Fig. 19B). There was no significant difference in the transport percentages between ANS/Tween® 80 and ANS/P188; the transport percentages did not show concentration-dependent differences. Taken together, these results indicate that the type of surfactant impacts the transport across enterocyte monolayers in-vitro. ANSs display enhanced transport through the intestinal barrier in-vitro compared to micronized suspension (Wellvone®).

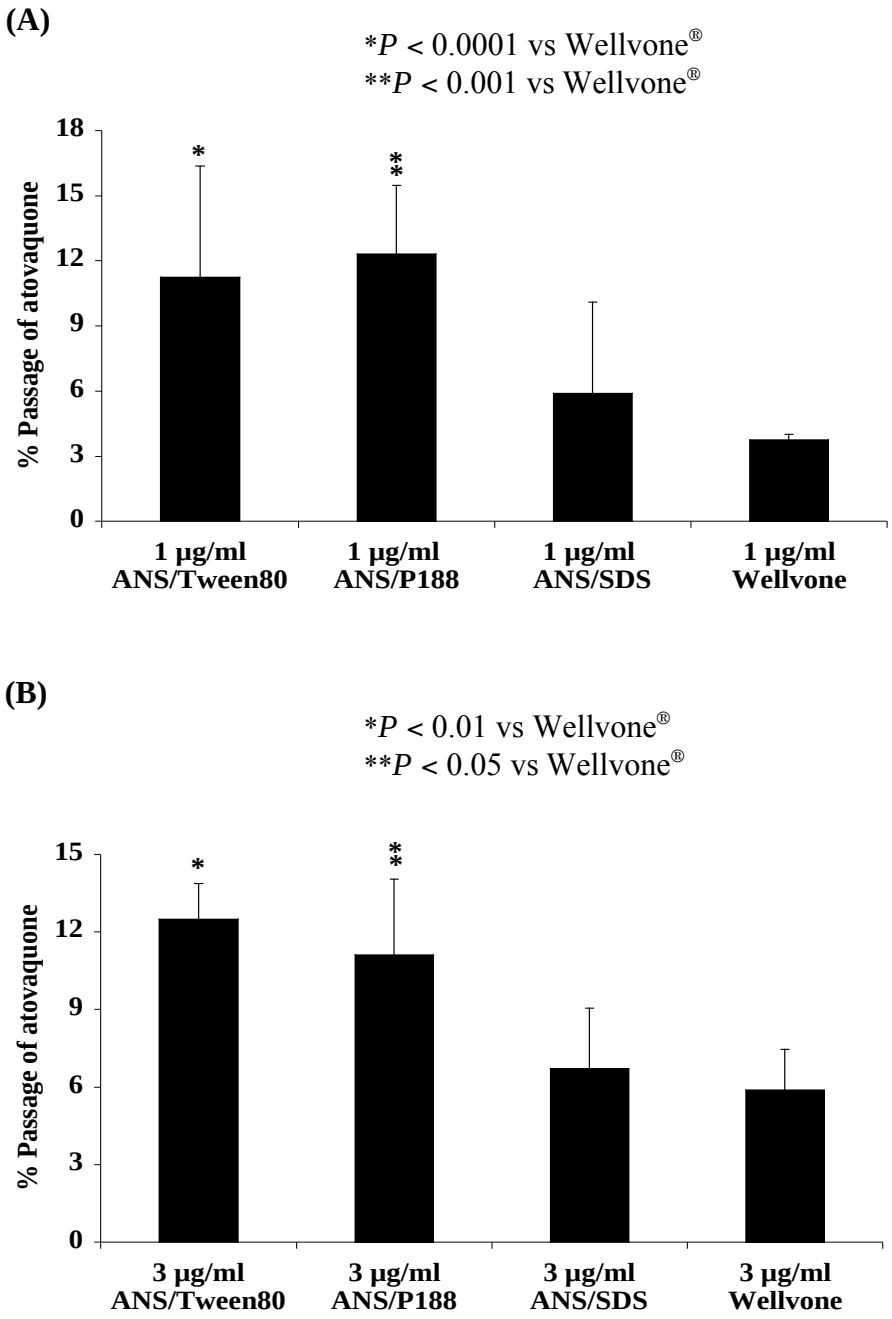

Fig. 19: Percentages of atovaquone transported through a mono-culture model of the intestinal barrier after 1h incubation with atovaquone compounds (Wellvone®, ANSs coated with Tween® 80, P188 and SDS) at 1 and 3 µg/ml (determined byHPLC). Results shown are pooled data from 3 transwell filters/atovaquone formulation ± SD

7.4 Transport of atovaquone across the BBB in a mono-culture model

The content of basolateral chambers of a mono-culture model of the BBB was analysed by HPLC to measure atovaquone concentrations after 1h incubation with ANSs and Wellvone®. At 1 µg/ml, ANS/P188 showed significantly higher passage (14.5%) than Wellvone® (9%), whereas ANS/Tween® 80 and ANS/SDS did not show enhanced transport compared to Wellvone® (Fig. 20). At 3 µg/ml we did not observe significant difference between individual preparations (data not shown).

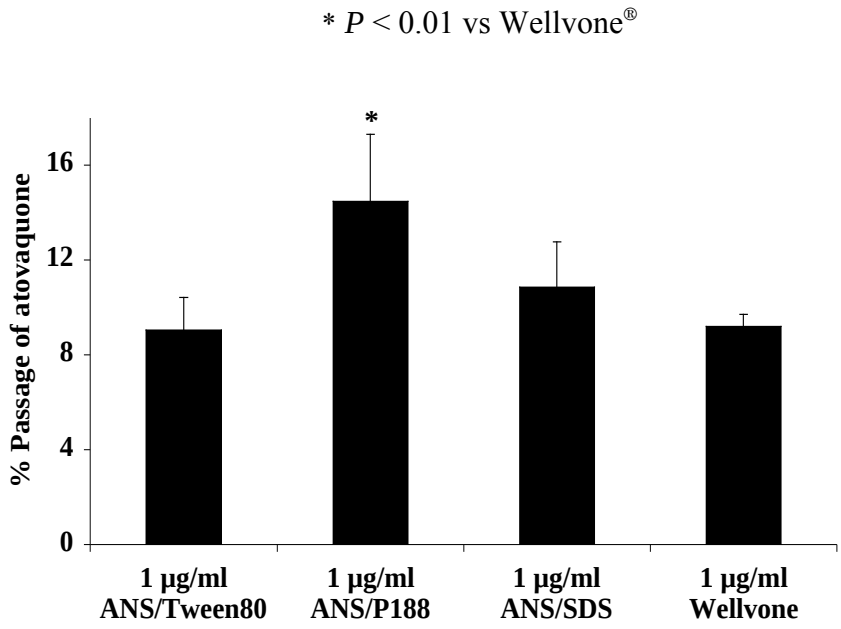

Fig. 20: Percent passage of ANSs and Wellvone® through a mono-culture model of the BBB after 1h incubation of ANSs coated with Tween® 80, P188, or SDS and Wellvone®. Results shown are pooled data from 3 transwell filters/atovaquone formulation ± SD

7.5 Transport of atovaquone across the BBB in a co-culture model

To investigate whether ANSs also show increased passage of the BBB, the most relevant barrier for the treatment of TE, we determined the passage of ANSs compared to Wellvone® through a co-culture model of the BBB. All atovaquone preparations showed between 13 and 19% passage at a concentration of 1 µg/ml. At a concentration of 1 µg/ml ANS/P188 showed a significantly higher transport rate than Wellvone® (16 vs. 13%, Fig. 21A); the passage of 1 µg/ml ANS/SDS or ANS/Tween 80 did not differ from that of Wellvone® and there was no significant difference between ANS/Tween® 80 and ANS/P188. At 3 µg/ml (Fig. 21B) the passage of ANSs and Wellvone® ranged from 8 to 24% but did not differ significantly between the nanosuspensions and micronized suspension. At a concentration of 3 µg/ml ANS/P188 showed significantly higher transport rate than ANS/SDS (24 vs. 8%, Fig. 21B).

(A)

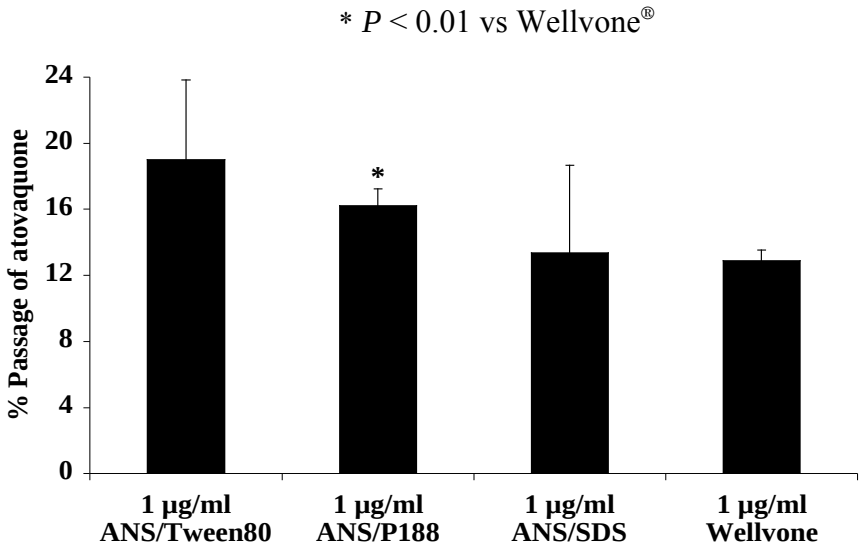

(B)

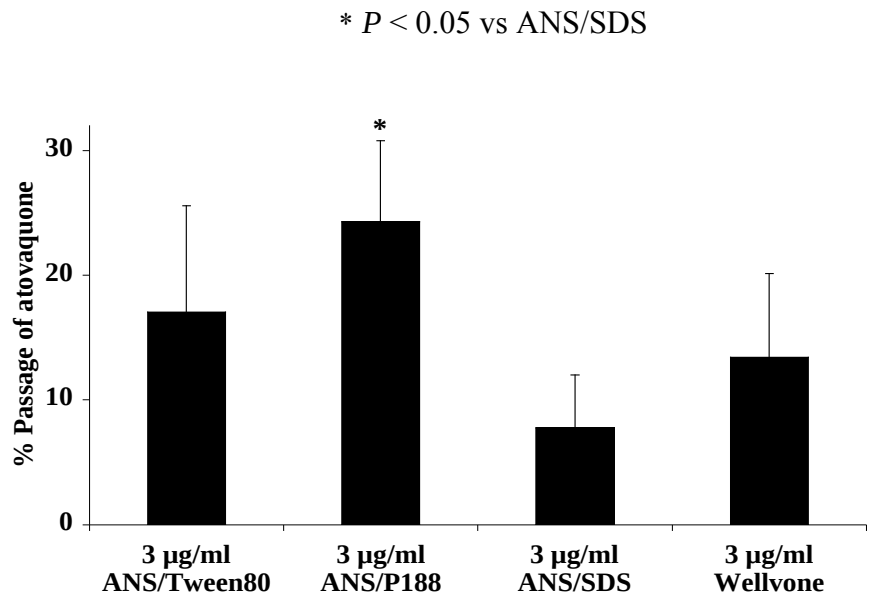

Fig. 21: Percentages of atovaquone transported through a co-culture model of the BBB after 1h incubation with ANSs coated with either Tween® 80, P188, or SDS compared to Wellvone® [all 1 (A) and 3 (B) µg/ml]. Results shown are pooled data from 3 transwell filters/atovaquone formulation ± SD

In summary, results of our in-vitro passage studies show that Tween® 80 and P188 but not SDS enhanced the passage of atovaquone through the intestinal barrier compared to the commercial suspension (Wellvone®).

Coating of ANSs with P188 enhanced the passage of atovaquone through BBB mono and co-cultures models compared to Wellvone®.

7.6 Antiparasitic effect of atovaquone in-vitro

To investigate the antiparasitic effect of atovaquone preparations in-vitro, I determined the reduction in the percentages of infected cells using flow cytometry. Using relatively high parasite-to-cell ratios (3:1) ANS/Tween® 80, ANS/P188, and ANS/SDS (3 µg/ml) inhibited parasite replication by 76, 57, and 36%, respectively, whereas Wellvone® inhibited parasite replication by only 26% (Fig. 22). These results suggest that ANSs have higher antiparasitic in-vitro efficacy than the micronized suspension (Wellvone®).

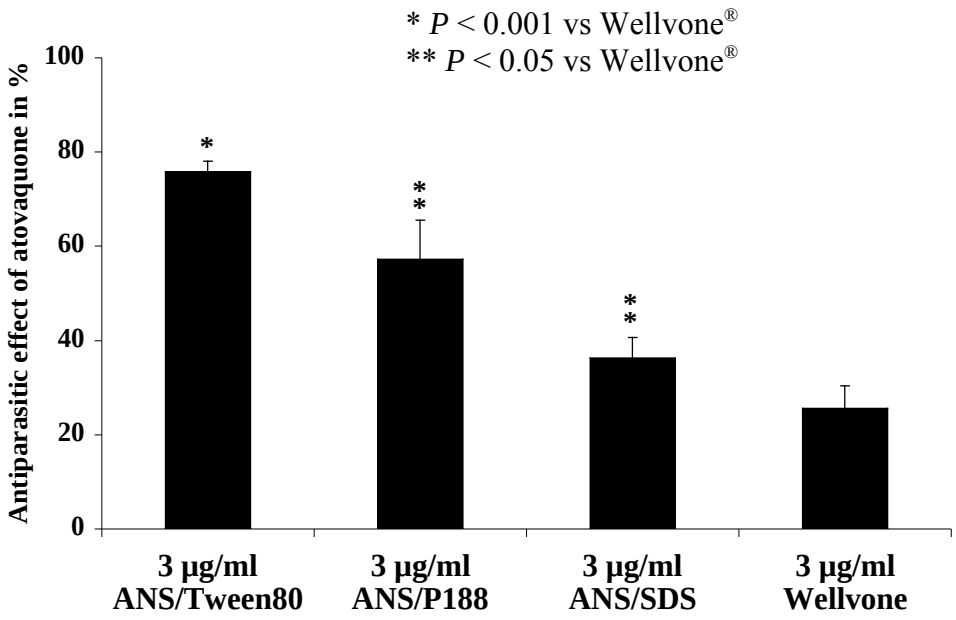

Fig. 22: Antiparasitic effects of ANSs and Wellvone® against *T. gondii* as determined by flow cytometry. MODE-K cells were incubated for 3h with GFP-containing RH tachyzoites at a parasite-to-cell ratio of 3:1 and treated with the respective ANSs or Wellvone® at 3 µg/ml for 48h. The antiparasitic effect was determined by comparing the percentage of infected treated cells with the percentage of infected cells in untreated control cells (set to be 100%). Results shown are pooled data from 4 wells/atovaquone formulation ± SD

7.7 Pharmacokinetics of ANSs in mice

In order to investigate the role of surfactants in oral uptake of atovaquone in-vivo, serum of naive C57BL/6J female mice was obtained 8, 24, and 48 hr after a single oral treatment with ANS/P188, ANS/SDS, and Wellvone® (50 mg/kg body weight). Using HPLC serum concentrations of atovaquone preparations were found to be highest at 8h post treatment, decreased after 24h respectively, and reached low levels at 48h post treatment. At 8 and 24h post treatment with ANS/SDS but not ANS/P188 showed significantly higher serum concentrations than Wellvone® (Fig. 23). At 48h there was no significant difference between serum levels of individual preparation.

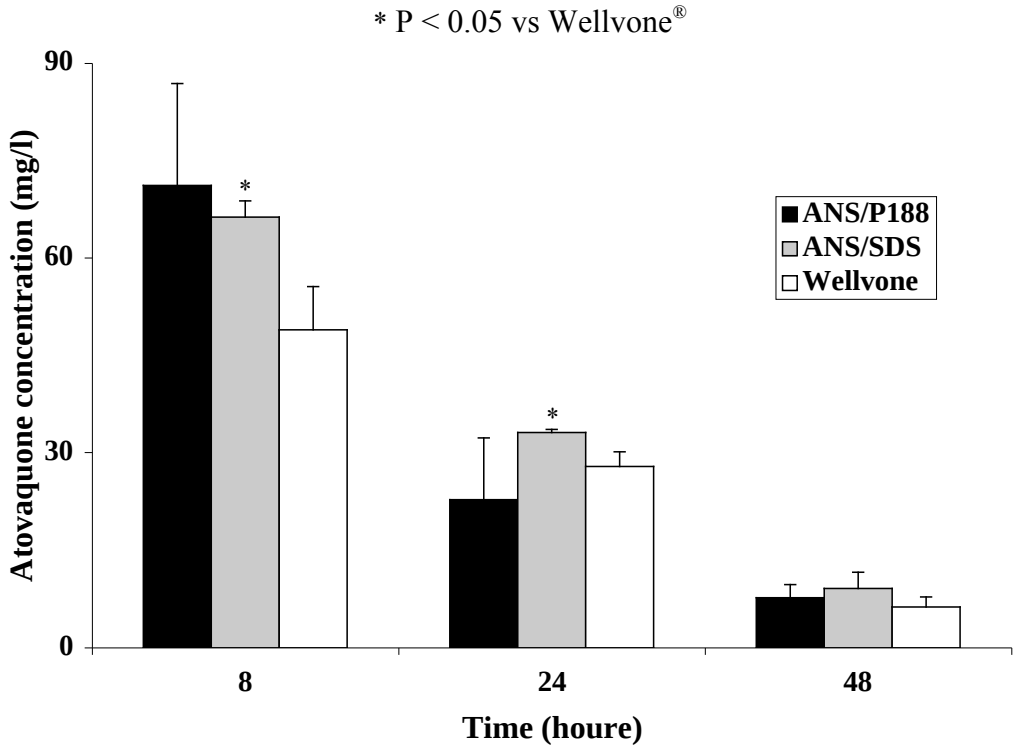

Fig. 23: Atovaquone concentrations in serum of C57BL/6J mice after a single oral treatment with atovaquone compounds (ANS/P188, ANS/SDS and Wellvone®) measured by HPLC. Results show pooled data from 4 mice/group ± SD

7.8 Therapeutic efficacy of atovaquone in a murine model of acute toxoplasmosis

To further investigate the role of surfactants in the passage of ANSs through the intestinal and brain barrier, I performed experiments in a murine model of acute toxoplasmosis. This model reflects the acute stage of infection in humans when parasite replication is high and cysts develop in the brain and muscle tissue. Concentrations of ANSs were determined in serum and organs and the antiparasitic effects of nanosuspesions were analysed in comparison with the micronized suspension (Wellvone®).

7.8.1 Therapeutic efficacy of atovaquone preparations at 50 mg/kg body weight

7.8.1.1 Atovaquone concentrations in serum and organs

Initially, mice were treated with 50 mg/kg body weight of ANSs coated with either Tween® 80, P188, or SDS; micronized suspension (Wellvone®) in the same dosage served as a control. All drugs were administered from day 5 to day 11 post infection.

To determine the bioavailability, distribution, and uptake of atovaquone, sera, brains, lungs, and livers were obtained on day 12 after infection of mice and processed by HPLC (Fig. 24). Atovaquone concentrations were significantly higher in sera and lungs of mice treated with SDS-coated ANS compared to Wellvone®-treated mice. In contrast, atovaquone concentrations in serum of mice treated with ANS/Tween® 80 were significantly lower than those in mice treated with Wellvone® (and SDS-coated ANS) whereas atovaquone concentrations in sera and lungs of mice treated with ANS/P188 and Wellvone® did not differ. In livers, I did not observe significant differences in atovaquone concentrations between individual groups.

Atovaquone was not detected in brains, most likely due to the limited sensitivity of HPLC in brains (data not shown).

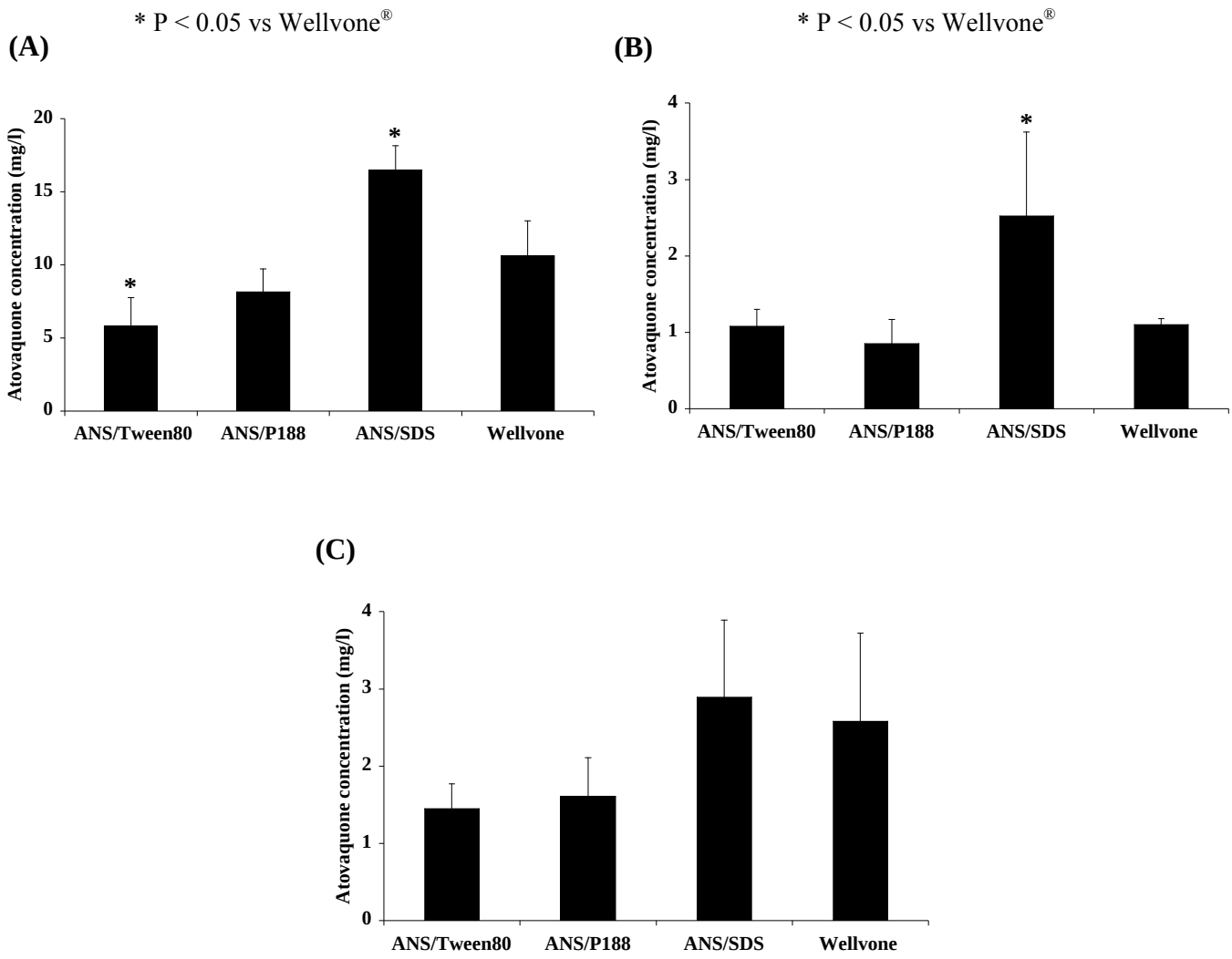

Fig. 24: Atovaquone concentrations in serum (A), lungs (B), and livers (C) of infected C57BL/6J mice after oral treatment with atovaquone compounds at 50 mg/kg body weight measured by HPLC. Results show pooled data from 3 to 4 mice/group ± SD

These results suggest that SDS-coated ANS have an increased bioavailability compared to the micronized suspension (Wellvone®). However, since atovaquone could not be detected in brains, we could not compare the uptake of individual formulations into the brain.

7.8.1.2 Antiparasitic effect of atovaquone

To investigate whether increased atovaquone concentrations in sera and organs of mice are accompanied by decreased histopathological changes and decreased parasite loads (DNA) in organs of infected mice, I stained brain tissues with H&E and PAP to quantify inflammatory foci and the parasite load. Quantitative PCR was performed to quantify parasite DNA in organs of ANSs-treated mice compared to Wellvone®-treated mice. Mice were treated with ANSs coated with Tween® 80, P188, or SDS, or treated with micronized suspension (Wellvone®) from day 5 to day 11 post infection. Untreated mice developed inflammatory foci in brains and livers (Fig. 25) and all preparations significantly reduced numbers of inflammatory foci in brains and livers compared to untreated control mice. ANS/SDS-treated mice showed significantly lower numbers of inflammatory foci in brains and livers compared to mice treated with Wellvone®. Numbers of inflammatory foci in brains of mice treated with ANS/Tween® 80 and ANS/P188 did not differ significantly from those in Wellvone®-treated mice (Fig. 25).

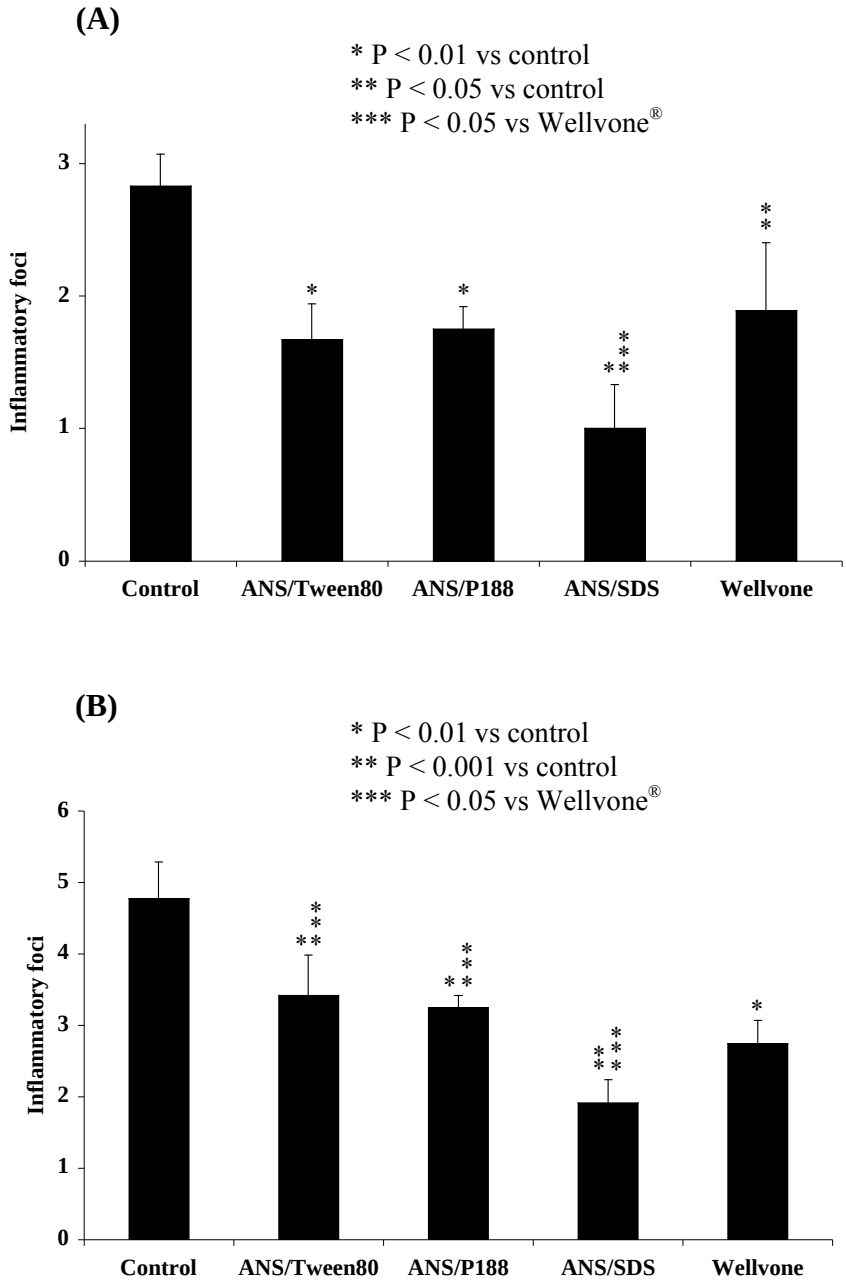

Fig. 25: Numbers of inflammatory foci (H&E) in brains (A) and livers (B) of C57BL/6J mice orally infected with *T. gondii* and treated orally with atovaquone compounds at 50 mg/kg body weight. Results show pooled data from 4 to 5 mice/group ± SD

To investigate whether decreased numbers of histopathological changes were caused by decreases in parasite numbers, I performed PAP immunohistological staining to determine parasite antigens in mice treated with ANSs compared to the micronized suspension (Wellvone®).

Histological findings in lungs, livers, and brains of mice infected with *T. gondii* and treated orally with ANS/Tween® 80, ANS/P188, ANS/SDS, and Wellvone® from day 5 to day 11 post infection are shown in Fig. 26. In lungs, livers, and brains, ANS/SDS significantly reduced parasite numbers compared to Wellvone® treated mice whereas parasite numbers did not differ in mice treated with ANS/Tween® 80, ANS/P188, and Wellvone® (except for ANS/P188 vs. Wellvone® in the liver). All preparations (except for ANS/Tween® 80 in the brain and Wellvone® in the liver) significantly reduced parasite numbers compared to untreated control mice.

These findings suggest that ANS/SDS has a higher therapeutic efficacy compared to Wellvone® by reducing parasite numbers and subsequently reducing the numbers of inflammatory foci in the brain.

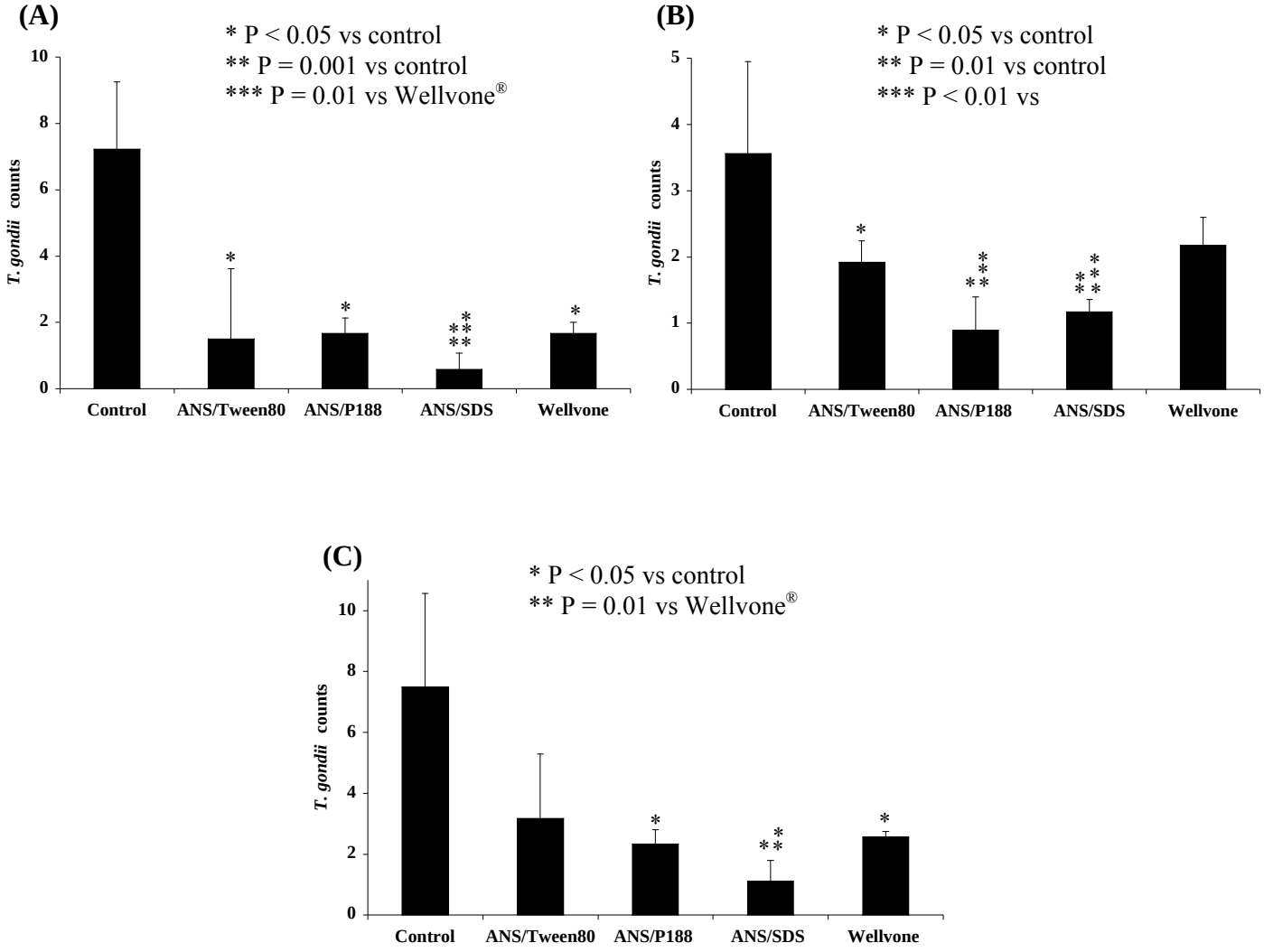

Fig. 26: Numbers of parasitophorous vacuoles and free parasite antigen as determined by immunoperoxidase staining in lungs (A), livers (B), and brains (C) of C57BL/6J mice orally infected with ME49 *T. gondii* and treated orally with atovaquone compounds at 50 mg/kg body weight. Results show pooled data from 4 to 5 mice/group ± SD

To investigate whether the histological findings are accompanied by reduction in parasite DNA LightCycler-PCR analysis was performed. All preparations significantly reduced parasite loads compared to untreated control mice (Fig. 27). Untreated control mice showed a high parasite load in lungs and brains. ANS/SDS-treated mice showed significantly lower parasite loads in lungs and brains compared to mice treated with Wellvone®. There was no significant difference in parasite loads in brains of mice treated with ANS/Tween® 80, ANS/P188, or Wellvone® (Fig. 27). In lungs ANS/P188 significantly reduced parasite load compared to Wellvone®.

These data confirm the histological findings suggesting that ANS/SDS has a higher antiparasitic effect than Wellvone® following infection with *T. gondii*.

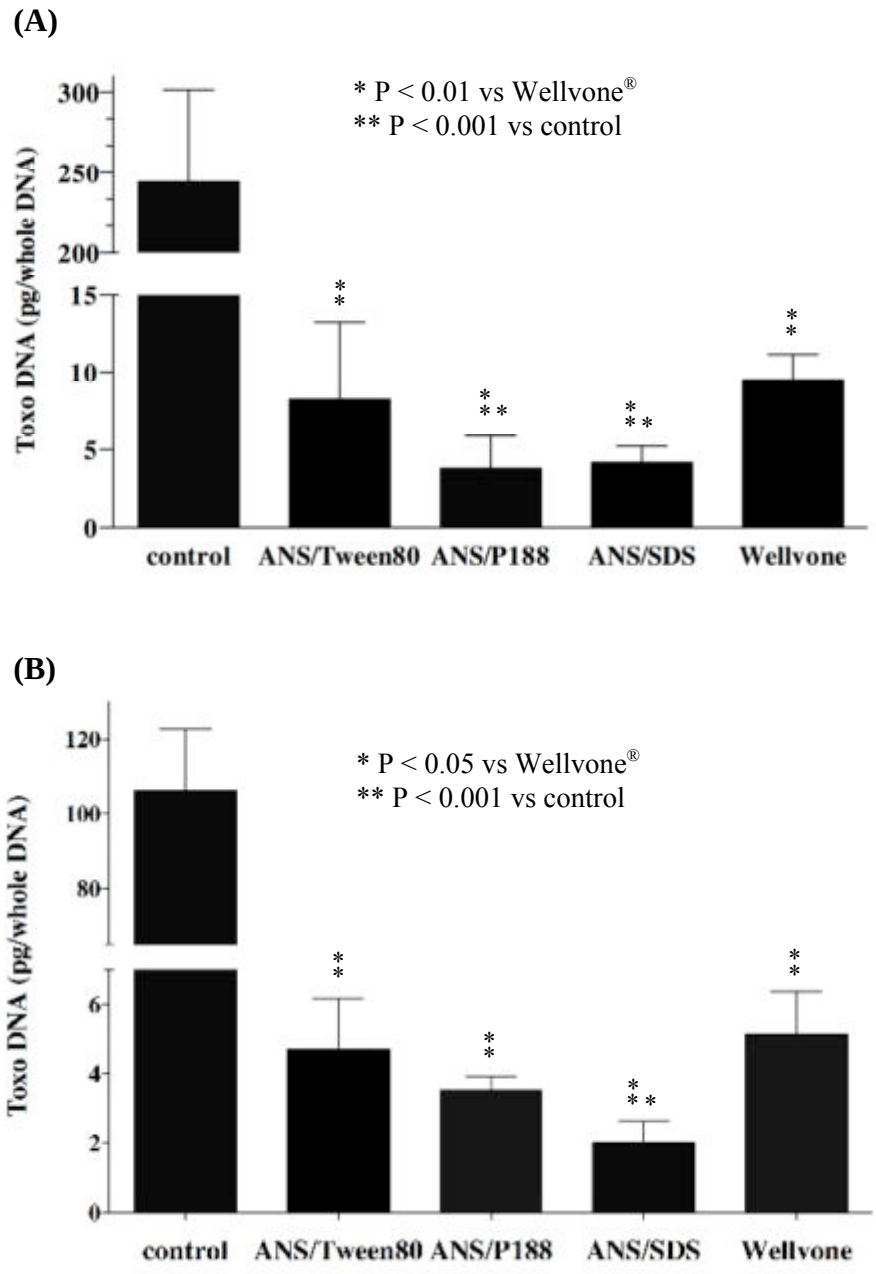

Fig. 27: *T. gondii* DNA load as determined by LightCycler-PCR in lungs (A) and brains (B) of C57BL/6J mice orally infected with 10 cysts ME49 *T. gondii* and treated orally with atovaquone compounds at 50 mg/kg body weight. Results show pooled data from 3 to 4 mice/group ± SD

7.8.2 Therapeutic efficacy of atovaquone preparations at 100 mg/kg body weight

Since atovaquone could not be detected in brains of *T. gondii*–infected mice treated orally with 50 mg/kg, I treated mice with 100 mg ANSs coated with P188 or SDS/kg body weight and compared the therapeutic efficacy with that of the micronized suspension (Wellvone®). Concentrations of atovaquone were determined in serum and organs by HPLC analysis, and the antiparasitic effects of nanosuspensions were analysed by microscopy and quantitative PCR.

7.8.2.1 Atovaquone concentrations in serum and organs

Following treatment with 100 mg/kg body weight atovaquone was detected in sera and organs including the brain of all mice (Fig. 28). Atovaquone concentrations were significantly higher in serum, brains, lungs, and livers in ANS/SDS-treated mice compared to Wellvone®-treated mice. Atovaquone concentrations in serum and organs of mice treated with ANS/P188 did not differ significantly from those in Wellvone®-treated mice.

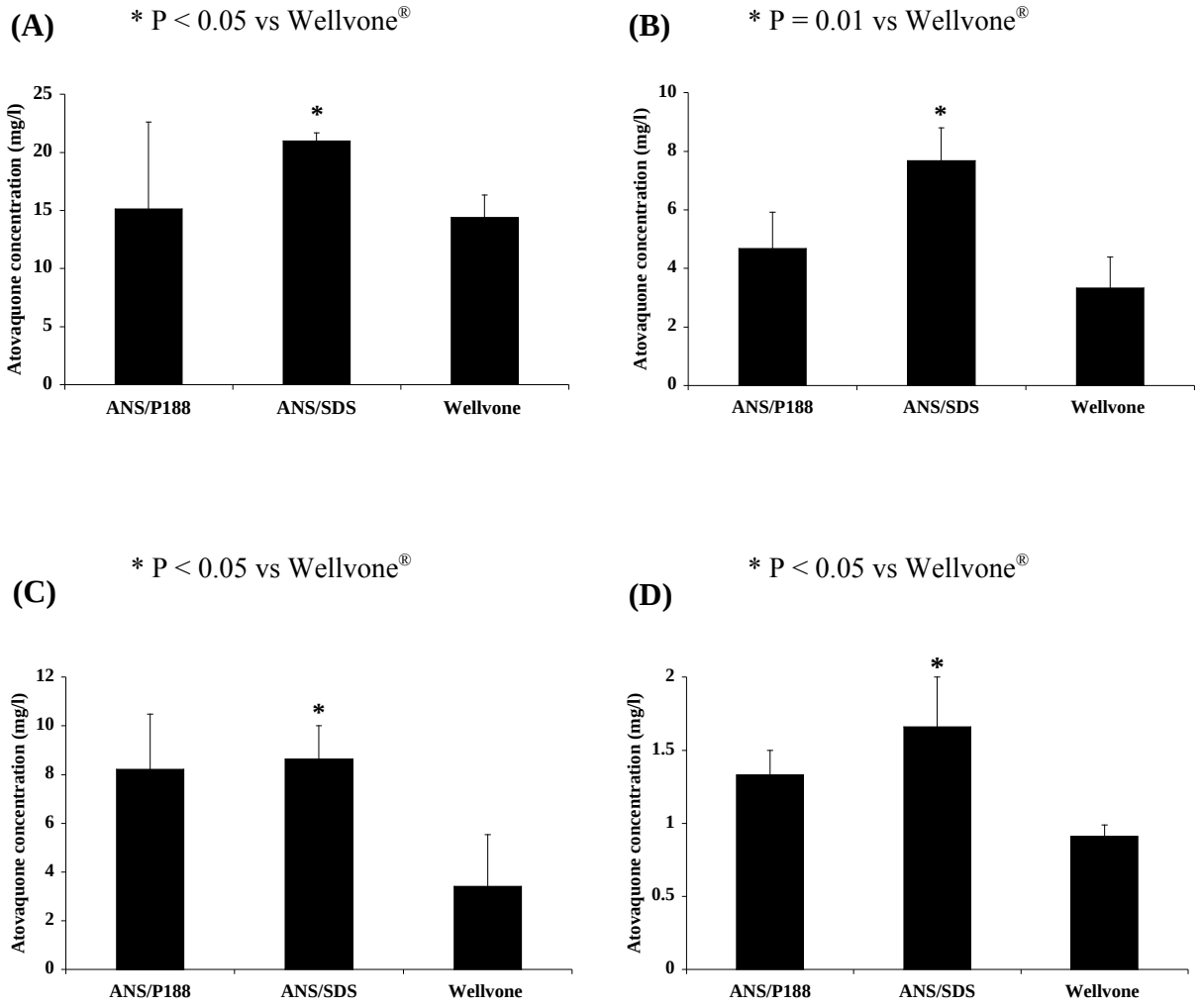

Fig. 28: Atovaquone concentrations in serum (A), lungs (B), livers (C), and brains (D) of infected C57BL/6J mice after oral treatment with atovaquone compounds at 100 mg/kg body weight measured by HPLC. Results show pooled data from 3 to 4 mice/group ± SD

7.8.2.2 Antiparasitic effect of atovaquone

Untreated control mice showed high numbers of inflammatory foci in brains and livers (Fig. 29). All preparations significantly lowered numbers of inflammatory foci compared to untreated control mice. ANS/SDS-treated mice showed significantly lower numbers of inflammatory foci in brains and livers compared to mice treated with Wellvone®. There was no significant difference in numbers of inflammatory foci in brains and livers of mice treated with ANS/P188 and Wellvone® (Fig. 29).

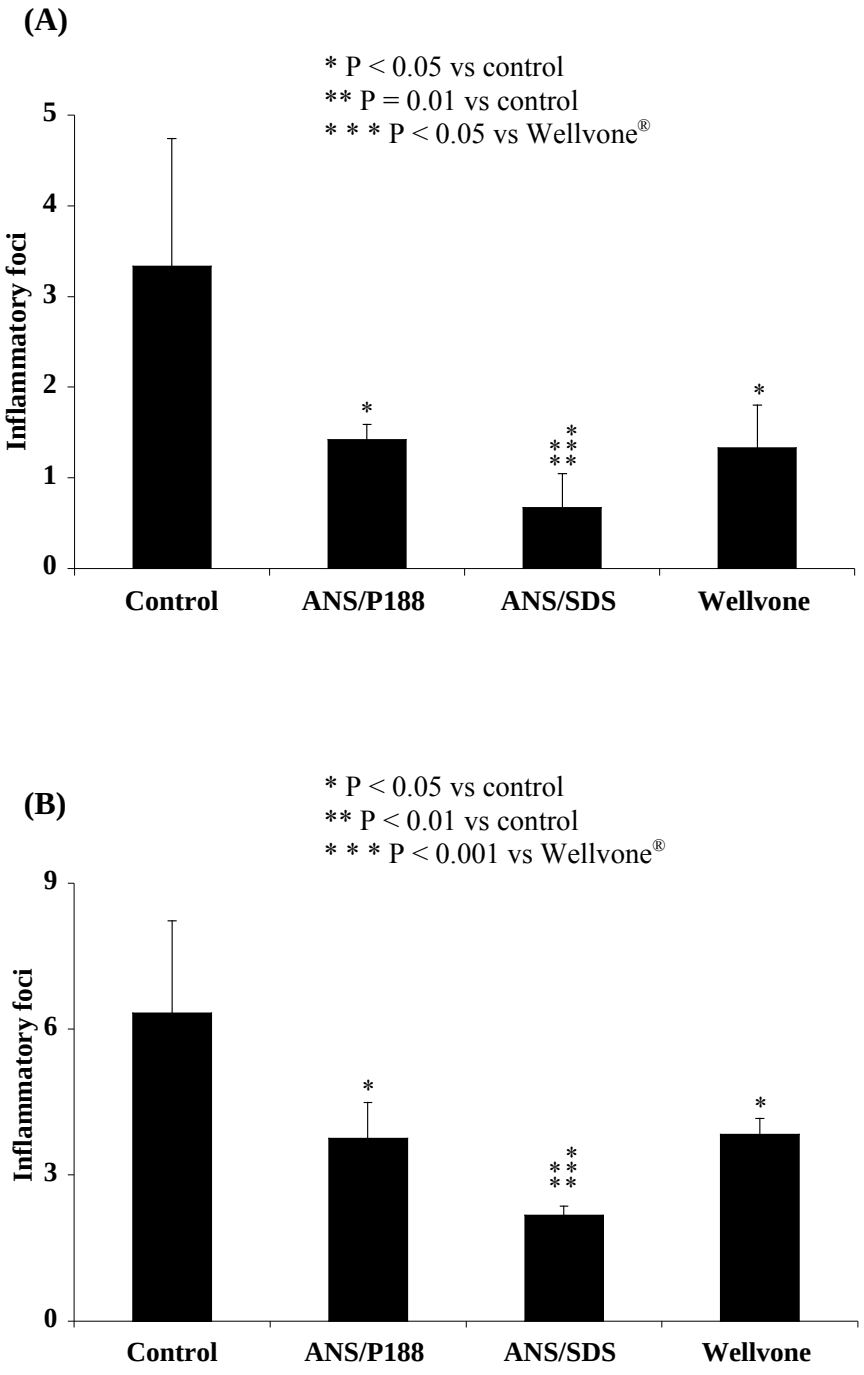

Fig. 29: Inflammatory foci (H&E) in brains (A) and livers (B) of C57BL/6J mice orally infected with *T. gondii* and treated orally with atovaquone compounds at 100 mg/kg body weight. Results show pooled data from 4 to 5 mice/group ± SD

Numbers of parasite in lungs, livers, and brains of *T. gondii* infected mice orally treated with atovaquone preparations as measured by immunohistology are shown in Fig. 30. All preparations (except for Wellvone® in the liver) significantly reduced parasite numbers compared to untreated control mice. In livers and brains, ANS/SDS significantly reduced parasite numbers compared to Wellvone® treated mice, whereas in lungs, livers, and brains, parasite numbers did not differ in mice treated with ANS/P188 and Wellvone® (Fig. 30).

These histological results suggest that ANS/SDS has a significantly higher therapeutic efficacy compared to Wellvone® by reducing parasite numbers and inflammatory foci following infection with *T. gondii*.

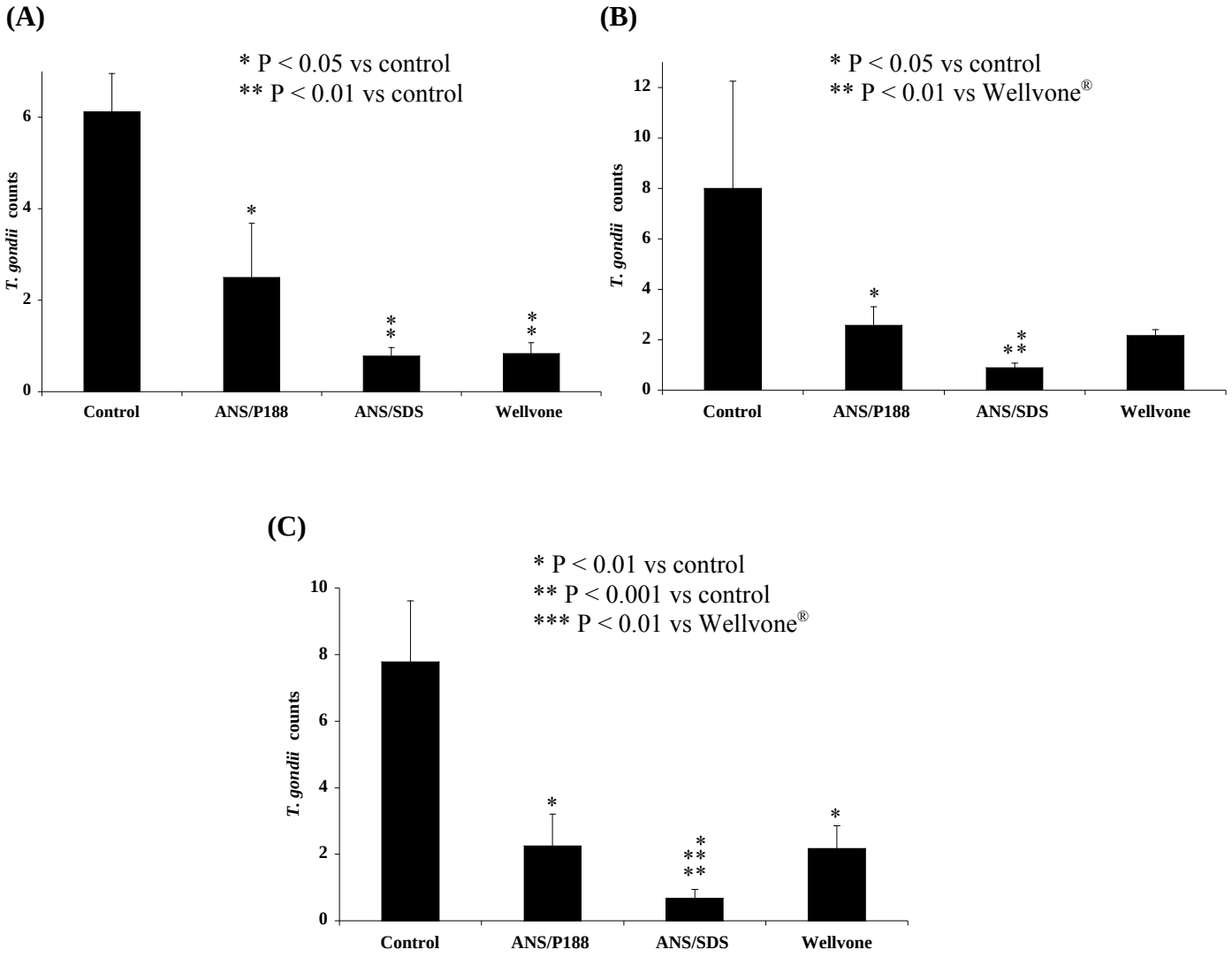

Fig. 30: Numbers of parasitophorous vacuoles and free parasite antigen as determined by immunoperoxidase staining in lungs (A), livers (B), and brains (C) of C57BL/6J mice orally infected with ME49 *T. gondii* and treated orally with atovaquone compounds at 100 mg/kg body weight. Results show pooled data from 4 to 5 mice/group ± SD

Antiparasitic effects of atovaquone preparations as measured by LightCycler-PCR are shown in Fig. 31. All compounds significantly lowered parasite loads in lungs and brains compared to untreated control mice. Lungs of ANS/SDS-treated mice showed significant lower numbers of parasite load (DNA) compared to Wellvone®-treated mice (Fig. 31). There was no significant difference between parasite loads in lungs and brains of mice treated with ANS/P188 and Wellvone®.

These data confirm the histological finding suggesting that ANS/SDS has significantly higher antiparasitic effect than the micronized suspension (Wellvone®) following infection with *T. gondii*.

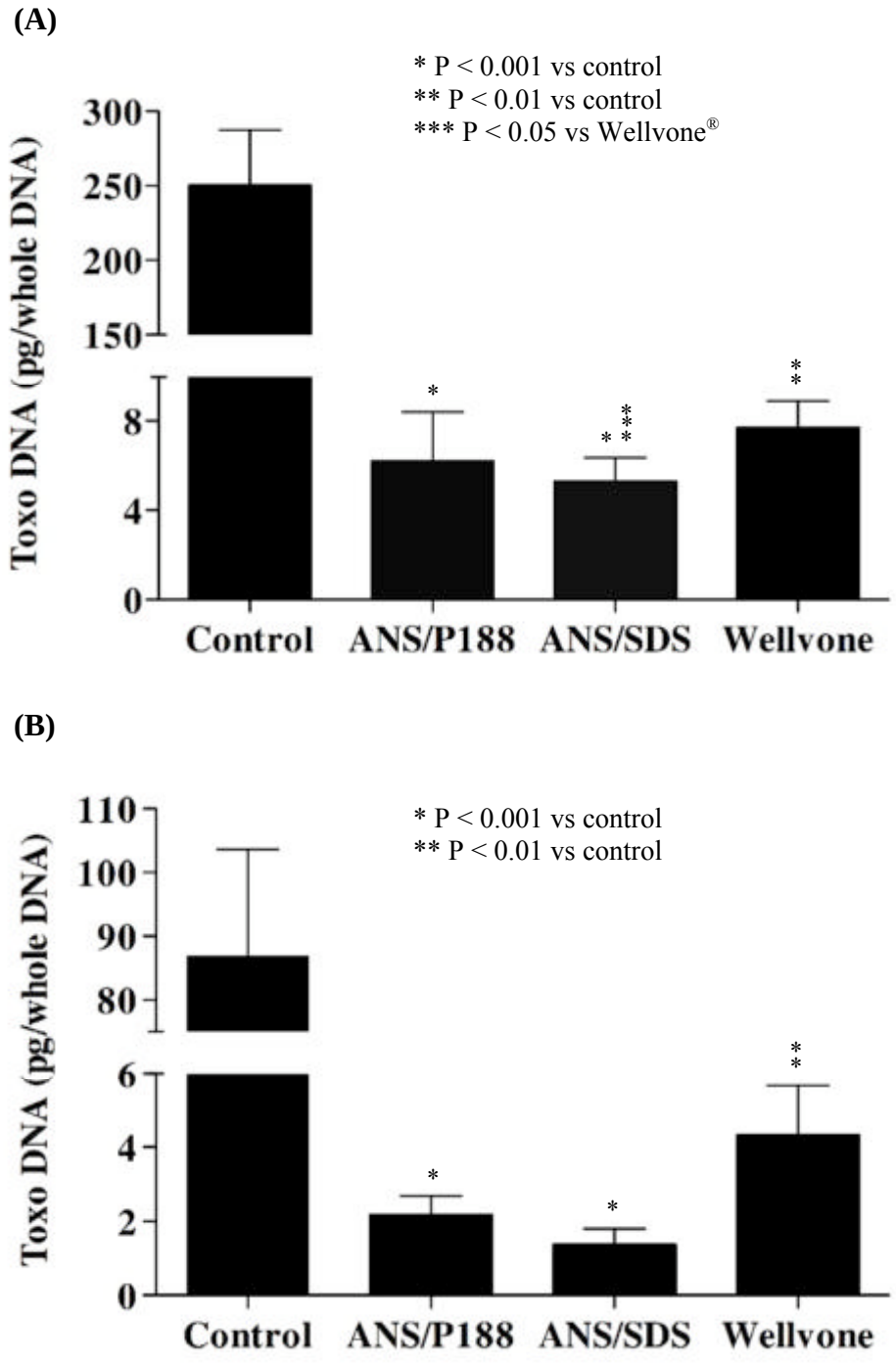

Fig. 31: *T. gondii* DNA load as determined by LightCycler-PCR in lungs (A) and brains (B) of C57BL/6J mice orally infected with 10 cysts ME49 *T. gondii* and treated orally with atovaquone compounds at 100 mg/kg body weight. Results show pooled data from 3 to 4 mice/group ± SD

7.9 Therapeutic efficacy of atovaquone in a murine model of reactivated toxoplasmosis

Since SDS-coated ANS enhanced oral and brain uptake of atovaquone, and showed higher antiparasitic effect compared to micronized suspension (Wellvone®) in a murine model of acute toxoplasmosis, I investigated the role of SDS in enhancing bioavailability and antiparasitic effects of atovaquone in mice with TE that mimics the reactivation of brain cysts observed in severly immunocompromised patients, i.e. AIDS patients.

7.9.1 Therapeutic efficacy of atovaquone preparations at 50 mg/kg body weight

Initially, mice were treated with 50 mg/kg body weight of ANSs coated with Tween® 80, P188, or SDS, or treated with micronized suspension (Wellvone®) from day 2 to day 8 after withdrawal of sulfadiazine (see Material and Methods).

7.9.1.1 Atovaquone concentrations in serum and organs

To determine the bioavailability, distribution, and uptake of atovaquone, sera, brains, lungs, and livers were obtained on day 9 after reactivation and processed by HPLC (Fig. 32).

Atovaquone concentrations were significantly higher in sera and brains of mice treated with SDS-coated ANS compared to Wellvone®-treated mice. In brains of mice treated with ANS/Tween® 80, atovaquone levels were significantly lower than in Wellvone®-treated mice whereas atovaquone concentrations in sera of mice treated with ANS/Tween® 80, ANS/P188 and Wellvone® did not differ.

These results indicate that in mice with reactivated toxoplasmosis SDS-coated ANS display increased bioavailability compared to micronized suspension (Wellvone®).

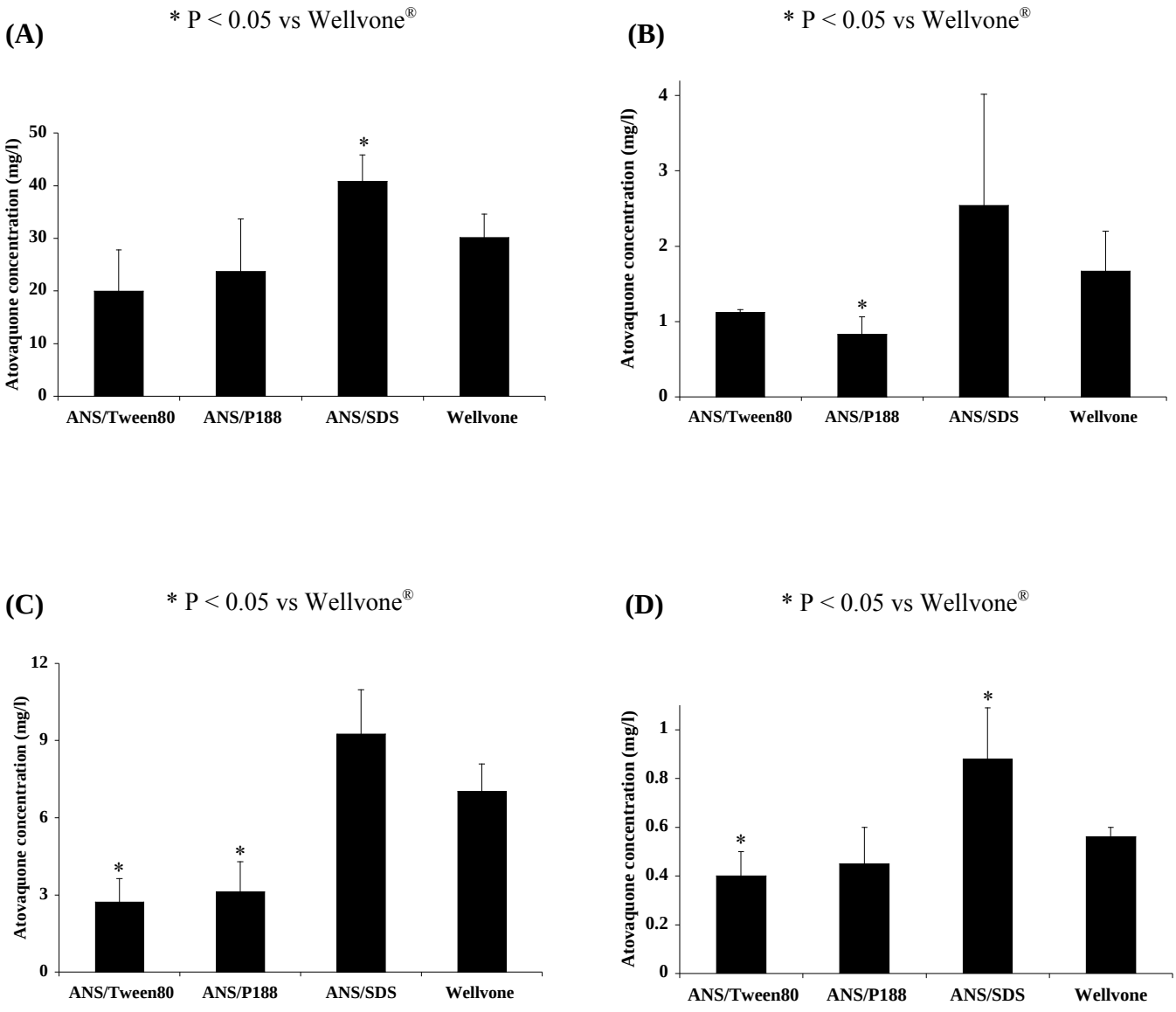

Fig. 32: Atovaquone concentrations in serum (A), lungs (B), livers (C), and brains (D) of infected IRF-8$^{-/-}$ mice after oral treatment with atovaquone compounds at 50 mg/kg body weight measured by HPLC. Results show pooled data from 3 to 4 mice/group ± SD

7.9.1.2 Antiparasitic effect of atovaquone

In order to investigate whether increased bioavailability of ANSs in mice with TE is accompanied by increased antiparasitic effects compared to micronized suspension (Wellvone®), immunohistological staining as well as LightCycler-PCR analysis were performed. Untreated mice developed inflammatory foci in brains and livers (Fig. 33). All preparations (except for Wellvone® in brains) significantly lowered numbers of inflammatory foci in brains and livers compared to untreated control mice. ANS/SDS-treated mice showed significantly lower numbers of inflammatory foci in brains and livers compared to mice treated with Wellvone®. There was no significant difference in numbers of inflammatory foci in brains of mice treated with ANS/Tween® 80, ANS/P188, or Wellvone® (Fig. 33).

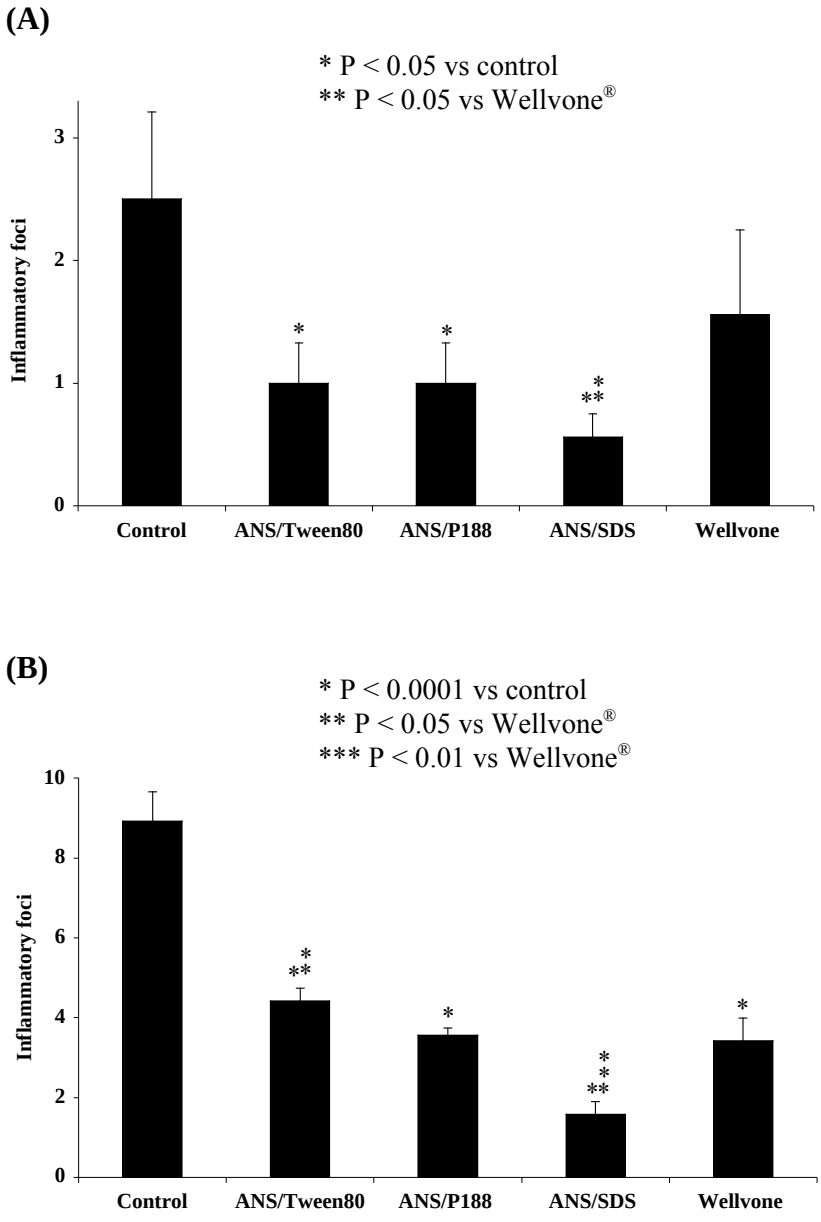

Fig. 33: Inflammatory foci (H&E) in brains (A) and livers (B) of IRF-8$^{-/-}$ mice orally infected with ME49 *T. gondii* and treated orally with atovaquone compounds at 50 mg/kg body weight. Results show pooled data from 4 to 5 mice/group ± SD

To investigate whether decreased numbers of histopathological changes were caused by decreases in parasite numbers, I microscopically determined numbers of parasite antigens in lungs, livers, and brains of mice treated with ANSs compared to mice treated with micronized suspension (Wellvone®).

ANS/SDS significantly reduced parasite numbers in livers and brains compared to Wellvone® treated mice (Fig. 34). All preparations (except for Wellvone® in livers and brains) significantly reduced parasite numbers compared to untreated control mice. All nanosuspensions significantly reduced parasite numbers in brains of mice compared to Wellvone®. In lungs and livers parasite numbers did not differ in mice treated with ANS/Tween® 80, ANS/P188, and Wellvone®.

Figure 35 show histological changes and parasites in brains of mice treated with atovaquone preparations.

In conclusion, these histological results suggest that ANS/SDS has a significantly higher therapeutic efficacy compared to Wellvone® by reducing parasite numbers and inflammatory foci following infection with *T. gondii*.

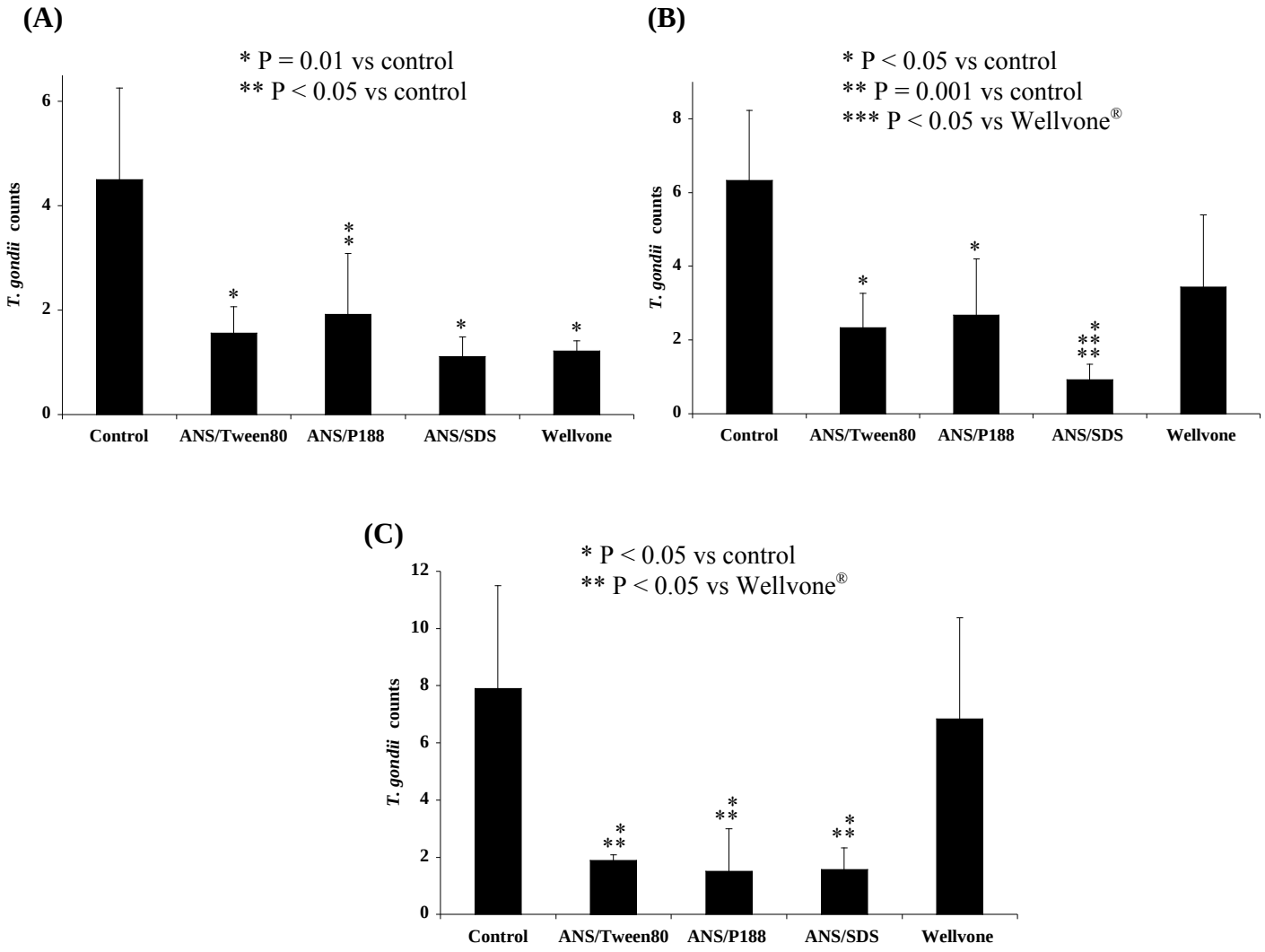

Fig. 34: Numbers of parasitophorous vacuoles and free parasite antigen as determined by immunoperoxidase staining in lungs (A), livers (B), and brains (C) of IRF-8$^{-/-}$ mice orally infected with ME49 *T. gondii* and treated orally with atovaquone compounds at 50 mg/kg body weight. Results show pooled data from 4 to 5 mice/group ± SD

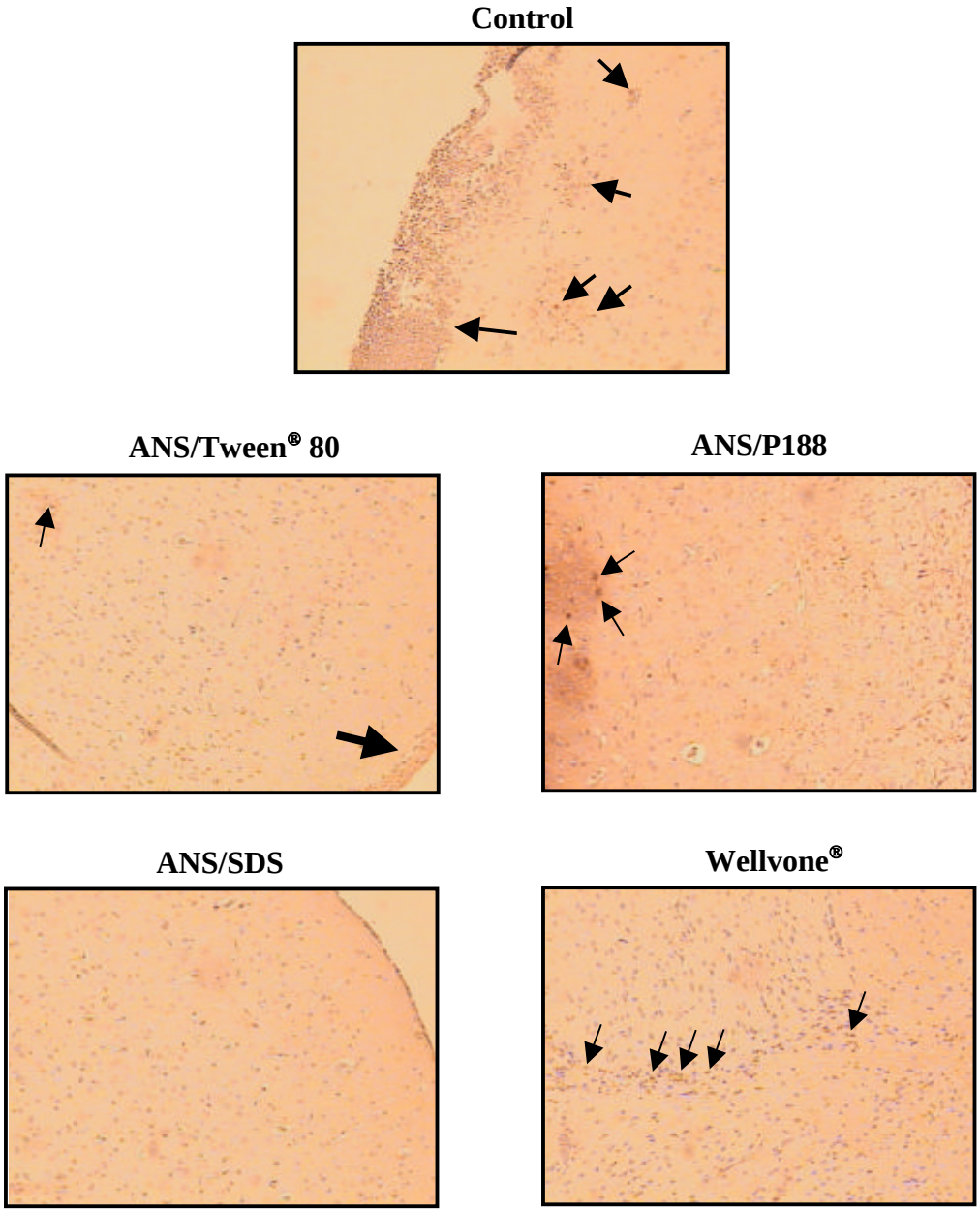

Fig. 35: Histologic changes in brains of IRF-8$^{-/-}$ mice with TE orally infected with ME49 *T. gondii* and treated orally with atovaquone compounds at 50 mg/kg. Small arrows indicate parasitic foci (parasitophorous vacuoles and parasitic antigen), large arrows indicate meningeal inflammation (immunoperoxidase staining, magnification x200). The sections shown are representative for at least four mice per group; experiments were repeated twice

To investigate whether histological findings are accompanied by a reduction in parasite load (DNA) in brains of mice (obtained on day 9 after reactivation of toxoplasmosis) and orally treated with atovaquone preparations (ANS/Tween® 80, ANS/P188, ANS/SDS, and Wellvone®) LightCycler-PCR analysis was performed.

Brains of mice treated with SDS-coated nanosuspensions showed a significant reduction in parasite load compared to brains of mice treated with micronized suspension (Wellvone®) (Fig. 36), whereas in mice treated with P188-coated nanosuspensions the parasite load was significantly higher than in mice treated with Wellvone®. Parasite load in brains of mice treated with ANS/Tween® 80 and Wellvone® did not differ.

These data confirm the histological finding suggesting that ANS/SDS has a significantly higher antiparasitic effect than the micronized suspension (Wellvone®) following infection with *T. gondii*.

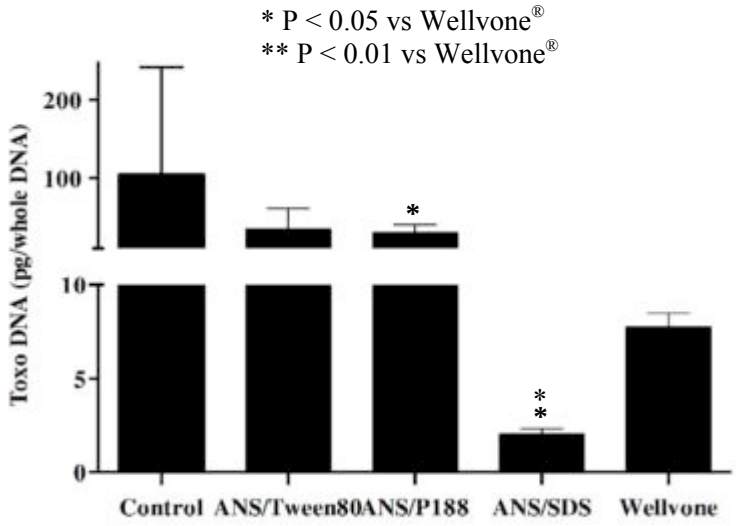

Fig. 36: *T. gondii* DNA load as determined by LightCycler-PCR in brains of IRF-8$^{-/-}$ mice orally infected with 10 cysts ME49 *T. gondii* and treated orally with atovaquone compounds at 50 mg/kg body weight. Results show pooled data from 3 to 4 mice/group ± SD

7.9.2 Therapeutic efficacy of atovaquone preparations at 100 mg/kg body weight

In order to investigate whether increased bioavailability of atovaquone by surfactants is established at higher dosages, I treated mice with ANSs coated with P188 or SDS at a concentration of 100 mg/kg body weight from day 2 to day 8 after reactivation of toxoplasmosis and compared the therapeutic efficacy with that of the micronized suspension (Wellvone®). Concentrations of atovaquone were determined in serum and organs by HPLC analysis, and the antiparasitic effects of nanosuspensions were analysed by microscopy and quantitative PCR.

7.9.2.1 Atovaquone concentrations in serum and organs

Following treatment with 100 mg/kg body weight atovaquone was detected in sera and organs including the brain of all mice (Fig. 37). Atovaquone concentrations were significantly higher in serum, brains, lungs, and livers in ANS/SDS-treated mice compared to Wellvone®-treated mice. Atovaquone concentrations in serum and organs (except in the liver) of mice treated with ANS/P188 did not differ significantly from those in Wellvone®-treated mice.

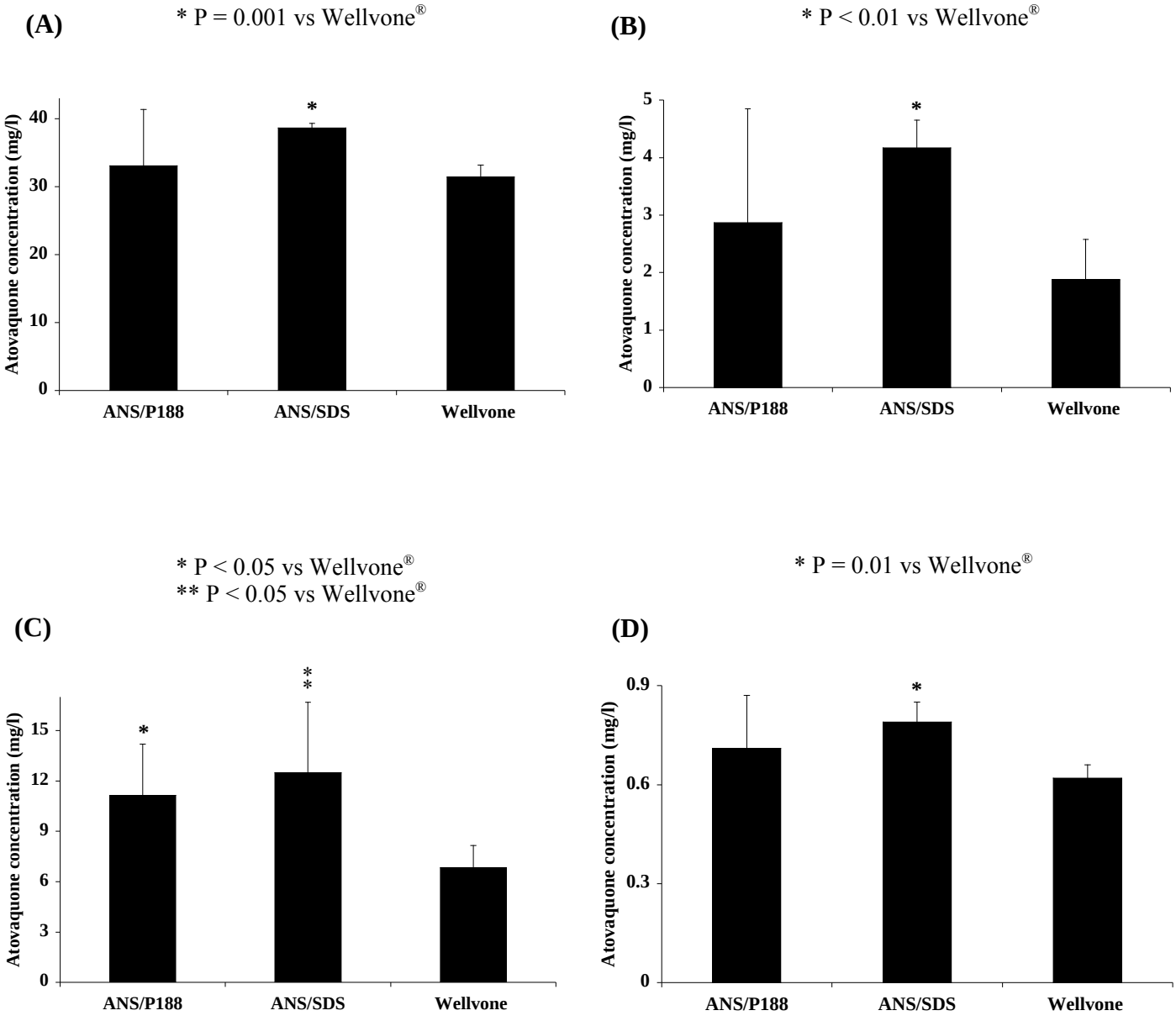

Fig. 37: Atovaquone concentrations in serum (A), lungs (B), livers (C), and brains (D) of infected IRF-8$^{-/-}$ mice after oral treatment with atovaquone compounds at 100 mg/kg body weight measured by HPLC. Results show pooled data from 3 to 4 mice/group ± SD

These results indicate that SDS-coated ANS appears to have an increased bioavailability compared to micronized suspension (Wellvone®) when given at higher dosages in mice with reactivated toxoplasmosis thereby underlining the observations obtained at lower dosages of atovaquone preparations.

7.9.2.2 Antiparasitic effect of atovaquone

H&E staining was performed on brains and livers of mice obtained on day 9 after reactivation of toxoplasmosis.

Untreated control mice showed high numbers of inflammatory foci in brains and livers (Fig. 38). All preparations significantly lowered numbers of inflammatory foci in livers compared to untreated control mice. ANS/SDS-treated mice showed significantly lower numbers of inflammatory foci in brains and livers compared to mice treated with Wellvone®. There was no significant difference in numbers of inflammatory foci in brains and livers of mice treated with ANS/P188 and Wellvone® (Fig. 38).

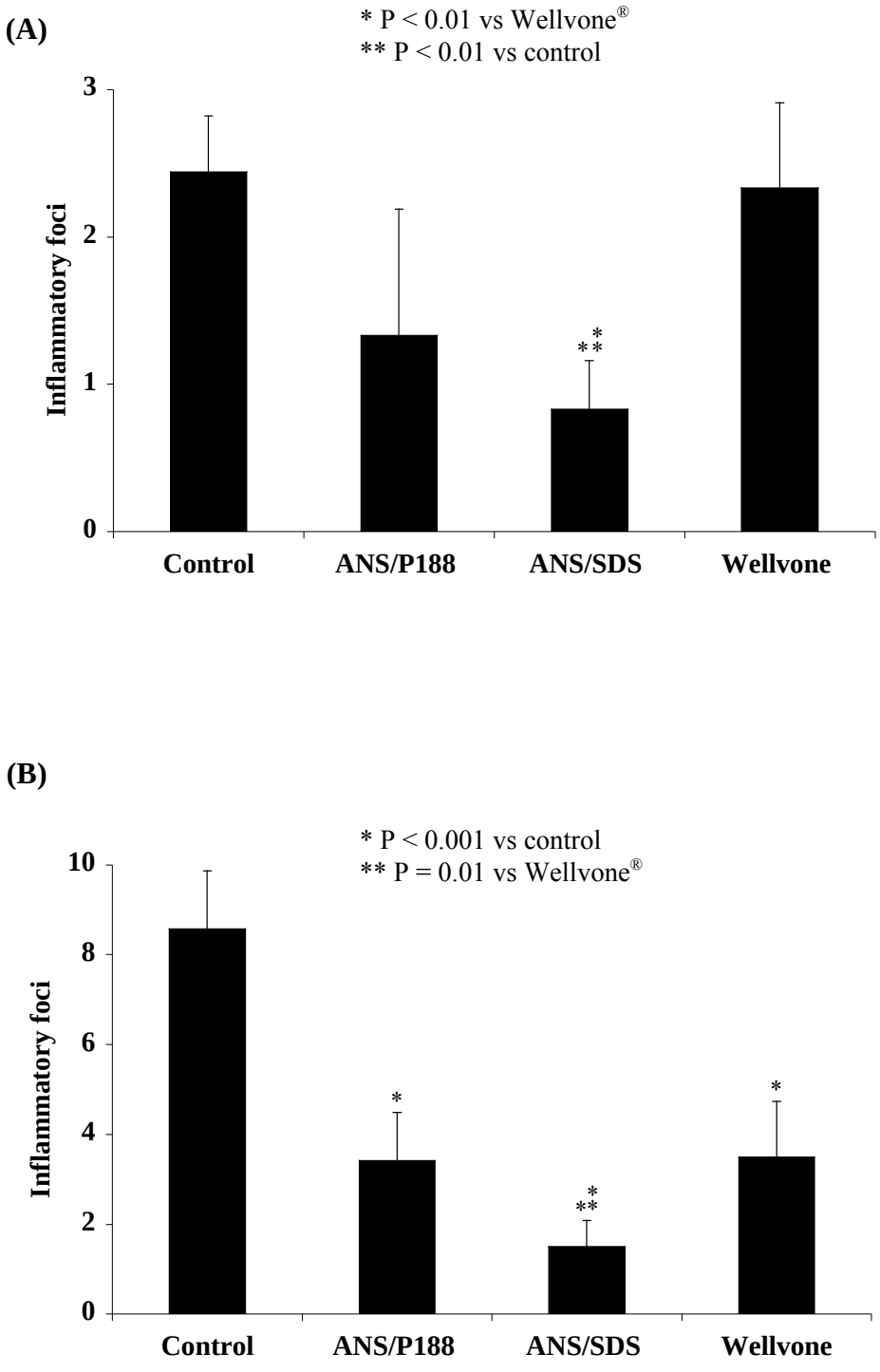

Fig. 38: Inflammatory foci (H&E) in brains (A) and livers (B) of IRF-8$^{-/-}$ mice orally infected with ME49 *T. gondii* and treated orally with atovaquone compounds at 100 mg/kg body weight. Results show pooled data from 4 to 5 mice/group ± SD

Numbers of parasites in lungs, livers, and brains of mice with TE and orally treated with atovaquone preparations as measured by immunohistology are shown in Fig. 39. All preparations (except Wellvone®) significantly reduced parasite numbers in lungs, livers, and brains compared to untreated control mice. In all organs, ANS/SDS significantly reduced parasite numbers compared to Wellvone® treated mice, whereas parasite numbers did not differ in mice treated with ANS/P188 and Wellvone® (Fig. 39).

These histological findings (H&E and PAP) indicate that SDS-coated nanosuspensions enhanced the antiparasitic effect compared to the micronized suspension (Wellvone®).

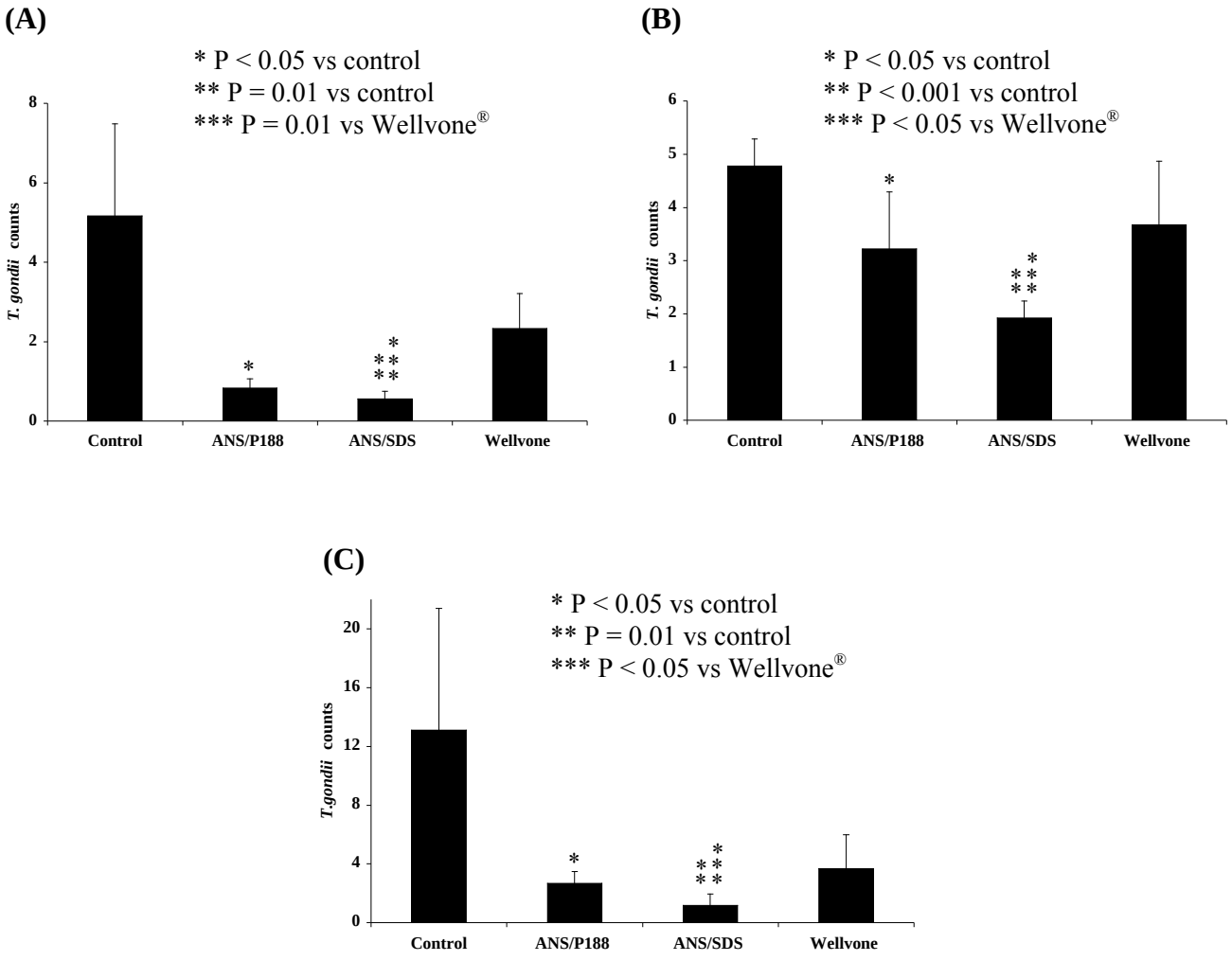

Fig. 39: Numbers of parasitophorous vacuoles and free parasite antigen as determined by immunoperoxidase staining in lungs (A), livers (B), and brains (C) of IRF-8$^{-/-}$ mice orally infected with ME49 *T. gondii* and treated orally with atovaquone compounds at 100 mg/kg body weight. Results show pooled data from 4 to 5 mice/group ± SD

Antiparasitic effects of atovaquone preparations as measured by LightCycler-PCR are shown in Fig. 40. P188 and SDS-coated ANSs (and not Wellvone®) significantly lowered parasite loads in brains compared to untreated control mice. Brains of ANS/SDS-treated mice showed significant lower numbers of parasite load (DNA) compared to Wellvone®-treated mice (Fig. 40). There was no significant difference between parasite loads in brains of mice treated with ANS/P188 and Wellvone®.

These data confirm the histological finding shown above suggesting that ANS/SDS has significantly higher antiparasitic effects than the micronized suspension (Wellvone®) following infection with *T. gondii*.

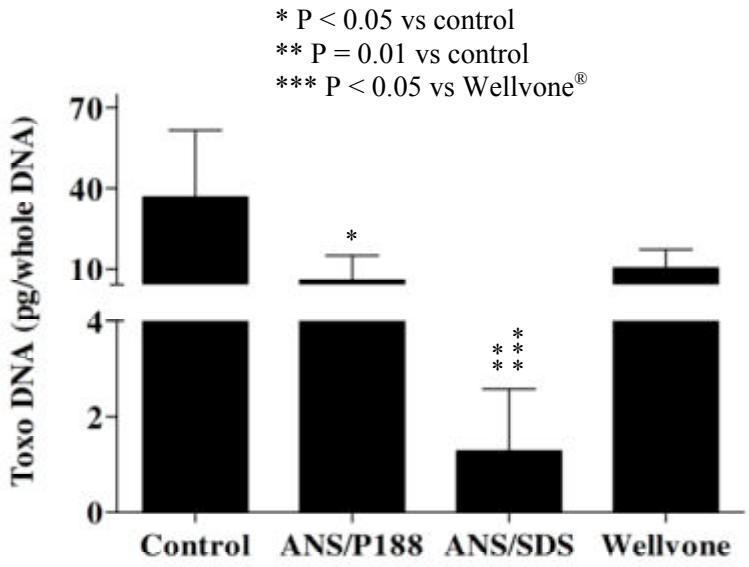

Fig. 40: *T. gondii* DNA load as determined by LightCycler-PCR in brains of IRF-8$^{-/-}$ mice orally infected with 10 cysts ME49 *T. gondii* and treated orally with atovaquone compounds at 100 mg/kg body weight. Results show pooled data from 3 to 4 mice/group ± SD

Since SDS enhanced oral and brain uptake and antiparasitic effect of atovaquone in murine acute and reactivated toxoplasmosis models compared to the micronized suspension (Wellvone®) when given in equal dosages, I was interested to investigate whether a lower dose of ANS coated with SDS (50 mg/kg) have similar or superior therapeutic effects compared to Wellvone® (administered in dosages equal to those used in humans 100 mg/kg body weight).

Atovaquone concentrations were significantly higher in sera of mice treated with SDS-coated ANSs (50 mg/kg) compared to Wellvone®-treated mice (50 or 100 mg/kg) and mice treated with ANS/Tween® 80 (Fig. 41A). Atovaquone concentrations in sera of mice treated with ANS/Tween® 80, ANS/P188 and Wellvone® did not differ (Fig. 41A).

Atovaquone concentrations were significantly higher in brains of mice treated with SDS-coated ANSs (50 mg/kg) compared to Wellvone®-, ANS/Tween® 80-, and ANS/P188-treated mice (all 50 mg/kg) (Fig. 41B). Atovaquone concentrations in brains of mice treated with ANS/SDS and Wellvone® (100 mg/kg) did not differ. Atovaquone concentrations were significantly higher in Wellvone®-treated mice (100 mg/kg body) compared to Wellvone®-treated mice (50 mg/kg body) (Fig. 41B).

These results indicate that SDS-coated ANSs administered at 50% of the clinical dosage showed similar bioavailabilities compared to full clinical doses of the micronized suspension (Wellvone®).

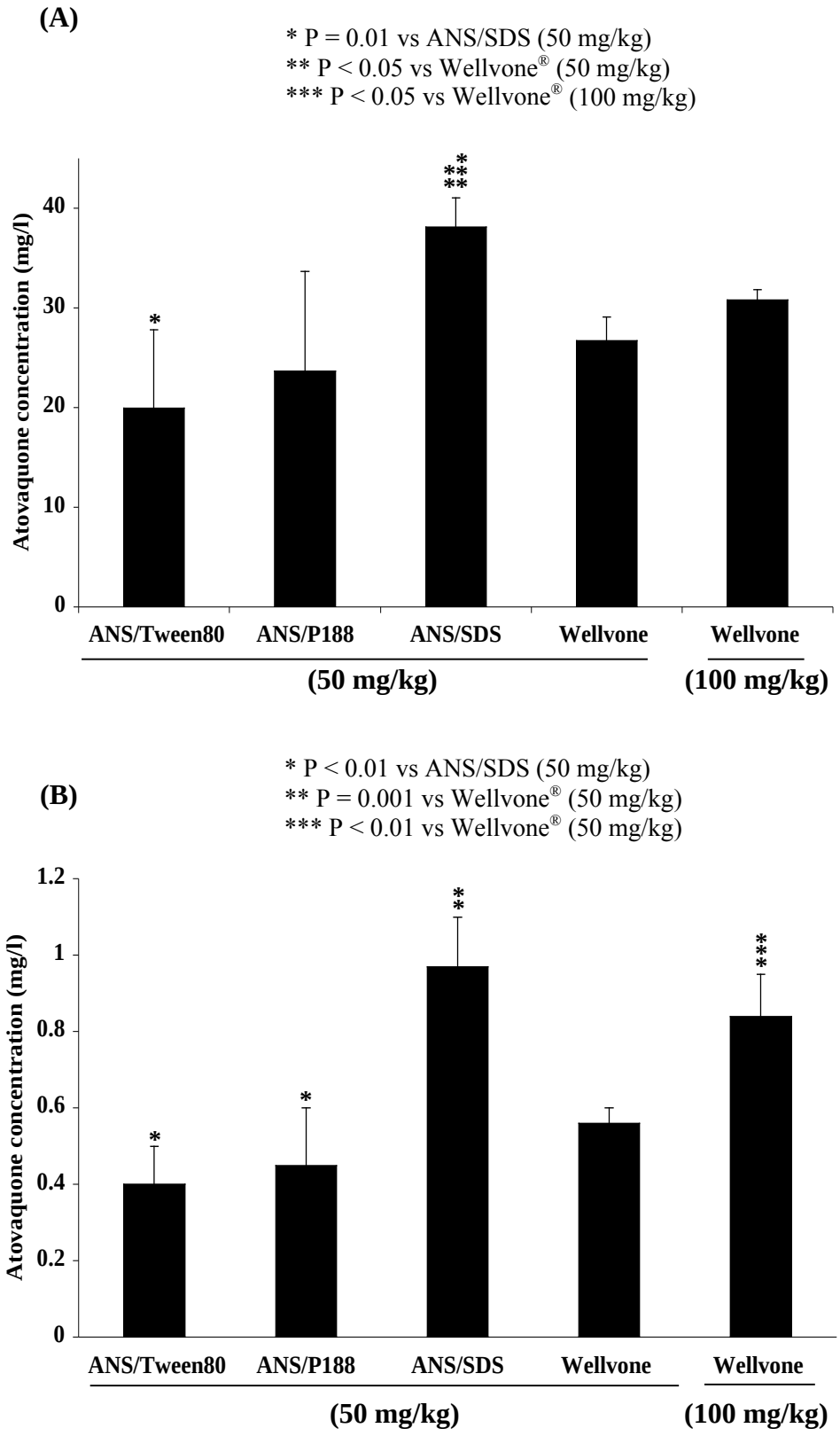

Fig. 41: Atovaquone concentrations in serum (A) and brains (B) of infected IRF-8$^{-/-}$ mice after oral treatment with atovaquone compounds at 50 mg/kg body weight (ANSs and Wellvone®) and 100 mg/kg body weight (Wellvone®) measured by HPLC. Results show pooled data from 3 to 4 mice/group ± SD

I then performed LightCycler-PCR analysis to investigate whether a 50% dosage of SDS-coated ANSs would result in similar antiparasitic effects as the full dosage of the micronized suspension (Wellvone®) in brains of mice orally infected with *T. gondii*.

ANS/SDS (50 mg/kg)-treated mice showed significantly lower parasite loads in brains compared to mice treated with Wellvone® (50 mg/kg) (Fig. 42). There was no significant difference in parasite loads in brains of mice treated with ANS/SDS (50 mg/kg) and Wellvone® (100 mg/kg) (Fig. 42) indicating similar antiparasitic effect. Wellvone® (100 mg/kg)-treated mice showed significantly lower parasite loads compared to mice treated with Wellvone® (50 mg/kg) (Fig. 42).

These data suggest that 50% dosages of SDS-coated ANSs due to the increased bioavailability result in similar antiparasitic effects compared to the micronized suspension (Wellvone®).

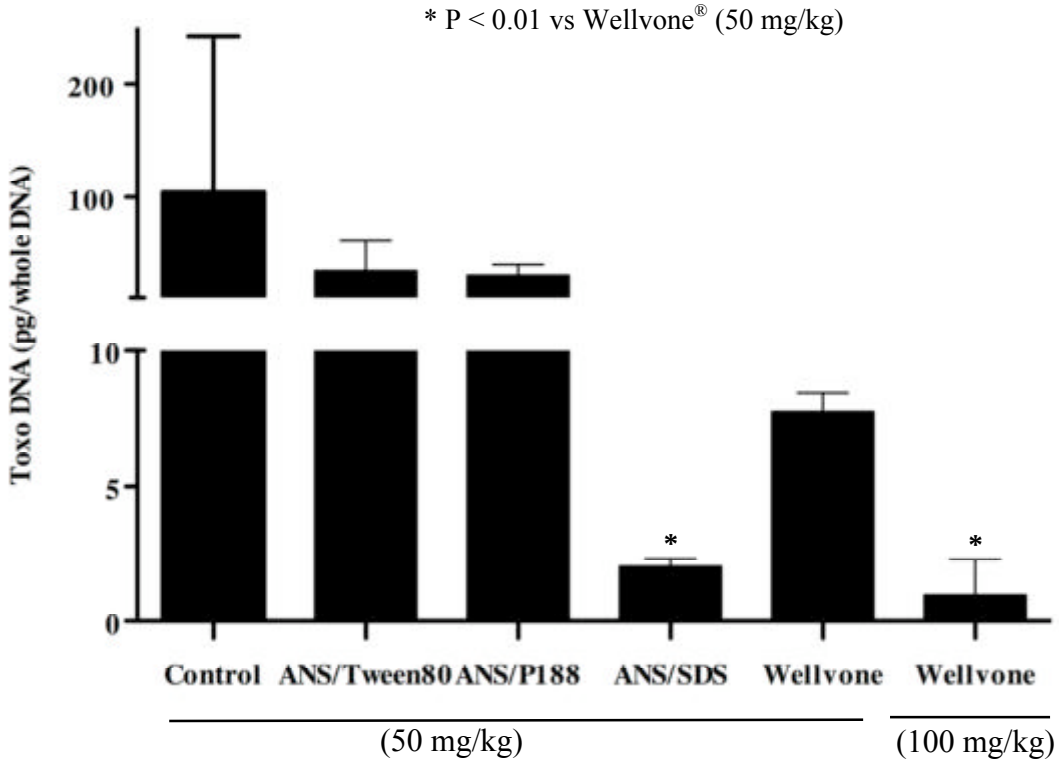

Fig. 42: *T. gondii* DNA load as determined by LightCycler-PCR in brains of IRF-8$^{-/-}$ mice orally infected with 10 cysts ME49 *T. gondii* and treated orally with atovaquone compounds at 50 mg/kg body weight (ANSs and Wellvone©) and 100 mg/kg body weight (Wellvone®). Results show pooled data from 3 to 4 mice/group ± SD

8 Discussion

TE continues to be a severe health problem in immunocompromised hosts including AIDS and transplant patients. Since numbers of transplantations are likely to increase further in the future and standard therapy against TE -the combination of pyrimethamine and sulfadiazine or clindamycin- is often accompanied by severe side effects, alternative therapeutic treatments are urgently needed. Since new compounds with strong antiparasitic effects and favorable safety profile are scarce modified formulations of established compound may be a successful strategy to improve treatment.

Atovaquone, a hydroxy-1,4-naphthoquinone, has an excellent safety profile (Hughes et al 1993, Hughes 1995) confirmed in volunteer studies in humans and shows excellent in-vitro inhibitory effects against *T. gondii* (Araujo et al 1991, Romand et al 1993). However, the present oral micronized suspension (Wellvone®) shows only poor bioavailability of 23% that increases to 47% when administered with meals.

Atovaquone is lipophilic with extremely low aqueous solubility (Rolan et al 1994) resulting in poor bioavailability after oral administration. More recently, nanosuspensions have emerged as a promising strategy for the efficient delivery of hydrophobic drugs because of their versatile features and unique advantages (Patravale et al 2004). Since nanocrystals improve the solubility of poorly water-soluble drugs (Keck & Mueller 2006, Mueller et al 1998), ANSs were synthesized and coated with different surfactants by our group (Dunay et al 2004, Scholer et al 2001, Shubar et al 2009).

Since reactivation of infection with *T. gondii* presents in the central nervous system, drugs for the treatment have to cross the gastrointestinal and blood-brain barrier when administered orally. The purpose of the present study was to investigate the passage of tissue barriers in the host by newly generated ANSs stabilized by different surfactants (Tween® 80, P188 and SDS) compared to the commercially available oral atovaquone suspension (Wellvone®).

To address this question experimentally, I initially used in-vitro models of the blood-brain and intestinal barriers to investigate the passage and toxicity of ANSs. After identification of appropriate candidate formulations of ANSs, I used murine models of acute and reactivated toxoplasmosis to confirm the antiparasitic effects of ANSs.

ANSs were produced by high-pressure homogenization under aseptic conditions (Dunay et al 2004, Scholer et al 2001, Shubar et al 2009). The high-pressure homogenization technique has several advantages over other techniques for production of nanocrystals including the simplicity of the process, ease of large-scale production, and a reduced product contamination (Keck & Mueller 2006). ANSs were then stabilized by surfactants (Bohm & Mueller 1999). As a result of the reduced size of the nanocrystals, the saturation solubility and dissolution velocity are increased accompanied by an increase in bioavailability.

Since many authors have shown that therapeutic agents can be transported across the BBB by binding them to PBCA nanoparticles coated with Tween® 80 (e.g. rivastigmine, dalargin, kytorphin, loperamide, and tubocurarine) (Alyautdin et al 1997, Alyautdin et al 1998, Kreuter et al 1995, Schroeder et al 1998, Wilson et al 2008a, Wilson et al 2008b), P188 is known as an efficient stabilizer of drug-loaded nanocrystals (e.g. docetaxel, amoxicillin, doxorubicin) (Fontana et al 2001, Keck 2006, Kreuter & Gelperina 2008, Mueller 1991, Yan et al 2009, Zhang & Fang 2008), and SDS is known to enhance transport of drug molecules across epithelial barrier (e.g. mannitol, 1-deamino-8-o-arginine-vasopressin, polyethylene glycothe, and tiludronate) (Anderberg & Artursson 1993, Boulenc et al 1995) and stabilizes drug-loaded nanoparticles (e.g. trimethoprim and ascorbyl palmitate) (Sun et al 2009, Teeranachaideekul et al 2008), therefore these surfactants –together with the physical properties of nanosuspensions- may be key to direct drugs across host barriers.

Furthermore, I used P188 as a stabilizer since it is used in the commercial micronized suspension of atovaquone (Wellvone®).

Before performing in-vitro and in-vivo experiments ANSs were characterized by LD and PCS. The mean sizes of nanosuspensions ranged between 415 and 469 nm whereas Wellvone® particles were markedly bigger (967 nm). Nanosuspensions had a narrow size distributions, whereas Wellvone® had a very broad size distribution. Furthermore, ANSs displayed a homogenously distributed solution as single particles whereas Wellvone® displayed a more clustered distribution pattern as measured by light microscopy. Since ANSs were found to be smaller in size and more uniform in shape than Wellvone®, they were considered as candidates for testing of the passage of host barriers in-vitro as well as bioavailability and antiparasitic effects in-vivo.

Coating of ANSs with the non-ionic surfactants Tween® 80 and P188 lead to a slight negative surface charge on the particles confirming the presumption that surfactants of this group do not change the surface charge of nanoparticles (Soukupová et al 2008).

In contrast, SDS has considerably influenced the surface charge of the ANSs. The adsorption of this surfactant is responsible, due to its active anionic part, for a considerable increase in the negative charge of the particles leading to a high negative ZP. Particles with ZP of higher than -30 mV are considered stable (Mishra et al 2008). Interestingly, the addition of ionic surfactants does not only lead to the stabilization of nanosuspensions (enhancing electrostatic potential by the adsorption of the surface-active substances on the nanoparticles surface) but it has also been reported to result in improved size distributions (Roux et al 1989, Soukupová et al 2008). Therefore, ANS/SDS can be considered more stable than the other preparations.

Recently, coating with P188 of docetaxel (an antitumor chemotherapeutic agent)-loaded PLGA [Poly(lactic-co-glycolic acid)] nanoparticles resulted in a more sustained release and increased efficacy in breast cancer chemotherapy due to its narrower particle size distribution, smaller mean diameter and greater ZP (Yan et al 2009). The cellular uptake of docetaxel-loaded PLGA/P188 nanoparticles by a human breast cancer cell line was higher than that of

PLGA nanoparticles without P188 (Yan et al 2009). Furthermore, there was an increased level of uptake and a faster drug release of PLGA/P188 nanoparticles in tumor cells when compared with PLGA nanoparticle formulations without P188 (Yan et al 2009).

Cytotoxicity of atovaquone preparations was analysed by MTT test a widely used colorimetric assay for cell viability (Wang et al 2006) based in its simple, rapid and reliable performance (Aziz 2006). All tovaquone preparations revealed only minor toxicity in higher concentrations (3 µg/ml). Cytotoxic effects of atovaquone were only observed at concentrations of >5 µg/ml in other studies (Romand et al 1993).

Since the physical characterization and the lack of cytotoxicity made ANSs likely candidates for improved bioavailability and passage of host barriers, I initially investigated their passage through the gastrointestinal barrier using an in-vitro mono-culture model of the intestinal epithelial barrier by culturing MODE-K cells on semi-permeable filters. After adding ANSs to the top chamber of the filters, passage through the filter was documented in the bottom chamber using HPLC. ANSs coated with P188 and Tween® 80 showed significantly increased passage compared to SDS-coated ANSs and Wellvone®. ANS/Tween® 80 and ANS/P188 crossed the transwell monolayer of MODE-K cells with significantly higher efficiency (11 and 12% recovery, respectively) compared to ANS/SDS (6%) and Wellvone® (3.75%). At higher concentrations of atovaquone (3 µg/ml) 12.5 and 11% recovery were observed for ANS/Tween® 80 and ANS/P188, respectively, compared to ANS/SDS (6.7%) and Wellvone® (6%). The relatively low rate of passage of all preparations could be due to the lipophilic nature of the preparations leading to adhesion to plastic surfaces.

Since the BBB represents the major host barrier shielding the central nervous system from the blood stream, I then investigated the passage of ANSs through the BBB using mono-culture (bEnd3 cells) and co-culture transwell systems of the BBB [PRBECs on the top side and astrocytes on the bottom side of semi-permeable filters (Deli et al 1993)]. P188-coated ANSs

showed significantly enhanced passage through the BBB in-vitro compared to Tween® 80-coated ANSs and Wellvone® in mono-culture, and to SDS-coated ANSs and Wellvone® in co-culture.

In-vitro results showing enhanced atovaquone passage through the BBB by the surfactant P188 are similar in mono and co-culture models of the BBB. However in the mono-culture model of the intestinal barrier both P188 and Tween® 80 enhanced passage of atovaquone.

There are several possible explanations for these results. First, Tween® 80 and P188 are nonionic surfactants whereas SDS is anionic surfactant. Since nonionized molecules may penetrate biologic membranes by lipid diffusion because they are much more lipid soluble this could explain the comparatively higher transport of P188 and Tween® 80-coated ANSs through the mono-culture of enterocytes, and the higher passage of P188-coated ANSs in mono and co-culture models of the BBB compared to SDS-coated ANSs and Wellvone®. Furthermore, the size of nanoparticles plays a key role in their adhesion to and interaction with cells (Win & Feng 2005). Generally nanoparticles have relatively higher intracellular uptake compared to microparticles and available to a wider range of biological targets due to their small size and relative mobility (Mohanraj & Chen 2006). Smaller particles have larger surface area, therefore, most of the drug associated would be at or near the particle surface, leading to fast drug release. Whereas, larger particles have large cores which allow more drug to be encapsulated and slowly diffuse out (Mohanraj & Chen 2006). Therefore this could explain the higher passage of ANSs versus the micronized suspension (Wellvone®).

Second, the negative charge of the endothelial cells lining the BBB (de Boer & Gaillard 2006) and the microvillus architecture of the intestinal barrier (Ford 2006) may repulse negatively charged compounds as SDS-coated ANSs more strongly than Tween® 80 and P188-coated ANSs and Wellvone® in in-vitro transport models.

Taken together, these results indicate that ANSs show increased passage through the intestinal barrier and BBB in comparison with the oral suspension Wellvone®. Furthermore, the type of surfactant appears to impact the transport across in-vitro models of the intestinal barrier and BBB. In-vitro, the coating of ANSs with either Tween® 80 or P188 displayed the strongest enhancement in transport through the intestinal and blood brain barriers compared to the micronized suspension (Wellvone®).

To investigate whether increased passage of host barriers by ANSs compared to Wellvone® also resulted in increased antiparasitic effects, the therapeutic efficacy of atovaquone was then analysed in-vitro by flow cytometry. Using percentages of *T. gondii*-infected cells as indicated by the presence of green-fluorescent parasites (Shubar et al 2008) I observed that ANSs coated with either Tween® 80 or P188 inhibited parasite replication by >50% (76 and 57% respectively), whereas ANS/SDS and the micronized suspension (Wellvone®) inhibited parasite replication by <50% (36 and 26% respectively). Thus, it appears that the increased passage of ANSs coated with Tween® 80 and P188 resulted in increased antiparasitic efficacy. Flow cytometry has been used in the past to determine the rates of parasite-infected cells (Di Giorgio et al 2000, Gay-Andrieu et al 1999, Moss et al 1999, Neumann et al 2000). The generation of transgenic parasites expression GFP has initially been used in a number of studies on the cell biology of *T. gondii* (Hu et al 2002b, Kamau et al 2001), however, in recent years the use in drug screens has gained increasing interest since GFP is stable throughout a wide spectrum of conditions and allows rapid screening of large numbers of samples compared to traditional microscopical analysis (Gubbels et al 2003, Tsien 1998).

Recently, I used flow cytometry to show excellent therapeutic activity of newly synthesized bisphosphonates against *T. gondii* tachyzoites carrying the GFP (Shubar et al 2008). *T. gondii* parasites expressing the yellow fluorescent protein have also been used to screen antiparasitic activity of pyrimethamine and clindamycin (Gubbels et al 2003). Alternatively, parasite

numbers have been measured by the incorporation of radioactive uracil (Pfefferkorn & Pfefferkorn 1977), by *T. gondii*-specific antibodies in an ELISA (Derouin & Chastang 1988, Merli et al 1985), or by transgenic expression of the bacterial β-galactosidase reporter gene (McFadden et al 1997).

In summary, coating of ANSs with Tween® 80 and P188 as surfactants showed significantly enhanced transport across the intestinal barrier in comparison to SDS-coated ANSs and Wellvone® suspension in-vitro, and ANSs coated with P188 showed significantly enhanced transport in comparison to Wellvone® in BBB mono and co-culture models. For ANSs coated with either Tween® 80 or P188 the increased passage through cell layers translated into significant increase in antiparasitic activity against *T. gondii* compared to Wellvone®.

Based on the increased passage of cell culture models of the BBB by ANSs compared to Wellvone®, I then investigated whether ANSs show increased bioavailability and uptake into the brain in-vivo. I also analysed whether these features would result in increased therapeutic efficacy compared to Wellvone® in the treatment of TE. I applied 2 mouse models of toxoplasmosis. The model of acute infection with *T. gondii* reflects the acute stage of infection in humans when parasite replication is high and cysts develop in the brain and muscle tissue. In contrast, the murine model of reactivated infection closely reflects the reactivated infection in immunocompromised hosts (Dunay et al 2004, Scholer et al 2001).

The therapeutic efficacy of ANSs coated with different surfactants and Wellvone® was analysed following oral administration of 50 and 100 mg of drug/kg body weight over 7 days. These dosages were used according to previous studies in which an atovaquone suspension administered at a dose of 100 mg/kg/day resulted in reduction in the numbers of cysts and a 100% survival rate in murine models of latent and chronic-progressive infection with *T. gondii* (Araujo et al 1991, Araujo et al 1992, Ferguson et al 1994). Furthermore maintenance therapy with atovaquone at daily doses of 50 or 100 mg/kg (body weight) protected mice

against reactivated TE and death in a murine model of reactivated toxoplasmosis (Dunay et al 2004). Most importantly, dosages of 100 mg/kg body weight given orally to mice are equivalent to those dosages used to treat patients.

Following treatment of mice with 50 mg/kg ANSs coated with Tween® 80, P188, and SDS I observed that the concentrations of atovaquone were significantly higher in the serum and brains of mice treated with SDS-coated ANSs compared to that in Wellvone®-treated mice; this observation was made in a murine model of acute toxoplasmosis. These increased serum and brain concentrations also resulted in decreased parasite loads and decreases in numbers of inflammatory foci in brains of mice treated with SDS-coated ANSs compared to untreated controls or to Wellvone®-treated mice. Furthermore, SDS-coated ANSs at 100 mg/kg also lead to significant increase in atovaquone concentrations in the serum and brains of mice compared to Wellvone®-treated mice. These increased serum and brain concentrations also resulted in decreased parasite loads and decreases in numbers of inflammatory foci in brains of mice treated with SDS-coated ANSs compared to untreated controls or to Wellvone®-treated mice.

In murine model of reactivated toxoplasmosis that closely mimics the reactivation of latent infection in immunocompromised hosts following treatment of mice with 50 mg/kg ANSs coated with Tween® 80, P188, and SDS I observed here also that the concentrations of atovaquone were significantly higher in the serum and brains of mice treated with SDS-coated ANSs compared to that in Wellvone®-treated mice. These increased serum and brain concentrations also resulted in decreased parasite loads and decreases in numbers of inflammatory foci in brains of mice treated with SDS-coated ANSs compared to untreated controls or to Wellvone®-treated mice. Same observations were obtained when mice were treated with SDS-coated ANSs at 100 mg/kg.

I then compared atovaquone concentrations in serum and brains in murine model of reactivated toxoplasmosis. When mice were treated orally with SDS-coated ANSs administered at 50% of the clinical dosage of Wellvone® (100 mg/kg), I observed similar bioavailabilities compared to full clinical doses of the micronized suspension (Wellvone®). Furthermore, 50% dosages of SDS-coated ANSs resulted in similar antiparasitic effects compared to the micronized suspension (Wellvone®).

There are several possible explanations for the increased therapeutic effects of SDS-coated ANSs. First, nanoparticles of negative ZP are better taken up through Peyer's patches in the gastrointestinal tract compared to positively charged nanoparticles (Shakweh et al 2005). Secondly, since SDS was reported to be incorporated into the lipid bilayer at low concentrations (Nakamura et al 2007) and to change the physical properties of cell membranes. Consequently, SDS is believed to open tight junctions (Amelsberg et al 1997, Anderberg & Artursson 1993, Boulenc et al 1995). Therefore, SDS could enhance oral and brain uptake of atovaquone via paracellular pathways and pave the way for drug passage both at the gastrointestinal and blood-brain barriers. Thirdly, since many molecules access the brain from the blood stream via receptor-mediated transport (RMT) across the BBB, this mechanism could be involved in the SDS-mediated transport of ANSs through the BBB (Jong & Huang 2005) by an unknown receptor binding.

Previous studies of atovaquone in animal models of infection with *T. gondii* revealed significantly increased survival and a reduction in brain cyst burden (Alves & Vitor 2005, Araujo et al 1992, Araujo et al 1998, Araujo et al 1993, Djurkovic-Djakovic et al 2002, Ferguson et al 1994, Romand et al 1993). In addition, the antiparasitic activity of orally administered atovaquone nanocapsules against *T. gondii* in-vitro and in-vivo was investigated (Sordet et al 1998). Atovaquone-loaded nanocapsules (15 mg/kg/day for 10 days) lead to 75% survival rate in mice acutely infected with the RH strain of *T. gondii* compared to untreated

controls and to mice treated with atovaquone suspension at the same dose regimen (Sordet et al 1998). Furthermore, in mice chronically infected with the ME49 strain and treated for six weeks (15 mg/kg/d atovaquone nanocapsules or suspension) resulted in a decrease in the parasite burden in the brain compared to untreated controls. However, since neither mice infected with the RH strain nor mice latently infected with the ME49 strain develop TE, the influence of atovaquone nanocapsules on inflammatory changes in the brain, survival, and/or time to death could not be investigated by these authors. The treatment of TE however represents the most important clinical challenge in immunocompromised patients.

I used atovaquone in nano-sized particles (mean size between 415 and 469 nm) with narrow size distributions and in homogenously distributed solutions that made them candidates for testing atovaquone bioavailability. For the first time, ANSs are used as an oral therapy in murine acute and reactivated toxoplasmosis and results obtained strongly argue that coating of ANSs with surfactants, i.e. SDS, increases the therapeutic efficacy of atovaquone when used in clinical setting (Wellvone®).

In past reports, Tween® 80 (Dunay et al 2004, Kreuter & Gelperina 2008, Kurakhmaeva et al 2008, Shubar et al 2009), P188 (Fontana et al 2001, Kreuter & Gelperina 2008, Scholer et al 2001, Zhang & Fang 2008), and SDS (Soukupová et al 2008, Sun et al 2009, Teeranachaideekul et al 2008) were used to stabilize nanoparticles.

Recently, nanoparticles made of PBCA or poly(lactic-co-glycolic acid) (PLGA) coated with polysorbate 80 or P188 were reported to transport doxorubicin across the BBB for the treatment of cerebral cancer (Kreuter & Gelperina 2008). SDS is an excellent electrostatic stabilizer with high affinity to particle surfaces leading to high ZPs. It is licensed as a stabilizer for oral dosage (Keck 2006), e.g. Janumet® tablets (Merck), and Rythmol® capsules (GlaxoSmithKline). SDS stabilizes amphoteric polyurethane nanoparticles making the complex particles smaller and more compact, and allowing redispersion into water stably

(Qiao et al 2007). SDS can also keep amphoteric polyurethane nanoparticles stable in a broad pH ranges from 1 to 14 (Qiao et al 2007). Furthermore, it was reported that SDS enhanced the transport of mannitols, 1-deamino-8-D-arginine-vasopressin, polyethylene glycol (Anderberg & Artursson 1993), and tiludronate (Boulenc et al 1995) across epithelial barrier in-vitro.

Recently, alumina-coated magnetite nanoparticles (Fe3O4/Al2O3 NPs) modified by SDS have successfully been applied for the extraction of trimethoprim (TMP) from environmental water samples due to the excellent adsorption capacity after surface modification by SDS (Sun et al 2009).

These reports obtained from the previous literature supports observations obtained from the present study indicating that SDS in murine models of acute and reactivated toxoplasmosis was superior to other surfactants (Tween® 80 and P188) and to the commercial oral suspension (Wellvone®) in enhancing oral and brain uptake of the poorly soluble antiparasitic drug (atovaquone).

Interestingly, results obtained in cell culture models do not correlate with those results obtained in murine models of acute and reactivated toxoplasmosis. Whereas ANSs coated with Tween® 80 and P188 showed enhanced transport of atovaquone across the intestinal barrier in-vitro, ANSs coated with P188 enhanced transport of atovaquone through the BBB (both mono- and co-culture models) compared to Wellvone® in-vitro. However, in-vivo, ANSs coated with SDS enhanced bioavailability and brain uptake of atovaquone and thereby improved the therapeutic efficacy of atovaquone in mice infected with *T. gondii*. Therefore, in-vitro models of host barriers (at least those used in the present study) do not appear to appropriately reflect the in-vivo situation. The complex in-vivo situation with at least 2 complex tissue barriers and dissemination in the blood stream may be difficult to represent in-vitro. Surfaces of in-vitro chamber may also impact the passage markedly.

Together the results clearly indicate that ANSs coated by surfactants, i.e. SDS, hold strong promise for the oral delivery of poorly bioavailable molecules like atovaquone. The findings of the present study should lead to further investigations into the detailed pharmacological properties of these drug formulations and may ultimately be used for the optimization of the treatment of patients with diseases that manifest in the central nervous system.

However, there are several limitations to the findings of the present study. First, to assess precisely the improvement in bioavailability, the full plasma concentration/time profiles need to be measured for calculation of the area under the curve, the maximum concentration of the drug in serum, and the time to maximum concentration of the drug in serum. Second, since nanoparticles when given orally pass through different anatomical locations in the gastrointestinal tract (exposed to different pH and different enzymatic conditions) their physicochemical properties, drug release behavior, and stability can be dramatically changed (Kalaria et al 2009). To test this, ANSs should be subjected to different pH media where a change in their properties must be elucidated by counter checking their particle size and polydispersity. Third, mortality study should be investigated in future in-vivo studies to prove that the reductions in inflammation and parasites will ultimately prevent death of mice.

Taken together, the results presented in this thesis will help to establish innovative, safe and efficacious strategies for the treatment of TE in humans.

9 Summary

Toxoplasma gondii is an intracellular parasite that is distributed worldwide. The seroprevalence in humans reaches up to 70% in Germany and France. Toxoplasmic encephalitis (TE) is the most common clinical manifestation of reactivated disease in immunocompromised patients that is lethal if untreated. Acute primary standard therapy for the treatment of TE is the combination of pyrimethamine plus sulfadiazine or clindamycin, but these combinations are associated with hematological toxicity and/or life threatening allergic reactions in 5 to 15% of patients. Therefore alternative treatment options are needed. Atovaquone, a hydroxy-1,4-naphthoquinone drug is safe and shows high efficacy against *T. gondii* in-vitro. However, in-vivo studies have shown less convincing results. Since the bioavailability of the present oral suspension (Wellvone®) is very poor and little is known about the uptake into the brain, modified formulations of atovaquone may be promising for the therapy of TE. Therefore, in the present thesis project, atovaquone nanosuspensions (ANSs) were synthesized and coated with different surfactants to enhance the oral bioavailability and passage through the blood brain barrier (BBB).

First, using an in-vitro model of the intestinal barrier I investigated the passage of ANSs compared to the commercial Wellvone® suspension. Coating of ANSs with polysorbate 80 (Tween® 80) and poloxamer 188 (P188) as surfactants showed significantly enhanced transport across the intestinal barrier in comparison to sodium dodecyl sulfate (SDS)-coated ANSs and Wellvone® suspension. Next, the passage of ANSs compared to Wellvone® suspension across the BBB was investigated using an in-vitro co-culture transwell model. I observed that ANSs coated with P188 showed significantly enhanced transport in comparison to Wellvone® suspension.

Finally, to prove whether ANSs show increased bioavailability, increased uptake into the brain, and superior therapeutic efficacy compared to Wellvone® in the treatment of TE in-vivo

I used mouse models of acute and reactivated toxoplasmosis. Concentrations of ANSs coated with SDS were significantly higher in the serum and brains of mice compared to Wellvone® suspension. Furthermore, parasite loads in brains determined by quantitative PCR and immunohistochemistry as well as numbers of inflammatory foci in brains of mice treated with SDS-coated ANSs were reduced compared to untreated controls and to Wellvone®-treated mice

In summary, whereas ANSs coated with Tween® 80 and P188 showed enhanced transport of atovaquone across the intestinal barrier in-vitro, ANS coated with P188 enhanced transport of atovaquone through the BBB compared to Wellvone® in-vitro. However, in-vivo, ANS coated with SDS enhanced bioavailability and brain uptake of atovaquone and thereby improved the therapeutic efficacy of atovaquone in mice infected with *T. gondii*.

In conclusion, modification of surface properties of ANSs markedly alters the capacity of drugs to cross host barriers. In-vitro models of host barriers do not appear to appropriately reflect the in-vivo situation. Only ANS coated with SDS improved the therapeutic efficacy of atovaquone for the treatment of TE. These results presented in this thesis project will help to establish innovative, safe and efficacious strategies for the treatment of TE in humans.

10 References

Abbott NJ, Ronnback L, Hansson E. 2006. Astrocyte-endothelial interactions at the blood-brain barrier. *Nat Rev Neurosci* 7: 41-53

Adams-Graves P, Kedar A, Koshy M, Steinberg M, Veith R, et al. 1997. RheothRx (poloxamer 188) injection for the acute painful episode of sickle cell disease: a pilot study. *Blood* 90: 2041-6

Alves CF, Vitor RW. 2005. Efficacy of atovaquone and sulfadiazine in the treatment of mice infected with Toxoplasma gondii strains isolated in Brazil. *Parasite* 12: 171-7

Alyautdin RN, Petrov VE, Langer K, Berthold A, Kharkevich DA, Kreuter J. 1997. Delivery of loperamide across the blood-brain barrier with polysorbate 80-coated polybutylcyanoacrylate nanoparticles. *Pharm Res* 14: 325-8

Alyautdin RN, Tezikov EB, Ramge P, Kharkevich DA, Begley DJ, Kreuter J. 1998. Significant entry of tubocurarine into the brain of rats by adsorption to polysorbate 80-coated polybutylcyanoacrylate nanoparticles: an in situ brain perfusion study. *J Microencapsul* 15: 67-74

Amelsberg A, Schteingart CD, Stein J, Simmonds WJ, Sawada GA, et al. 1997. Intestinal absorption of sodium dodecyl sulfate in the rodent: evidence for paracellular absorption. *Am J Physiol* 272: G498-506

Anderberg EK, Artursson P. 1993. Epithelial transport of drugs in cell culture. VIII: Effects of sodium dodecyl sulfate on cell membrane and tight junction permeability in human intestinal epithelial (Caco-2) cells. *J Pharm Sci* 82: 392-8

Araujo FG, Huskinson J, Remington JS. 1991. Remarkable in vitro and in vivo activities of the hydroxynaphthoquinone 566C80 against tachyzoites and tissue cysts of Toxoplasma gondii. *Antimicrob Agents Chemother* 35: 293-9

Araujo FG, Huskinson-Mark J, Gutteridge WE, Remington JS. 1992. In vitro and in vivo activities of the hydroxynaphthoquinone 566C80 against the cyst form of Toxoplasma gondii. *Antimicrob Agents Chemother* 36: 326-30

Araujo FG, Khan AA, Bryskier A, Remington JS. 1998. Use of ketolides in combination with other drugs to treat experimental toxoplasmosis. *J Antimicrob Chemother* 42: 665-7

Araujo FG, Lin T, Remington JS. 1993. The activity of atovaquone (566C80) in murine toxoplasmosis is markedly augmented when used in combination with pyrimethamine or sulfadiazine. *J Infect Dis* 167: 494-7

Aziz DM. 2006. Assessment of bovine sperm viability by MTT reduction assay. *Anim Reprod Sci* 92: 1-8

Baggish AL, Hill DR. 2002. Antiparasitic agent atovaquone. *Antimicrob Agents Chemother* 46: 1163-73

Balimane PV, Han YH, Chong S. 2006. Current industrial practices of assessing permeability and P-glycoprotein interaction. *AAPS J* 8: E1-13

Ballabh P, Braun A, Nedergaard M. 2004. The blood-brain barrier: an overview: structure, regulation, and clinical implications. *Neurobiol Dis* 16: 1-13

Ballas SK, Files B, Luchtman-Jones L, Benjamin L, Swerdlow P, et al. 2004. Safety of purified poloxamer 188 in sickle cell disease: phase I study of a non-ionic surfactant in the management of acute chest syndrome. *Hemoglobin* 28: 85-102

Batrakova EV, Kabanov AV. 2008. Pluronic block copolymers: evolution of drug delivery concept from inert nanocarriers to biological response modifiers. *J Control Release* 130: 98-106

Bertschy S, Opravil M, Cavassini M, Bernasconi E, Schiffer V, et al. 2006. Discontinuation of maintenance therapy against toxoplasma encephalitis in AIDS patients with sustained response to anti-retroviral therapy. *Clin Microbiol Infect* 12: 666-71

Bischoff KM, Shi L, Kennelly PJ. 1998. The detection of enzyme activity following sodium dodecyl sulfate-polyacrylamide gel electrophoresis. *Anal Biochem* 260: 1-17

Bohm BH, Mueller RH. 1999. Lab-scale production unit design for nanosuspensions of sparingly soluble cytotoxic drugs. *Pharm Sci Technolo Today* 2: 336-9

Boothroyd JC, Grigg ME. 2002. Population biology of Toxoplasma gondii and its relevance to human infection: do different strains cause different disease? *Curr Opin Microbiol* 5: 438-42

Boulenc x, Breul T, Gautier JC, Saudemon P, Joyeux H, et al. 1995. Sodium lauryl sulphate increases tiludronate paracellular transport using human epithelial caco-2 monolayers *International Journal of Pharmaceutics* 123: 71-83

Brannon-Peppas L, Blanchette JO. 2004. Nanoparticle and targeted systems for cancer therapy. *Adv Drug Deliv Rev* 56: 1649-59

Buda A, Sands C, Jepson MA. 2005. Use of fluorescence imaging to investigate the structure and function of intestinal M cells. *Adv Drug Deliv Rev* 57: 123-34

Chirgwin K, Hafner R, Leport C, Remington J, Andersen J, et al. 2002. Randomized phase II trial of atovaquone with pyrimethamine or sulfadiazine for treatment of toxoplasmic encephalitis in patients with acquired immunodeficiency syndrome: ACTG 237/ANRS 039 Study. AIDS Clinical Trials Group 237/Agence Nationale de Recherche sur le SIDA, Essai 039. *Clin Infect Dis* 34: 1243-50

Chopra D, Gulati M, Saluja V, Pathak P, Bansal P. 2008. Brain permeable nanoparticles. *Recent Pat CNS Drug Discov* 3: 216-25

Clark MA, Hirst BH, Jepson MA. 2000. Lectin-mediated mucosal delivery of drugs and microparticles. *Adv Drug Deliv Rev* 43: 207-23

Conley FK, Jenkins KA, Remington JS. 1981. Toxoplasma gondii infection of the central nervous system. Use of the peroxidase-antiperoxidase method to demonstrate toxoplasma in formalin fixed, paraffin embedded tissue sections. *Hum Pathol* 12: 690-8

Darde ML. 2004. Genetic analysis of the diversity in Toxoplasma gondii. *Ann Ist Super Sanita* 40: 57-63

de Boer AG, Gaillard PJ. 2006. Blood-brain barrier dysfunction and recovery. *J Neural Transm* 113: 455-62

Deli MA, Abraham CS, Kataoka Y, Niwa M. 2005. Permeability studies on in vitro blood-brain barrier models: physiology, pathology, and pharmacology. *Cell Mol Neurobiol* 25: 59-127

Deli MA, Joo F, Krizbai I, Lengyel I, Nunzi MG, Wolff JR. 1993. Calcium/calmodulin-stimulated protein kinase II is present in primary cultures of cerebral endothelial cells. *J Neurochem* 60: 1960-3

Derouin F, Chastang C. 1988. Enzyme immunoassay to assess effect of antimicrobial agents on Toxoplasma gondii in tissue culture. *Antimicrob Agents Chemother* 32: 303-7

des Rieux A, Fievez V, Garinot M, Schneider YJ, Preat V. 2006. Nanoparticles as potential oral delivery systems of proteins and vaccines: a mechanistic approach. *J Control Release* 116: 1-27

Devalapally H, Chakilam A, Amiji MM. 2007. Role of nanotechnology in pharmaceutical product development. *J Pharm Sci* 96: 2547-65

Di Giorgio C, Ridoux O, Delmas F, Azas N, Gasquet M, Timon-David P. 2000. Flow cytometric detection of Leishmania parasites in human monocyte-derived

macrophages: application to antileishmanial-drug testing. *Antimicrob Agents Chemother* 44: 3074-8

Djurkovic-Djakovic O, Milenkovic V, Nikolic A, Bobic B, Grujic J. 2002. Efficacy of atovaquone combined with clindamycin against murine infection with a cystogenic (Me49) strain of Toxoplasma gondii. *J Antimicrob Chemother* 50: 981-7

Dubey JP. 2008. The history of Toxoplasma gondii--the first 100 years. *J Eukaryot Microbiol* 55: 467-75

Dubey JP, Jones JL. 2008. Toxoplasma gondii infection in humans and animals in the United States. *Int J Parasitol* 38: 1257-78

Dubey JP, Lindsay DS, Speer CA. 1998. Structures of Toxoplasma gondii tachyzoites, bradyzoites, and sporozoites and biology and development of tissue cysts. *Clin Microbiol Rev* 11: 267-99

Dunay IR, Heimesaat MM, Bushrab FN, Mueller RH, Stocker H, et al. 2004. Atovaquone maintenance therapy prevents reactivation of toxoplasmic encephalitis in a murine model of reactivated toxoplasmosis. *Antimicrob Agents Chemother* 48: 4848-54

Duncan R. 2003. The dawning era of polymer therapeutics. *Nat Rev Drug Discov* 2: 347-60

Emerich DF, Thanos CG. 2007. Targeted nanoparticle-based drug delivery and diagnosis. *J Drug Target* 15: 163-83

Ferguson DJ, Huskinson-Mark J, Araujo FG, Remington JS. 1994. An ultrastructural study of the effect of treatment with atovaquone in brains of mice chronically infected with the ME49 strain of Toxoplasma gondii. *Int J Exp Pathol* 75: 111-6

Fitzhugh AL. 1998. Clindamycin as a composite analogue of the transfer RNA fragments L-Pro-Met and D-ribosyl ring of adenosine. *Bioorg. Med Chem. Lett.* 8: 87-92

Florence AT. 2005. Nanoparticle uptake by the oral route: fulfilling its potential? *Drug Discov. Today. Technol.* 2: 75-81

Fontana G, Licciardi M, Mansueto S, Schillaci D, Giammona G. 2001. Amoxicillin-loaded polyethylcyanoacrylate nanoparticles: influence of PEG coating on the particle size, drug release rate and phagocytic uptake. *Biomaterials* 22: 2857-65

Ford HR. 2006. Mechanism of nitric oxide-mediated intestinal barrier failure: insight into the pathogenesis of necrotizing enterocolitis. *J Pediatr Surg* 41: 294-9

Francis K, van Beek J, Canova C, Neal JW, Gasque P. 2003. Innate immunity and brain inflammation: the key role of complement. *Expert Rev Mol Med* 5: 1-19

Frenkel JK, and G. H. Hitchings. 1957. Relative reversal by vitamins (p-aminobezoic, folic acids) of the effects of sulfadiazine and pyrimethamine on Toxoplasma, mouse and man. *Antibiot. Chemother.* 7: 630-8

Frey A, Neutra MR. 1997. Targeting of mucosal vaccines to Peyer's patch M cells. *Behring Inst Mitt*: 376-89

Fricker G, Miller DS. 2004. Modulation of drug transporters at the blood-brain barrier. *Pharmacology* 70: 169-76

Fung HB, Kirschenbaum HL. 1996. Treatment regimens for patients with toxoplasmic encephalitis. *Clin Ther* 18: 1037-56; discussion 6

Gaillard PJ, Voorwinden LH, Nielsen JL, Ivanov A, Atsumi R, et al. 2001. Establishment and functional characterization of an in vitro model of the blood-brain barrier, comprising a co-culture of brain capillary endothelial cells and astrocytes. *Eur J Pharm Sci* 12: 215-22

Galindo-Rodriguez SA, Allemann E, Fessi H, Doelker E. 2005. Polymeric nanoparticles for oral delivery of drugs and vaccines: a critical evaluation of in vivo studies. *Crit Rev Ther Drug Carrier Syst* 22: 419-64

Gay-Andrieu F, Cozon GJ, Ferrandiz J, Kahi S, Peyron F. 1999. Flow cytometric quantification of Toxoplasma gondii cellular infection and replication. *J Parasitol* 85: 545-9

Gebert A, Rothkotter HJ, Pabst R. 1996. M cells in Peyer's patches of the intestine. *Int Rev Cytol* 167: 91-159

Gil ES, Li J, Xiao H, Lowe TL. 2009. Quaternary Ammonium beta-Cyclodextrin Nanoparticles for Enhancing Doxorubicin Permeability across the In Vitro Blood-Brain Barrier. *Biomacromolecules*

Groneberg DA, Giersig M, Welte T, Pison U. 2006. Nanoparticle-based diagnosis and therapy. *Curr Drug Targets* 7: 643-8

Gubbels MJ, Li C, Striepen B. 2003. High-throughput growth assay for Toxoplasma gondii using yellow fluorescent protein. *Antimicrob Agents Chemother* 47: 309-16

Ha E, Wang W, Wang YJ. 2002. Peroxide formation in polysorbate 80 and protein stability. *J Pharm Sci* 91: 2252-64

Hannan SL, Ridout GA, Jones AE. 1996. Determination of the potent antiprotozoal compound atovaquone in plasma using liquid-liquid extraction followed by reversed-phase high-performance liquid chromatography with ultraviolet detection. *J Chromatogr B Biomed Appl* 678: 297-302

Hansson AG, Mitchell S, Jatlow P, Rainey PM. 1996. Rapid high-performance liquid chromatographic assay for atovaquone. *J Chromatogr B Biomed Appl* 675: 180-2

Hu K, Mann T, Striepen B, Beckers CJ, Roos DS, Murray JM. 2002a. Daughter cell assembly in the protozoan parasite Toxoplasma gondii. *Mol Biol Cell* 13: 593-606

Hu K, Roos DS, Murray JM. 2002b. A novel polymer of tubulin forms the conoid of Toxoplasma gondii. *J Cell Biol* 156: 1039-50

Hughes W, Leoung G, Kramer F, Bozzette SA, Safrin S, et al. 1993. Comparison of atovaquone (566C80) with trimethoprim-sulfamethoxazole to treat Pneumocystis carinii pneumonia in patients with AIDS. *N Engl J Med* 328: 1521-7

Hughes WT. 1995. The role of atovaquone tablets in treating Pneumocystis carinii pneumonia. *J Acquir Immune Defic Syndr Hum Retrovirol* 8: 247-52

Jacobs C, Mueller RH. 2002. Production and characterization of a budesonide nanosuspension for pulmonary administration. *Pharm Res* 19: 189-94

Jong A, Huang SH. 2005. Blood-brain barrier drug discovery for central nervous system infections. *Curr Drug Targets Infect Disord* 5: 65-72

Jordan MK, Burstein AH, Rock-Kress D, Alfaro RM, Pau AK, et al. 2004. Plasma pharmacokinetics of sulfadiazine administered twice daily versus four times daily are similar in human immunodeficiency virus-infected patients. *Antimicrob Agents Chemother* 48: 635-7

Kalaria DR, Sharma G, Beniwal V, Ravi Kumar MN. 2009. Design of biodegradable nanoparticles for oral delivery of doxorubicin: in vivo pharmacokinetics and toxicity studies in rats. *Pharm Res* 26: 492-501

Kamau SW, Grimm F, Hehl AB. 2001. Expression of green fluorescent protein as a marker for effects of antileishmanial compounds in vitro. *Antimicrob Agents Chemother* 45: 3654-6

Kaplan JE, Benson C, Holmes KH, Brooks JT, Pau A, Masur H. 2009. Guidelines for prevention and treatment of opportunistic infections in HIV-infected adults and adolescents: recommendations from CDC, the National Institutes of Health, and the HIV Medicine Association of the Infectious Diseases Society of America. *MMWR Recomm Rep* 58: 1-207; quiz CE1-4

Katlama C, Mouthon B, Gourdon D, Lapierre D, Rousseau F. 1996. Atovaquone as long-term suppressive therapy for toxoplasmic encephalitis in patients with AIDS and multiple drug intolerance. Atovaquone Expanded Access Group. *Aids* 10: 1107-12

Kawasaki ES, Player A. 2005. Nanotechnology, nanomedicine, and the development of new, effective therapies for cancer. *Nanomedicine* 1: 101-9

Keck CM. 2006. *Cyclosporine Nanosuspensions: Optimised Size Characterisation & Oral Formulations* Free University, Berlin, Germany

Keck CM, Mueller RH. 2006. Drug nanocrystals of poorly soluble drugs produced by high pressure homogenisation. *Eur J Pharm Biopharm* 62: 3-16

Kerns EH, Li D. 2008. *Drug-like Properties: Concepts, Structure Design and Methods : from ADME to Toxicity Optimization*: Academic Press. 526 pp.

Kerwin BA. 2008. Polysorbates 20 and 80 used in the formulation of protein biotherapeutics: structure and degradation pathways. *J Pharm Sci* 97: 2924-35

Kovacs JA. 1992. Efficacy of atovaquone in treatment of toxoplasmosis in patients with AIDS. The NIAID-Clinical Center Intramural AIDS Program. *Lancet* 340: 637-8

Kraehenbuhl JP, Neutra MR. 2000. Epithelial M cells: differentiation and function. *Annu Rev Cell Dev Biol* 16: 301-32

Kreuter J. 2001. Nanoparticulate systems for brain delivery of drugs. *Adv Drug Deliv Rev* 47: 65-81

Kreuter J, Alyautdin RN, Kharkevich DA, Ivanov AA. 1995. Passage of peptides through the blood-brain barrier with colloidal polymer particles (nanoparticles). *Brain Res* 674: 171-4

Kreuter J, Gelperina S. 2008. Use of nanoparticles for cerebral cancer. *Tumori* 94: 271-7

Kuhn S, Gill MJ, Kain KC. 2005. Emergence of atovaquone-proguanil resistance during treatment of Plasmodium falciparum malaria acquired by a non-immune north American traveller to west Africa. *Am J Trop Med Hyg* 72: 407-9

Kurakhmaeva KB, Voronina TA, Kapica IG, Kreuter J, Nerobkova LN, et al. 2008. Antiparkinsonian effect of nerve growth factor adsorbed on polybutylcyanoacrylate nanoparticles coated with polysorbate-80. *Bull Exp Biol Med* 145: 259-62

Lambkin I, Pinilla C. 2002. Targeting approaches to oral drug delivery. *Expert Opin Biol Ther* 2: 67-73

LaVan DA, Lynn DM, Langer R. 2002. Moving smaller in drug discovery and delivery. *Nat Rev Drug Discov* 1: 77-84

Lundsted LG, and I. R. Schmolka. 1976. The synthesis and properties of block copolymer polyol surfactants. *In R. J. Ceresa (ed.)* 2: 1-103

Mansouri S, Cuie Y, Winnik F, Shi Q, Lavigne P, et al. 2006. Characterization of folate-chitosan-DNA nanoparticles for gene therapy. *Biomaterials* 27: 2060-5

Masur H, Kaplan JE, Holmes KK. 2002. Guidelines for preventing opportunistic infections among HIV-infected persons--2002. Recommendations of the U.S. Public Health Service and the Infectious Diseases Society of America. *Ann Intern Med* 137: 435-78

Maynard C, Swenson R, Paris JA, Martin JS, Hallstrom AP, et al. 1998. Randomized, controlled trial of RheothRx (poloxamer 188) in patients with suspected acute myocardial infarction. RheothRx in Myocardial Infarction Study Group. *Am Heart J* 135: 797-804

McFadden DC, Seeber F, Boothroyd JC. 1997. Use of Toxoplasma gondii expressing beta-galactosidase for colorimetric assessment of drug activity in vitro. *Antimicrob Agents Chemother* 41: 1849-53

Merli A, Canessa A, Melioli G. 1985. Enzyme immunoassay for evaluation of Toxoplasma gondii growth in tissue culture. *J Clin Microbiol* 21: 88-91

Miller DW, Batrakova EV, Waltner TO, Alakhov V, Kabanov AV. 1997. Interactions of pluronic block copolymers with brain microvessel endothelial cells: evidence of two potential pathways for drug absorption. *Bioconjug Chem* 8: 649-57

Mishra PR, Shaal LA, Mueller RH, Keck CM. 2008. Production and characterization of Hesperetin nanosuspensions for dermal delivery. *Int J Pharm*

Misra A, Ganesh S, Shahiwala A, Shah SP. 2003. Drug delivery to the central nervous system: a review. *J Pharm Pharm Sci* 6: 252-73

Moghimi SM, Hunter AC, Dadswell CM, Savay S, Alving CR, Szebeni J. 2004. Causative factors behind poloxamer 188 (Pluronic F68, Flocor)-induced complement activation in human sera. A protective role against poloxamer-mediated complement activation by elevated serum lipoprotein levels. *Biochim Biophys Acta* 1689: 103-13

Moghimi SM, Murray JC. 1996. Poloxamer-188 revisited: a potentially valuable immune modulator. *J Natl Cancer Inst* 88: 766-8

Mohanraj VJ, Chen Y. 2006. Nanoparticles – A Review *Tropical Journal of Pharmaceutical Research* 5: 561-73

Montoya JG, Liesenfeld O. 2004. Toxoplasmosis. *Lancet* 363: 1965-76

Mosmann T. 1983. Rapid colorimetric assay for cellular growth and survival: application to proliferation and cytotoxicity assays. *J Immunol Methods* 65: 55-63

Moss DM, Croppo GP, Wallace S, Visvesvara GS. 1999. Flow cytometric analysis of microsporidia belonging to the genus Encephalitozoon. *J Clin Microbiol* 37: 371-5

Mueller RH. 1991. *Colloidal Carriers for Controlled Drug Delivery and Targeting*. Stuttgart: Wissenschaftliche Verlagsgesellschaft mbH

Mueller RH, Benita S, Böhm BHL. 1998. *Emulsions and nanosuspensions for the formulation of poorly soluble drugs*. Stuttgart, Germany: medpharm Verlag GmbH

Myatt AV, Coatney GR, Hernandez T, Burton HW. 1953. A further study of the toxicity of pyrimethamine (daraprim) in mna. *Am J Trop Med Hyg* 2: 1000-1

Nakamura T, Yamada M, Teshima M, Nakashima M, To H, et al. 2007. Electrophysiological characterization of tight junctional pathway of rabbit cornea treated with ophthalmic ingredients. *Biol Pharm Bull* 30: 2360-4

Nema S, Washkuhn RJ, Brendel RJ. 1997. Excipients and their use in injectable products. *PDA J Pharm Sci Technol* 51: 166-71

Neumann NF, Gyurek LL, Gammie L, Finch GR, Belosevic M. 2000. Comparison of animal infectivity and nucleic acid staining for assessment of Cryptosporidium parvum viability in water. *Appl Environ Microbiol* 66: 406-12

Orive G, Hernandez RM, Rodriguez Gascon A, Dominguez-Gil A, Pedraz JL. 2003. Drug delivery in biotechnology: present and future. *Curr Opin Biotechnol* 14: 659-64

Orringer EP, Casella JF, Ataga KI, Koshy M, Adams-Graves P, et al. 2001. Purified poloxamer 188 for treatment of acute vaso-occlusive crisis of sickle cell disease: A randomized controlled trial. *JAMA* 286: 2099-106

Palmer JS, Cromie WJ, Lee RC. 1998. Surfactant administration reduces testicular ischemia-reperfusion injury. *J Urol* 159: 2136-9

Patel MM, Goyal BR, Bhadada SV, Bhatt JS, Amin AF. 2009. Getting into the brain : approaches to enhance brain drug delivery. *CNS Drugs* 23: 35-58

Patravale VB, Date AA, Kulkarni RM. 2004. Nanosuspensions: a promising drug delivery strategy. *J Pharm Pharmacol* 56: 827-40

Perriere N, Demeuse P, Garcia E, Regina A, Debray M, et al. 2005. Puromycin-based purification of rat brain capillary endothelial cell cultures. Effect on the expression of blood-brain barrier-specific properties. *J Neurochem* 93: 279-89

Pfefferkorn ER, Nothnagel RF, Borotz SE. 1992. Parasiticidal effect of clindamycin on Toxoplasma gondii grown in cultured cells and selection of a drug-resistant mutant. *Antimicrob Agents Chemother* 36: 1091-6

Pfefferkorn ER, Pfefferkorn LC. 1977. Specific labeling of intracellular Toxoplasma gondii with uracil. *J Protozool* 24: 449-53

Porter SB, Sande MA. 1992. Toxoplasmosis of the central nervous system in the acquired immunodeficiency syndrome. *N Engl J Med* 327: 1643-8

Qiao Y, Zhang S, Lin O, Deng L, Dong A. 2007. Complexation between sodium dodecyl sulfate and amphoteric polyurethane nanoparticles. *J Phys Chem B* 111: 11134-9

Reischl U, Bretagne S, Kruger D, Ernault P, Costa JM. 2003. Comparison of two DNA targets for the diagnosis of Toxoplasmosis by real-time PCR using fluorescence resonance energy transfer hybridization probes. *BMC Infect Dis* 3: 7

Ribatti D, Nico B, Crivellato E, Artico M. 2006. Development of the blood-brain barrier: a historical point of view. *Anat Rec B New Anat* 289: 3-8

Rolan PE, Mercer AJ, Weatherley BC, Holdich T, Meire H, et al. 1994. Examination of some factors responsible for a food-induced increase in absorption of atovaquone. *Br J Clin Pharmacol* 37: 13-20

Romand S, Pudney M, Derouin F. 1993. In vitro and in vivo activities of the hydroxynaphthoquinone atovaquone alone or combined with pyrimethamine, sulfadiazine, clarithromycin, or minocycline against Toxoplasma gondii. *Antimicrob Agents Chemother* 37: 2371-8

Roux FS, Mokni R, Hughes CC, Clouet PM, Lefauconnier JM, Bourre JM. 1989. Lipid synthesis by rat brain microvessel endothelial cells in tissue culture. *J Neuropathol Exp Neurol* 48: 437-47

Schmidt DR, Hogh B, Andersen O, Hansen SH, Dalhoff K, Petersen E. 2005. Treatment of infants with congenital toxoplasmosis: tolerability and plasma concentrations of sulfadiazine and pyrimethamine. *Eur J Pediatr*

Schmolka IR. 1991. Poloxamers in the pharamceutical industry. *In P. J. Tarcha (ed.).* 190-208

Scholer N, Krause K, Kayser O, Mueller RH, Borner K, et al. 2001. Atovaquone nanosuspensions show excellent therapeutic effect in a new murine model of reactivated toxoplasmosis. *Antimicrob Agents Chemother* 45: 1771-9

Schroeder U, Sommerfeld P, Ulrich S, Sabel BA. 1998. Nanoparticle technology for delivery of drugs across the blood-brain barrier. *J Pharm Sci* 87: 1305-7

Shakweh M, Besnard M, Nicolas V, Fattal E. 2005. Poly (lactide-co-glycolide) particles of different physicochemical properties and their uptake by peyer's patches in mice. *Eur J Pharm Biopharm* 61: 1-13

Shubar HM, Dunay IR, Lachenmaier S, Dathe M, Bushrab FN, et al. 2009. The role of apolipoprotein E in uptake of atovaquone into the brain in murine acute and reactivated toxoplasmosis. *J Drug Target*: 1-11

Shubar HM, Mayer JP, HopfenMueller W, Liesenfeld O. 2008. A new combined flow-cytometry-based assay reveals excellent activity against Toxoplasma gondii and low toxicity of new bisphosphonates in vitro and in vivo. *J Antimicrob Chemother* 61: 1110-9

Soppimath KS, Aminabhavi TM, Kulkarni AR, Rudzinski WE. 2001. Biodegradable polymeric nanoparticles as drug delivery devices. *J Control Release* 70: 1-20

Sordet F, Aumjaud Y, Fessi H, Derouin F. 1998. Assessment of the activity of atovaquone-loaded nanocapsules in the treatment of acute and chronic murine toxoplasmosis. *Parasite* 5: 223-9

Soukupová J, Kvítek L, Paná_ek A, Nev__ná T, Zbo_il R. 2008. *Comprehensive study on surfactant role on silver nanoparticles (NPs) prepared via modified Tollens process* Elsevier

Spector DL, Goldman RD. 2006. *Basic Methods in Microscopy*. NY, USA: Cold Spring Harbor Laboratory Press. 382 pp.

Sun L, Zhang C, Chen L, Liu J, Jin H, et al. 2009. Preparation of alumina-coated magnetite nanoparticle for extraction of trimethoprim from environmental water samples based on mixed hemimicelles solid-phase extraction. *Anal Chim Acta* 638: 162-8

Teeranachaideekul V, Junyaprasert VB, Souto EB, Mueller RH. 2008. Development of ascorbyl palmitate nanocrystals applying the nanosuspension technology. *Int J Pharm* 354: 227-34

Torres RA, Weinberg W, Stansell J, Leoung G, Kovacs J, et al. 1997. Atovaquone for salvage treatment and suppression of toxoplasmic encephalitis in patients with AIDS. Atovaquone/Toxoplasmic Encephalitis Study Group. *Clin Infect Dis* 24: 422-9

Toth K, Bogar L, Juricskay I, Keltai M, Yusuf S, et al. 1997. The effect of RheothRx Injection on the hemorheological parameters in patients with acute myocardial infarction. *Clin Hemorheol Microcirc* 17: 117-25

Tsien RY. 1998. The green fluorescent protein. *Annu Rev Biochem* 67: 509-44

Ulbrich K, Hekmatara T, Herbert E, Kreuter J. 2009. Transferrin- and transferrin-receptor-antibody-modified nanoparticles enable drug delivery across the blood-brain barrier (BBB). *Eur J Pharm Biopharm* 71: 251-6

Van Eerdenbrugh B, Vermant J, Martens JA, Froyen L, Van Humbeeck J, et al. 2009. A screening study of surface stabilization during the production of drug nanocrystals. *J Pharm Sci* 98: 2091-103

Veszelka S, Pasztoi M, Farkas AE, Krizbai I, Ngo TK, et al. 2007. Pentosan polysulfate protects brain endothelial cells against bacterial lipopolysaccharide-induced damages. *Neurochem Int* 50: 219-28

Wang B, Siahaan TJ, Soltero RA. 2005. *Drug Delivery: Principles and Applications*: Wiley-IEEE

Wang X, Ge J, Wang K, Qian J, Zou Y. 2006. Evaluation of MTT assay for measurement of emodin-induced cytotoxicity. *Assay Drug Dev Technol* 4: 203-7

Weber K, Osborn M. 1969. The reliability of molecular weight determinations by dodecyl sulfate-polyacrylamide gel electrophoresis. *J Biol Chem* 244: 4406-12

Weiss LM, Dubey JP. 2009. Toxoplasmosis: A history of clinical observations. *Int J Parasitol*

Weiss LM, Kim K. 2007. *Toxoplasma Gondii: The Model Apicomplexan : Perspectives and Methods*: Academic Press. 777 pp.

Wilson B, Samanta MK, Santhi K, Kumar KP, Paramakrishnan N, Suresh B. 2008a. Poly(n-butylcyanoacrylate) nanoparticles coated with polysorbate 80 for the targeted delivery of rivastigmine into the brain to treat Alzheimer's disease. *Brain Res* 1200: 159-68

Wilson B, Samanta MK, Santhi K, Kumar KP, Paramakrishnan N, Suresh B. 2008b. Targeted delivery of tacrine into the brain with polysorbate 80-coated poly(n-butylcyanoacrylate) nanoparticles. *Eur J Pharm Biopharm* 70: 75-84

Win KY, Feng SS. 2005. Effects of particle size and surface coating on cellular uptake of polymeric nanoparticles for oral delivery of anticancer drugs. *Biomaterials* 26: 2713-22

Wu G, Lee KY. 2009. Effects of Poloxamer 188 on Phospholipid Monolayer Morphology: An Atomic Force Microscopy Study. *Langmuir*

Wu G, Majewski J, Ege C, Kjaer K, Weygand MJ, Lee KY. 2005. Interaction between lipid monolayers and poloxamer 188: an X-ray reflectivity and diffraction study. *Biophys J* 89: 3159-73

Wuelfing WP, Kosuda K, Templeton AC, Harman A, Mowery MD, Reed RA. 2006. Polysorbate 80 UV/vis spectral and chromatographic characteristics--defining boundary conditions for use of the surfactant in dissolution analysis. *J Pharm Biomed Anal* 41: 774-82

Yamamoto E, Yamaguchi S, Nagamune T. 2008. Effect of beta-cyclodextrin on the renaturation of enzymes after sodium dodecyl sulfate-polyacrylamide gel electrophoresis. *Anal Biochem* 381: 273-5

Yan F, Zhang C, Zheng Y, Mei L, Tang L, et al. 2009. The effect of Poloxamer 188 on nanoparticle morphology, size, cancer cell uptake and cytotoxicity. *Nanomedicine*

Zhang L, Gu FX, Chan JM, Wang AZ, Langer RS, Farokhzad OC. 2008. Nanoparticles in medicine: therapeutic applications and developments. *Clin Pharmacol Ther* 83: 761-9

Zhang W, Fang XL. 2008. [Significant role of poloxamer in drug transport across blood-brain barrier]. *Yao Xue Xue Bao* 43: 890-7

11 Addition

Curriculum Vitae

For reasons of data protection,
the curriculum vitae is not included in the online version

ACADEMIC GRANTS

2003-2009 Libyan General Peoples Committee Secretary For Higher Education Doctoral Scholarship

WORK EXPERIENCE

1998-2000 Private Pharmacies, Tripoli, Libya
Retailer pharmacist, providing prescribed medications, drugs and other pharmaceuticals needed for patient care

2000-2003 Department of Microbiology and Immunity, Al-Fateh University, Tripoli, Libya
Laboratory demonstrater

PUBLICATIONS

1. A new combined flow-cytometry-based assay reveals excellent activity against Toxoplasma gondii and low toxicity of new bisphosphonates in vitro and in vivo. Shubar HM, Mayer JP, Hopfenmüller W, Liesenfeld O. J Antimicrob Chemother. 2008 May; 61(5):1110-9. Epub 2008 Feb 19. PMID: 18285314.
2. The role of apolipoprotein E in uptake of atovaquone into the brain in murine acute and reactivated toxoplasmosis. Shubar HM, Dunay IR, Lachenmaier S, Dathe M, Bushrab FN, Mauludin R, Mueller RH, Fitzner R, Borner K, Liesenfeld O. J Drug Target. 2009 Mar 2:1-11. PMID: 19255896.

PRESENTATIONS

1. 8th blood-brain barrier expert meeting, Bad Herrenalb, Germany, Mai 22nd to 24th 2006:

   "Effect of different surfactants and apolipoprotein E peptides on the passage of atovaquone nanosuspensions through the blood-brain barrier"

2. Institute for Microbiology and Hygiene, Charité Medical School, Campus Benjamin Franklin, Berlin, Germany, Oktober 30th 2006:

   "Atovaquone nanosuspensions for treatment and prophylaxis of toxoplasmosis: effect of surfactants and apolipoprotein E on bioavailability and uptake through the blood-brain barrier"

3. Institute for Microbiology and Hygiene, Charité Medical School, Campus Benjamin Franklin, Berlin, Germany, November 5th 2007

   "Atovaquone nanosuspensions for treatment of acute and reactivated toxoplasmosis"

POSTERS

1. 10th Symposium "Signal transduction in the blood-brain barrier", Potsdam, Germany September 13th to 16th 2007, Shubar HM, Liesenfeld O, Mauludin R, Bushrab FN, Mueller RH, Fitzner R

   "Passage of atovaquone nanosuspensions through the blood-brain barrier in a murine model of acute and reactivated toxoplasmosis"

2. 11th Scientific Meeting of the Association of Colleges of Pharmacy in the Arab World (ACPAW), Tripoli, Libya, December 7th to 9th 2007, Shubar HM, Liesenfeld O, Mayer JP, HopfenMueller W

   "A new combined flow-cytometry-based assay reveals excellent activity against Toxoplasma gondii and low toxicity of new bisphosphonates in-vitro and in-vivo"

PARTICIPATION

1. 7th blood-brain barrier expert meeting, Bad Herrenalb, Germany, May 2nd to 4th 2005
2. Symposium *"Targets, Drugs and Carriers"*, Department of Biology, Chemistry, and Pharmacy, Institute of Pharmacy, Free University, Berlin (FG 463), May 31 to 2nd June 2007
3. 9th blood-brain barrier expert meeting, Bad Herrenalb, Germany, May 21 to 23rd 2007

FURTHER EDUCATION

2nd Symposium *"Quality Assurance in Medical Laboratory Impact and Current Problems"* Institute of Virology, Charité Medical School, Campus Benjamin Franklin, Berlin, Germany, June 16th to 18th 2005

COOPERATION PROJECTS

1. Dr. Margitta Dathe, Peptide Lipid Interaction/Peptide Transport, Leibniz Institute for Molecular Pharamacology, Campus Buch, Berlin, Germany

2. Dr. Gabriele Schönian and Dr. Ahmed Amro, Genetic Variability in Leishmania and Candida, Institute of Microbiology and Hygiene, Charité Medical School, Campus Charité Mitte, Berlin, Germany

DECLARATION

Herewith I declare, that I did the present work without the help of others and without using different sources than mentioned in the work. All citations and explanation, which were taken literally or analogously are noted as such.

Berlin, 27.07.2009

Hend Muammar Shubar